AN ABSTRACT OF THE THESIS OF

SUBODH KUMAR SAXENA for the DOCTOR OF PHILOSOPHY
(Name) (Degree)

in SOIL SCIENCE presented on [illegible]
(Major) (Date)

Title: THEORETICAL AND EXPERIMENTAL EVALUATION OF TRANSFER OF 2,4-DICHLOROPHENOXYACETIC ACID IN POROUS MEDIA

Redacted for Privacy

Abstract approved: _____
Larry Boersma

Experiments were conducted to study the effect of pore size distribution on the diffusion of 2,4-Dichlorophenoxyacetic acid (carbon-14) through water saturated porous media. Eight size fractions of glass beads were used representing the porous media. It was found that as the average particle radius, and hence pore radius, increased, the value of the diffusion coefficient also increased. A relation was obtained between pore radius and the ratio of porous material diffusion coefficient and free chemical diffusion coefficient. Results indicate that the diffusion coefficients of various chemicals can be obtained from self-diffusion coefficients.

Two methods were used to measure self-diffusion coefficients. The agar method consisted of bringing two columns of agar media together having the same concentration of the ion under investigation,

but one column having the ion labelled. Agar media of various concentrations were used and the value of the self-diffusion coefficient was determined by extrapolating the values of self-diffusion coefficients to zero concentration of agar. This method did not give reliable results of the self-diffusion coefficients for 2,4-Dichlorophenoxyacetic acid (carbon-14) and Calcium Chloride (calcium-45). The cell diffusion method was then used and the values of the self-diffusion coefficients were obtained. This method involved the immersion of a short capillary tube filled with a solution containing a labelled ion in a bath containing a solution of the same concentration, but not labelled. It was found that cell diffusion method yielded reliable estimates of the self-diffusion coefficients of the chemicals considered.

Experiments were designed to evaluate theoretical dispersion models proposed by Lindstrom et al. (1967) and Lindstrom and Boersma (1971) for non-sorbing as well as sorbing porous materials. As the average particle radius, and hence pore radius, increased, the shape of the experimental curve varied indicating that pore size distribution effects the movement of the chemicals. The experimental and theoretical curves were compared and found in agreement within the experimental error. The results indicated that the mathematical theory well describes the movement of chemicals.

Theoretical and experimental curves for sorbing media were compared and found to be in agreement within the experimental error

as well. This suggests that the proposed dispersion models may be used to predict the effects of pore size distribution and adsorption on the transport of chemicals.

Theoretical and Experimental Evaluation of Transfer of 2,4-Dichlorophenoxyacetic Acid in Porous Media

by

Subodh Kumar Saxena

A THESIS

submitted to

Oregon State University

in partial fulfillment of
the requirements for the
degree of

Doctor of Philosophy

June 1972

APPROVED:

Redacted for Privacy

Professor of Soil Science

in charge of major

Redacted for Privacy

Head of Department of Soil Science

Redacted for Privacy

Dean of Graduate School

Date thesis is presented

Typed by Clover Redfern for Subodh Kumar Saxena

ACKNOWLEDGMENTS

I wish to express my gratitude and deep appreciation to Dr. Larry Boersma for his valuable guidance, encouragement and constructive criticism during the course of this study.

My appreciation is also expressed to Dr. M. E. Harward, Department of Soil Science; Dr. J. W. Nibler, Department of Chemistry; Dr. D. R. Thomas, Department of Statistics and Dr. G. E. Blanch, Department of Agricultural Economics for acting as members of my Graduate Committee and for their valuable advice in selecting courses relevant to this study.

A special acknowledgment goes to Dr. F. T. Lindstrom, Research Mathematician, Department of Agricultural Chemistry, for his help, criticism and guidance in preparing the parts of this thesis relating to mathematical models and computer analysis. It would have been difficult to complete this dissertation without his assistance.

I wish to express gratitude to my parents, whose encouragement made my ambition for advanced study possible. I wish to dedicate this thesis to them.

Financial support from the Office of Water Resources Research, United States Department of the Interior (grant No. B-001-ORE), the Oregon Agricultural Experiment Station (project 419), and the Soil and Water Conservation Division of the Agricultural Research Service is gratefully acknowledged.

TABLE OF CONTENTS

LIST OF TABLES

LIST OF FIGURES

THEORETICAL AND EXPERIMENTAL EVALUATION OF TRANSFER OF 2,4-DICHLOROPHENOXYACETIC ACID IN POROUS MEDIA

INTRODUCTION

Though extensive literature exists concerning the movement of chemicals through soils it is not adequate to predict the movement of these chemicals through soil. Research in this field has not been widely applicable to practical soil problems of fertility, plant nutrition and pollution control.

Basic research at the molecular level to determine the distribution of ions between the solution and solid phase, properties of water in the proximity of soil colloids and an estimate of the effective cross-sectional area available for diffusion of ions is required. Different parameters such as tortuosity, pore size distribution, texture, negative adsorption, capacity factor and viscosity have been reported to influence the movement of ions. But to predict this movement a quantitative estimation of these parameters is needed.

Experiments were designed to measure the diffusion coefficient of 2,4-Dichlorophenoxyacetic acid as a function of pore size and to evaluate theoretical models developed to describe the movement of this chemical in porous media. Glass beads were used to represent the porous media. To obtain media of different pore size distributions, several size fractions of glass beads were used.

Measurement of the diffusion coefficient was based on several methods reported in the literature. Among those considered and used were the cell diffusion method of Anderson and Saddington (1949) and the agar media method most recently described by Elgawhary et al. (1970) for the measurement of the self-diffusion coefficient. Porous media diffusion coefficients in glass bead beds were measured by a technique described by Lindstrom et al. (1968).

The study of the movement of 2, 4-D in porous media was based on dispersion models proposed by Lindstrom et al. (1967) and Lindstrom and Boersma (1971). The effect of adsorption on the transfer was studied by coating glass beads with powdered resin and ferric hydroxide to create adsorption sites.

PORE SIZE DISTRIBUTIONS

Introduction

Pore size distributions of soils presently are obtained from soil water characteristic curves (Schofield, 1939; Leamer and Lutz, 1940; Childs, 1940). However, the reliability of this procedure has been one of its main disadvantages. Lack of reproducibility, effect of plate impedance, and the fact that the procedure is time consuming made it desirable to consider alternate methods. Mercury intrusion has recently been used as an alternative method. Mercury is forced into pores under pressure. The pressure and the volume of mercury intruded are simultaneously recorded. The relationship between the pressure applied and the pore radius (Washburn, 1921) is:

$$P = \frac{2\sigma \cos \theta}{r}, \qquad (1)$$

where P is the applied pressure, r is the radius of the pore, σ is the surface tension, and θ is the angle of contact between the fluid and solid. The value of θ for mercury was considered by several investigators. Juhola and Wiig (1949) obtained a value of 140 degrees when they forced mercury into calibrated glass capillaries at known pressures. Winslow and Shapiro (1959) suggested 130 degrees to be an average value. Purcell (1949) compared mercury

capillary pressure curves with curves obtained with water and air for various types of rock formations. He found a close agreement between the two values of 140 and 130 degrees over the range of porosities tested.

Using a value of $\theta = 130$ degrees and a surface tension of 473 dynes/cm of mercury obtains,

$$D = \frac{175}{P} \tag{2}$$

where D is the pore diameter in microns and P is the absolute pressure (psia). Since the pores are irregular in shape, Equation (2) gives an effective pore diameter.

Equipment

The Aminco-Winslow Porosimeter (Figure 1) was used to determine pore size distributions of the porous media to be used in the transfer studies. It has a pressure range of 0-5000 psia. The penetrometer assembly (Figure 2) consists of a uniform bore graduated stem 23.3 cm long, fused to a 3.2 cm high glass sample holder which is sealed with a ground glass plate held in place by a threaded collar and lock ring. The maximum possible sample pore volume is controlled by the penetrometer stem volume which was 0.2 ml. In order to control the packing of the sample, it was necessary to place it in

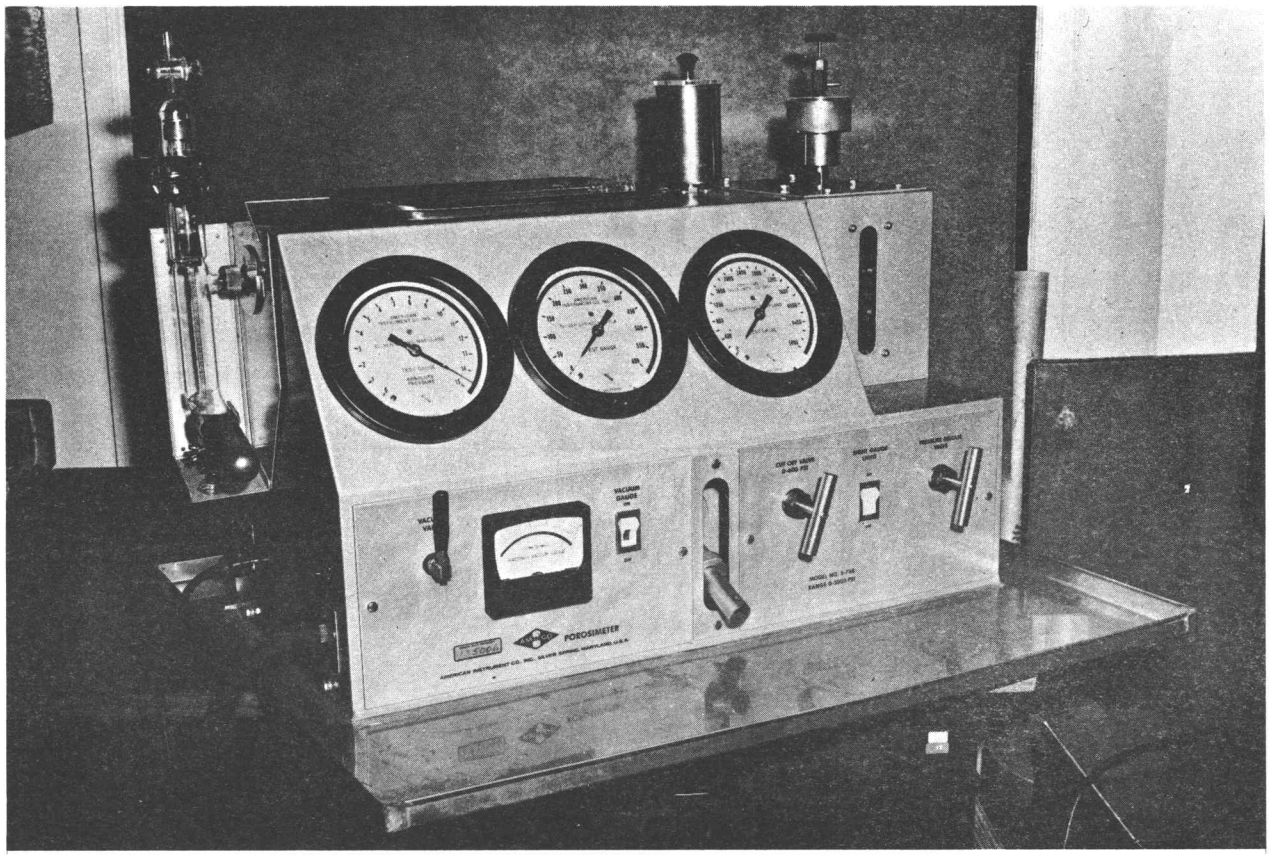

Figure 1. Front view of the mercury intrusion porosimeter.

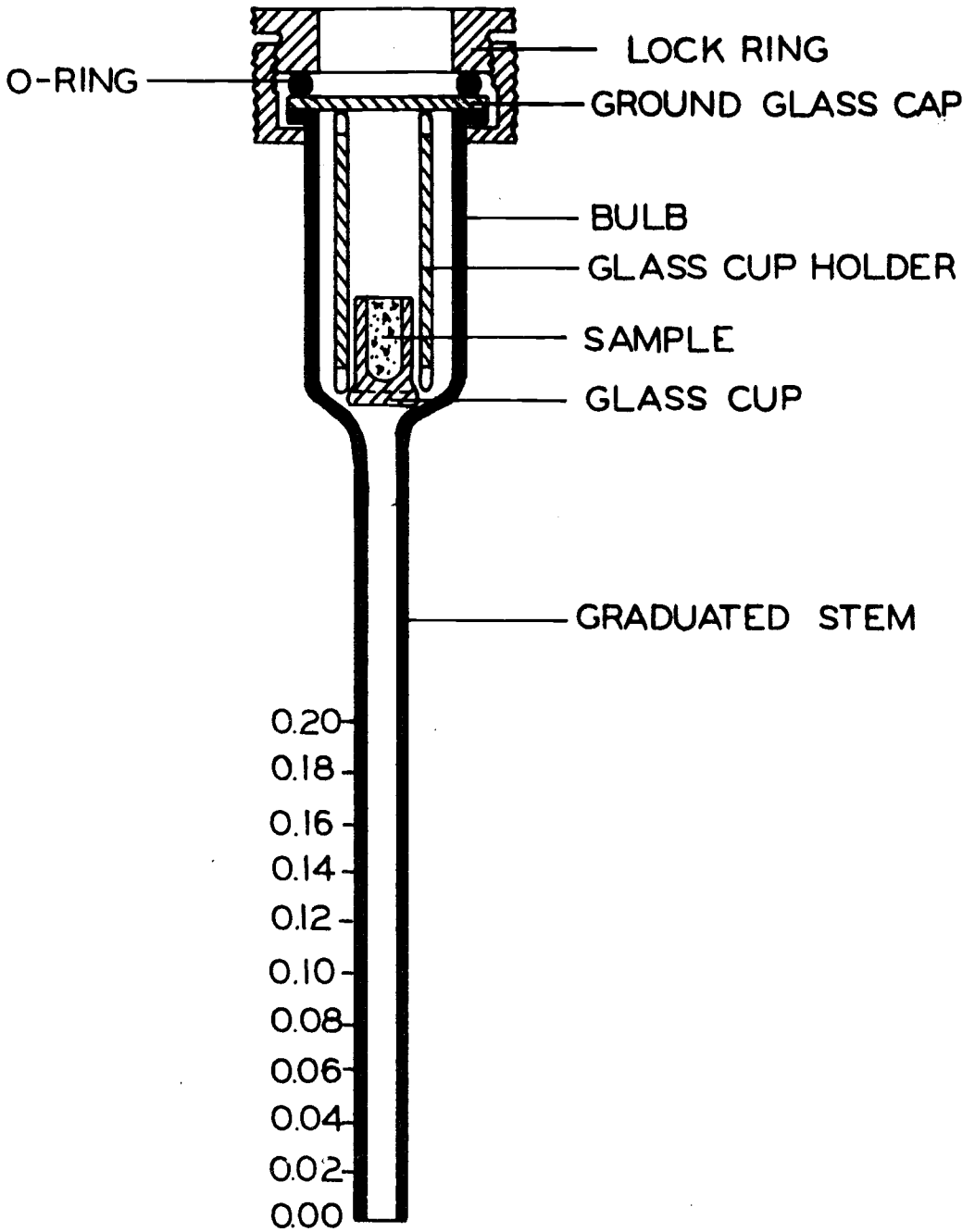

Figure 2. Mercury intrusion porosimeter penetrometer assembly.

cups. These were made from glass tubing and had a length of 1.9 cm, an inside diameter of 0.4 cm, and an outside diameter of 0.6 cm. The volume of these cups was calibrated with mercury. Cup holders (Figure 2) were also constructed to avoid spilling the sample in the penetrometer assembly.

Procedure

An empty cup was weighed and an extension was adapted to the cup. The cup was filled with the sample with occasional tapping to get uniform packing. When the cup was filled completely, the extension was removed and the cup was weighed before transferring to the cup holder. The cup in the holder was then slid gently into the penetrometer assembly which in turn was inserted into the filling device (Figure 3).

The filling device was evacuated to a pressure of less than 50 microns. Once this pressure was reached, the lower tip of the penetrometer was immersed into the mercury pool in the bottom of the filling device by tilting the lower end of the filling device forward. Pressure was released slowly until it read 6.0 psia on the 0-15 psia gauge. This initial pressure filled the penetrometer with mercury. The filling device was rotated backward and the reading on the graduated stem was recorded. The pressure was increased in increments to 14.7 psia and with each pressure increase, the penetrometer stem

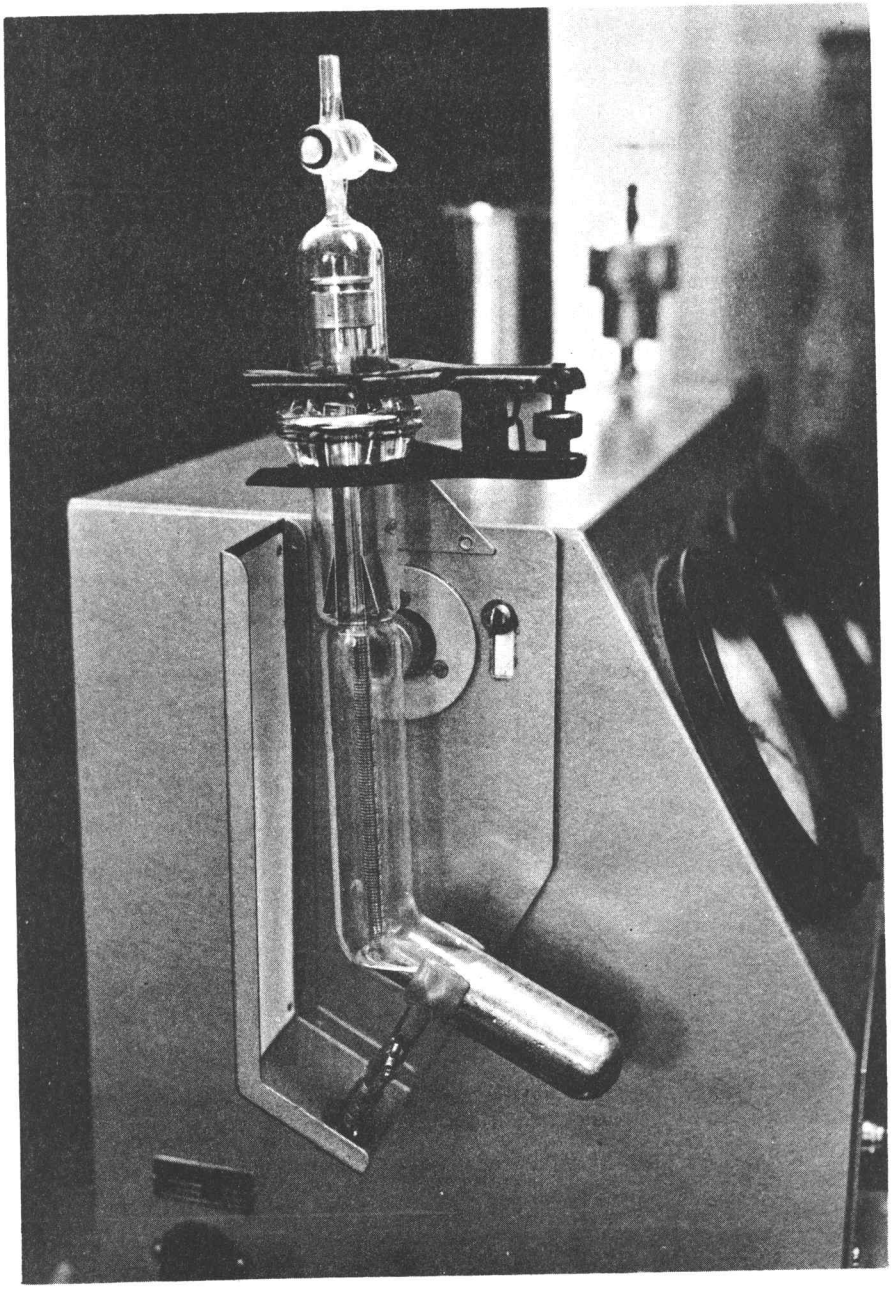

Figure 3. Side view of the filling device for the mercury intrusion porosimeter penetrometer.

reading was recorded. After atmospheric pressure was reached, the penetrometer assembly was placed in the pressure vessel. Large increments of pressure were used in the pressure vessel and subsequent stem readings were recorded (Table 1).

Calculations

Tables 1 through 8 show results of the pore size distribution determinations for the glass bead materials used in later studies as determined by the mercury intrusion porosimeter. Column 1 shows the value of mercury head which is the pressure exerted by the hanging mercury column. It is used to correct the pressure applied to yield absolute pressure (column 4). Pressure corrections corresponding to certain penetrometer stem readings are given in Table 9. The sum of columns 2 + 3 gives the total pressure applied and column 4 is equal to column (2 + 3) minus column 1. Column 5, stem reading, indicates total volume of pores filled with mercury. The maximum value of the stem reading was assumed to indicate the total cumulative pore volume as shown in column 6. It indicates the cumulative volume of pores smaller in diameter than the corresponding diameter indicated in column 7. Equation 2 was used to calculate the pore diameter (column 7) by using the values of absolute pressure from column 4. Column 8 indicates relative pore volumes calculated as follows:

$$\text{Pore volume} = \frac{\text{Cumulative pore volume}}{\text{Total cumulative pore volume}} \times 100.$$

Results

Results of the pore size distribution determinations for the glass bead fractions of <10, 10-20, 30-40, 40-50, <30, 28-53, 105-149 and 149-210 microns (in diameter) are shown in Tables 1 through 8. These results were used in subsequent studies to calculate the contribution of each pore size increment to the transfer of chemicals by diffusion or mass flow.

Table 1. Pore size distribution determination of <10 microns glass beads with mercury intrusion porosimeter.

Mercury Head (1)	0-15 Gauge (2)	Pressure Gauge (3)	Absolute Pressure (4)	Stem Reading (5)	Cumulative Pore Volume (6)	Pore Diameter (7)	Pore Volume (8)
psia	psia	psia	psia	cm^3	cm^3	micron	percent
5.029	6.0	0.0	.971	.000	.086	180.2	100.0
5.016	7.0	0.0	1.984	.001	.085	88.2	98.8
5.016	8.0	0.0	2.984	.001	.085	58.6	98.8
5.016	9.0	0.0	3.984	.001	.085	43.9	98.8
5.016	10.0	0.0	4.984	.001	.085	35.1	98.8
5.016	11.0	0.0	5.984	.001	.085	29.2	98.8
5.016	12.0	0.0	5.984	.001	.085	25.1	98.8
5.002	13.0	0.0	7.998	.002	.084	21.9	97.7
5.002	14.0	0.0	8.998	.002	.084	19.4	97.7
4.989	14.7	0.0	9.711	.003	.083	18.0	96.5
4.949	14.7	2.0	11.751	.006	.080	14.9	93.0
4.936	14.7	4.0	13.764	.007	.079	12.7	91.9
4.910	14.7	6.0	15.790	.009	.077	11.1	89.5
4.896	14.7	10.0	19.804	.010	.076	8.8	88.4
4.830	14.7	20.0	29.870	.015	.071	5.9	82.6
4.141	14.7	50.0	60.559	.067	.019	2.9	22.1
3.942	14.7	100.0	110.758	.082	.004	1.6	4.7
3.916	14.7	250.0	260.784	.084	.002	.67	2.3
3.903	14.7	500.0	510.797	.085	.001	.34	1.2
3.903	14.7	1000.0	1010.797	.085	.001	.17	1.2
3.903	14.7	2000.0	2010.797	.085	.001	.09	1.2
3.889	14.7	4000.0	4010.811	.086	.000	.04	0.0

Table 2. Pore size distribution determination of 10-20 microns glass beads with mercury intrusion porosimeter.

Mercury Head (1)	0-15 Gauge (2)	Pressure Gauge (3)	Absolute Pressure (4)	Stem Reading (5)	Cumulative Pore Volume (6)	Pore Diameter (7)	Pore Volume (8)
psia	psia	psia	psia	cm^3	cm^3	micron	percent
5.029	6.0	0.0	.971	.000	.078	180.2	100.0
5.029	7.0	0.0	1.971	.000	.078	88.8	100.0
5.029	8.0	0.0	2.971	.000	.078	58.9	100.0
5.029	9.0	0.0	3.971	.000	.078	44.1	100.0
5.016	10.0	0.0	4.984	.001	.077	35.1	98.7
5.016	11.0	0.0	5.984	.001	.077	29.2	98.7
5.016	12.0	0.0	6.984	.001	.077	25.1	98.7
5.016	13.0	0.0	7.984	.001	.077	21.9	98.7
5.016	14.0	0.0	8.984	.001	.077	19.5	98.7
4.989	14.7	0.0	9.711	.003	.075	18.0	96.2
4.976	14.7	2.0	11.724	.004	.074	14.9	94.9
4.976	14.7	4.0	13.724	.004	.074	12.8	94.9
4.976	14.7	6.0	15.724	.004	.074	11.1	94.9
4.963	14.7	10.0	19.737	.005	.073	8.9	93.6
4.684	14.7	20.0	30.016	.026	.052	5.8	66.7
4.075	14.7	50.0	60.625	.072	.006	2.9	7.7
4.022	14.7	100.0	110.678	.076	.002	1.6	2.6
4.009	14.7	250.0	260.691	.077	.001	.67	1.3
4.009	14.7	500.0	510.691	.077	.001	.34	1.3
4.009	14.7	1000.0	1010.691	.077	.001	.17	1.3
4.009	14.7	2000.0	2010.691	.077	.001	.09	1.3
3.995	14.7	4000.0	4010.705	.078	.000	.04	1.3

Table 3. Pore size distribution determination of 30-40 microns glass beads with mercury intrusion porosimeter.

Mercury Head (1)	0-15 Gauge (2)	Pressure Gauge (3)	Absolute Pressure (4)	Stem Reading (5)	Cumulative Pore Volume (6)	Pore Diameter (7)	Pore Volume (8)
psia	psia	psia	psia	cm^3	cm^3	micron	percent
5.029	6.0	0.0	.971	.000	.059	180.2	100.0
5.029	7.0	0.0	1.971	.000	.059	88.8	100.0
5.029	8.0	0.0	2.971	.000	.059	58.9	100.0
5.029	9.0	0.0	3.971	.000	.059	44.1	100.0
5.029	10.0	0.0	4.971	.000	.059	35.2	100.0
5.029	11.0	0.0	5.971	.000	.059	29.3	100.0
5.016	12.0	0.0	6.984	.001	.058	25.1	98.3
5.016	13.0	0.0	7.984	.001	.058	21.9	98.3
5.016	14.0	0.0	8.984	.001	.058	19.5	98.3
4.989	14.7	0.0	9.711	.003	.056	18.0	94.9
4.910	14.7	2.0	11.790	.009	.050	14.8	84.7
4.552	14.7	4.0	14.148	.036	.023	12.4	39.0
4.406	14.7	6.0	16.294	.047	.012	10.7	20.3
4.327	14.7	10.0	20.373	.053	.006	8.6	10.2
4.287	14.7	20.0	30.413	.056	.003	5.8	5.1
4.260	14.7	50.0	60.440	.058	.001	2.9	1.7
4.260	14.7	100.0	110.440	.058	.001	1.6	1.7
4.260	14.7	250.0	260.440	.058	.001	.67	1.7
4.260	14.7	500.0	510.440	.058	.001	.34	1.7
4.247	14.7	1000.0	1010.453	.059	.000	.17	0.0
4.247	14.7	2000.0	2010.453	.059	.000	.09	0.0
4.247	14.7	4000.0	4010.453	.059	.000	.04	0.0

Table 4. Pore size distribution determination of 40-50 microns glass beads with mercury intrusion porosimeter.

Mercury Head (1)	0-15 Gauge (2)	Pressure Gauge (3)	Absolute Pressure (4)	Stem Reading (5)	Cumulative Pore Volume (6)	Pore Diameter (7)	Pore Volume (8)
psia	psia	psia	psia	cm^3	cm^3	micron	percent
5.029	6.0	0.0	.971	.000	.084	180.2	100.0
5.016	7.0	0.0	1.984	.001	.083	88.2	98.8
5.016	8.0	0.0	2.984	.001	.083	58.6	98.8
5.016	9.0	0.0	3.984	.001	.083	43.9	98.8
5.016	10.0	0.0	4.984	.001	.083	35.1	98.8
5.016	11.0	0.0	5.984	.001	.083	29.2	98.8
5.002	12.0	0.0	6.998	.002	.082	25.0	97.6
5.002	13.0	0.0	7.998	.002	.082	21.9	97.6
5.002	14.0	0.0	8.998	.002	.082	19.4	97.6
4.936	14.7	0.0	9.764	.007	.077	17.9	91.7
4.247	14.7	2.0	12.453	.059	.025	14.1	29.8
4.088	14.7	4.0	14.612	.071	.013	12.0	15.5
4.048	14.7	6.0	16.652	.074	.010	10.5	11.9
3.995	14.7	10.0	20.705	.078	.006	8.5	7.1
3.956	14.7	20.0	30.744	.081	.003	5.7	3.6
3.942	14.7	50.0	60.758	.082	.002	2.9	2.4
3.929	14.7	100.0	110.771	.083	.001	1.6	1.2
3.929	14.7	250.0	260.771	.083	.001	.67	1.2
3.929	14.7	500.0	510.771	.083	.001	.34	1.2
3.929	14.7	1000.0	1010.771	.083	.001	.17	1.2
3.929	14.7	2000.0	2010.771	.083	.001	.09	1.2
3.916	14.7	4000.0	4010.784	.084	.000	.04	0.0

Table 5. Pore size distribution determination of <30 microns glass beads with mercury intrusion porosimeter.

Mercury Head (1)	0-15 Gauge (2)	Pressure Gauge (3)	Absolute Pressure (4)	Stem Reading (5)	Cumulative Pore Volume (6)	Pore Diameter (7)	Pore Volume (8)
psia	psia	psia	psia	cm^3	cm^3	micron	percent
5.029	6.0	0.0	0.971	.000	.059	180.20	100.00
4.989	7.0	0.0	2.011	.003	.056	87.02	94.91
4.963	8.0	0.0	3.037	.005	.054	57.62	91.53
4.949	9.0	0.0	4.051	.006	.053	43.19	89.83
4.949	10.0	0.0	5.051	.006	.053	34.65	89.83
4.949	11.0	0.0	6.051	.006	.053	28.92	89.83
4.949	12.0	0.0	7.051	.006	.053	24.82	89.83
4.949	13.0	0.0	8.051	.006	.053	21.74	89.83
4.949	14.0	0.0	9.051	.006	.053	19.33	89.83
4.936	14.7	0.0	9.764	.007	.052	17.92	88.14
4.936	14.7	2.0	11.764	.007	.052	14.88	88.14
4.936	14.7	4.0	13.764	.007	.052	12.71	88.14
4.896	14.7	6.0	15.804	.01	.049	11.07	86.44
4.552	14.7	10.0	20.148	.036	.023	8.69	38.98
4.300	14.7	20.0	30.400	.055	.004	5.76	6.78
4.260	14.7	50.0	60.440	.058	.001	2.90	1.69
4.260	14.7	100.0	110.440	.058	.001	1.58	1.69
4.260	14.7	250.0	260.440	.058	.001	0.67	1.69
4.247	14.7	500.0	510.453	.059	.000	0.34	0.00
4.247	14.7	1000.0	1010.453	.059	.000	0.17	0.00
4.247	14.7	2000.0	2010.453	.059	.000	0.087	0.00
4.247	14.7	4000.0	4010.453	.059	.000	0.044	0.00

Table 6. Pore size distribution determination of 28-53 microns glass beads with mercury intrusion porosimeter.

Mercury Head (1)	0-15 Gauge (2)	Pressure Gauge (3)	Absolute Pressure (4)	Stem Reading (5)	Cumulative Pore Volume (6)	Pore Diameter (7)	Pore Volume (8)
psia	psia	psia	psia	cm^3	cm^3	micron	percent
5.029	6.0	0.0	0.971	.000	.067	180.2	100.00
5.029	7.0	0.0	1.971	.000	.067	88.79	100.00
5.029	8.0	0.0	2.971	.000	.067	58.90	100.00
5.029	9.0	0.0	3.971	.000	.067	44.07	100.00
5.029	10.0	0.0	4.971	.000	.067	35.20	100.00
5.023	11.0	0.0	5.977	.0005	.0665	14.64	99.25
5.023	12.0	0.0	6.977	.0005	.0665	25.08	99.25
5.023	13.0	0.0	7.977	.0005	.0665	21.94	99.25
5.016	14.0	0.0	8.984	.001	.066	19.48	98.50
5.002	14.7	0.0	9.698	.002	.065	18.04	97.01
5.260	14.7	2.0	12.440	.058	.009	14.07	13.43
4.221	14.7	4.0	14.479	.061	.006	12.09	8.96
4.207	14.7	6.0	16.493	.062	.005	10.61	7.46
4.181	14.7	10.0	20.519	.064	.003	8.53	4.48
4.168	14.7	20.0	30.532	.065	.002	5.73	2.99
4.154	14.7	50.0	60.546	.066	.001	2.89	1.49
4.141	14.7	100.0	110.559	.067	.000	1.58	0.00
4.141	14.7	250.0	260.559	.067	.000	0.67	0.00
4.141	14.7	500.0	510.559	.067	.000	0.34	0.00
4.141	14.7	1000.0	1010.559	.067	.000	0.17	0.00
4.141	14.7	2000.0	2010.559	.067	.000	0.087	0.00
4.141	14.7	4000.0	4010.559	.067	.000	0.044	0.00

Table 7. Pore size distribution determination of 105-149 microns glass beads with mercury intrusion porosimeter.

Mercury Head (1)	0-15 Gauge (2)	Pressure Gauge (3)	Absolute Pressure (4)	Stem Reading (5)	Cumulative Pore Volume (6)	Pore Diameter (7)	Pore Volume (8)
psia	psia	psia	psia	cm^3	cm^3	micron	percent
5.029	6.0	0.0	0.971	.000	.074	180.22	100.00
5.002	7.0	0.0	1.998	.002	.072	87.59	97.30
4.989	8.0	0.0	3.011	.003	.071	58.12	95.95
4.963	9.0	0.0	4.037	.005	.069	43.35	93.24
4.181	10.0	0.0	5.819	.064	.010	15.04	13.51
4.128	11.0	0.0	6.872	.068	.006	25.47	8.11
4.115	12.0	0.0	7.885	.069	.005	22.19	6.75
4.088	13.0	0.0	8.912	.071	.003	19.64	4.05
4.088	14.0	0.0	9.912	.071	.003	17.65	4.05
4.088	14.7	0.0	10.612	.071	.003	16.49	4.05
4.075	14.7	2.0	12.625	.072	.002	13.86	2.70
4.075	14.7	4.0	14.625	.072	.002	11.96	2.70
4.062	14.7	6.0	16.638	.073	.001	10.52	1.35
4.062	14.7	10.0	10.638	.073	.001	8.48	1.35
4.062	14.7	20.0	30.638	.073	.001	5.71	1.35
4.062	14.7	50.0	60.638	.073	.001	2.89	1.35
4.062	14.7	100.0	110.638	.073	.001	1.58	1.35
4.062	14.7	250.0	260.638	.073	.001	0.67	1.35
4.062	14.7	500.0	510.638	.073	.001	0.34	1.35
4.062	14.7	1000.0	1010.638	.073	.001	0.17	1.35
4.062	14.7	2000.0	2010.638	.073	.001	0.087	1.35
4.048	14.7	4000.0	4010.652	.074	.000	0.044	0.00

Table 8. Pore size distribution determination of 149-210 microns glass beads with mercury intrusion porosimeter.

Mercury Head (1)	0-15 Gauge (2)	Pressure Gauge (3)	Absolute Pressure (4)	Stem Reading (5)	Cumulative Pore Volume (6)	Pore Diameter (7)	Pore Volume (8)
psia	psia	psia	psia	cm^3	cm^3	micron	percent
5.029	6.0	0.0	0.971	.000	.083	180.2	100.00
4.989	7.0	0.0	2.011	.003	.080	79.1	96.38
4.207	8.0	0.0	3.793	.062	.021	45.0	25.30
4.075	9.0	0.0	4.925	.072	.011	35.5	13.25
4.035	10.0	0.0	5.965	.075	.008	29.3	9.64
4.009	11.0	0.0	6.991	.077	.006	25.0	7.23
3.995	12.0	0.0	8.005	.078	.005	21.9	6.02
3.995	13.0	0.0	9.005	.078	.005	19.4	6.02
3.982	14.0	0.0	10.018	.079	.004	17.5	4.82
3.969	14.7	0.0	10.731	.080	.003	16.3	3.61
3.956	14.7	2.0	12.744	.081	.002	13 7	2.41
3.956	14.7	4.0	14.744	.081	.002	11.9	2.41
3.956	14.7	6.0	16.744	.081	.002	10.5	2.41
3.956	14.7	10.0	20.744	.081	.002	8.4	2.41
3.956	14.7	20.0	30.744	.081	.002	5.7	2.41
3.942	14.7	50.0	60.758	.082	.001	2.9	1.21
3.942	14.7	100.0	110.758	.082	.001	1.6	1.21
3.942	14.7	250.0	260.758	.082	.001	0.7	1.21
3.942	14.7	500.0	510.758	.082	.001	0.3	1.21
3.942	14.7	1000.0	1010.758	.082	.001	0.17	1.21
3.942	14.7	2000.0	2010.758	.082	.001	0.087	1.21
3.929	14.7	4000.0	4010.771	.083	.000	0.044	0.00

Table 9. Pressure correction for the hanging mercury column in the penetrometer.

Penetrometer Reading	Pressure Correction
cm^3	psia
0.00	5.029
0.01	4.896
0.02	4.764
0.03	4.631
0.04	4.499
0.05	4.366
0.06	4.234
0.07	4.101
0.08	3.969
0.09	3.836
0.10	3.704
0.11	3.571
0.12	3.439
0.13	3.306
0.14	3.174
0.15	3.041
0.16	2.909
0.17	2.776
0.18	2.644
0.19	2.511
0.20	2.379

DIFFUSION

Introduction

Graham (1850) first studied experimentally the process of diffusion in solution. Fick (1855), by considering diffusion as analogous to the flow of heat, and assuming that the amount of solute that diffused across a given cross-section per unit time was proportional to the concentration gradient at that point, was able to set up a differential equation describing diffusion processes. This equation, known as Fick's law is

$$\frac{\partial c}{\partial t} = D \frac{\partial^2 c}{\partial x^2},$$

where c is the concentration of the solute, t is the time, and x is the distance along the diffusion path. The diffusion coefficient D represents the amount of solute that will diffuse across a unit cross-section of the diffusion cell per unit time if the concentration gradient at that point is unity.

The subject of diffusion is one of great practical and theoretical importance in biological sciences. A knowledge of the speeds at which ions diffuse in soils is of both basic and agronomic importance. Mass flow and diffusion of ions are considered to be main processes responsible for making nutrients available to plant roots. Barber

(1962) proposed a plant nutrient availability concept for plants growing in soil based on the movement of nutrients through the soil to the root surface. He stated that diffusion is the dominant factor controlling availability when mass flow brings only a small fraction of the nutrients required by the plant. Barber et al. (1963) gave some quantitative values for the amounts of nutrients available to the plants and the amounts that roots would reach and showed the significance of diffusion and mass flow.

Extensive literature exists about diffusion of ions in biological systems yet it lacks in reporting quantitative values of diffusion coefficients, and the effects properties of the media have on them. Many investigators (Barrer, 1951; Call, 1956; Crank, 1956; Klute and Letey, 1958; Bouldin, 1961; Brenner, 1961; Lai and Mortland, 1961; Dutt and Low, 1962; Lai and Mortland, 1968) have proposed mathematical models to determine diffusion coefficients quantitatively. These models are based on Fick's law and employ linear diffusion type partial differential equations. They are summarized in Appendix 1. These models represent various boundary conditions and have been developed to suit the investigator's specific experiment. Numerous soil properties such as bulk density, water content, texture, kind and amount of clay, organic matter content, kind and quantity of cations on the exchange complex, soluble salts, and temperature may affect the diffusion rate of plant nutrients in the soil.

Olsen et al. (1962) and Olsen and Watanabe (1963) first reported the effect of soil texture on the diffusion of phosphorus. They mentioned that tortuosity and ionic interaction factors of the porous system must be known in order to calculate effective diffusion coefficients. Lindstrom et al. (1967) developed a mathematical model for the movement of a herbicide in saturated soil based on Fick's law, conservation of energy, and sorption isotherms. They incorporated, in the model, conditions like saturation, chemical diffusion coefficient, percolation velocity of water, sorbtive properties of the soil, the average particle size of the soil and the fractional number of sorbing sites on the particle surface.

According to Olsen et al. (1962) and Olsen and Watanabe (1963) different values of diffusion coefficients were obtained because of variation in soil texture. However a clear concept of this variation can be obtained only if pore size and pore size distribution is known. To test the hypothesis that pore size and pore size distribution is important for diffusion of ions and chemicals in soil, the present study was carried out.

Diffusion Apparatus

Equipment was designed and constructed to study diffusion rates as a function of pore sizes and pore size distributions of porous media. The method used was based on the measurement of the distribution of

a chemical allowed to diffuse into a water saturated porous bed, from a reservoir in contact with the bed. The principle of the method used is shown in Figure 4. The equipment used consisted of sample holder, reservoir, column stand, and sampling tools.

Equipment

Sample Holder. The porous medium sample was held in brass rings contained in a hollow brass cylinder 6.0 in. high with an inside diameter of 1.0 in. and an outside diameter of 1 25/32 in. (Figure 4A). The assembly was secured to a platform with a projecting steel rod 9/16 in. long and 1/4 in. in diameter, 3/8 in. from the bottom of this cylinder. The top 1/2 in. of the column was machined to an outside diameter of 1 11/16 in. and the bottom 1 1/8 in. was machined to give an outside diameter of 1 5/8 in.

The brass rings containing the sample had an inside diameter of 3/4 in. and an outside diameter of 1.0 in. Twenty rings were used of which 6 were 0.1 in. high, 7 were 0.2 in. high, 4 were 0.4 in. high, and 3 were 0.8 in. high, for a total column height of 6.0 in. when all rings were used. A lucite plug with two 0-rings was used to seal the bottom of the cylinder. With the plug and rings in place in the sample holder, it was packed with glass beads.

Reservoir. A hollow brass cylinder 6.0 in. high with an inside diameter of 3/4 in. and an outside diameter of 1 9/32 in. was used to

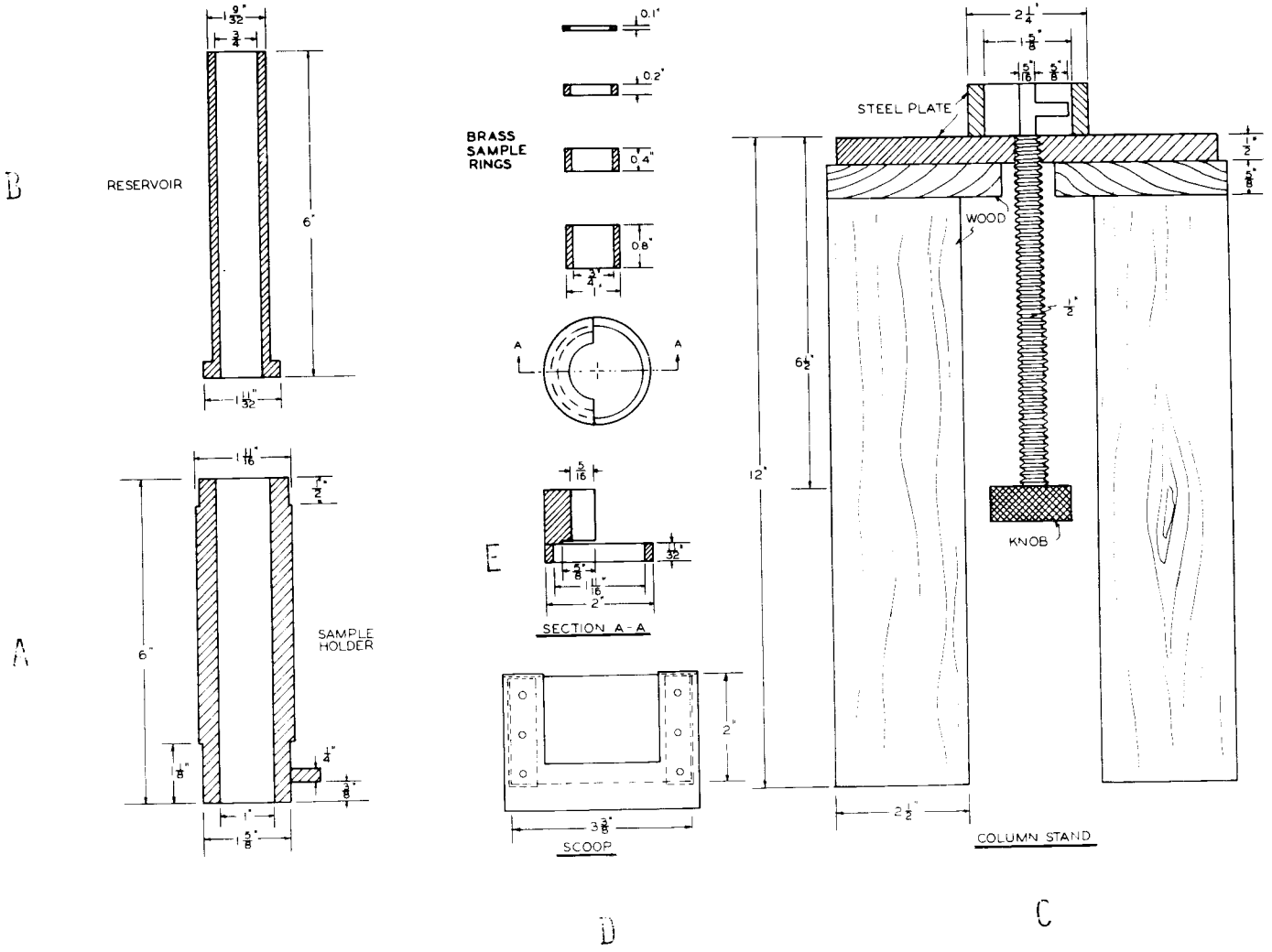

Figure 4. Diffusion apparatus. (A) sample holder; (B) reservoir; (C) column stand; (D) scoop.

contain the solution with the diffusing chemical. A collar 5/16 in. high, with an inside diameter of 3/4 in. and an outside diameter of 1 11/16 in. provided the contact surface with the sample holder. The contact surfaces were sealed with vacuum grease (Figure 4B).

Column Stand. This assembly was used to mount the sample holder for extraction of the sample rings for analysis. A 7.0 in. x 7.0 in. steel plate was mounted in a wooden stand 12.0 in. high. In the center of this plate, an aluminum ring with an inside diameter of 1 5/8 in. was attached. This ring was notched with a 5/8 in. long groove which held the projected steel rod (A) of the sample holder. A threaded rod 9 in. long with a knurled knob was attached to the bottom of the steel plate. With the sample column in place, turning the knob raised the rod, pushing against the brass rings, raising them 0.05 in. per revolution (Figure 4C).

Scoop. Upon completion of an experimental run, the reservoir was removed and the sample holder was fitted on the column stand to obtain the samples for analysis. The column was raised in increments, each one being equal to the thickness of a sample ring. The ring protruding above the holder was removed with a specially constructed scoop. It consisted of a rectangular (2.0 in. x 3 3/8 in.) steel plate 1/32 in. thick, held in a U-shaped clamp (Figure 4D). To avoid pushing the sample of the stand without picking it up, a backing was provided against which the sample ring was blocked when being picked up

by the scoop. It is shown in Figure 4E. The lower half was machined to fit on the machined upper portion of the sample holder with an inside diameter of 1 11/16 in., an outside diameter of 2.0 in. and a height of 11/32 in. The upper half was a half circle wall holding the sample ring in position with an inside diameter of 1.0 in., an outside diameter of 2.0 in. and a height of 1.0 in. Slightly more than half of the upper ring was cut away leaving a distance of 29/32 in. from the center of the inner face to the outer surface of the ring. At the joining surfaces of the two halves of this assembly, a groove was cut to accommodate the scoop as it was used to cut away the sample. The groove was 3/64 in. high and extended slightly beyond the inside surface of the upper ring to a distance of 3/8 in. from the outside surface of the assembly. This entire assembly was made from 2.0 in. diameter aluminum rod stock (Figure 4E).

Vacuum Chamber. To avoid air pockets in the porous beds, they were saturated with water in a vacuum chamber (Figure 5) 13.0 in. high with an inside diameter of 2 29/32 in. made of lucite. It was sealed at the top with an 0-ring and a lid tightened down with 6 wing-nuts. It was connected to a mercury manometer and a vacuum pump.

Chemical Preparation

The experiments were done with the herbicide 2,4-Dichlorophenoxyacetic acid (2,4-D). Carbon-14 labelled

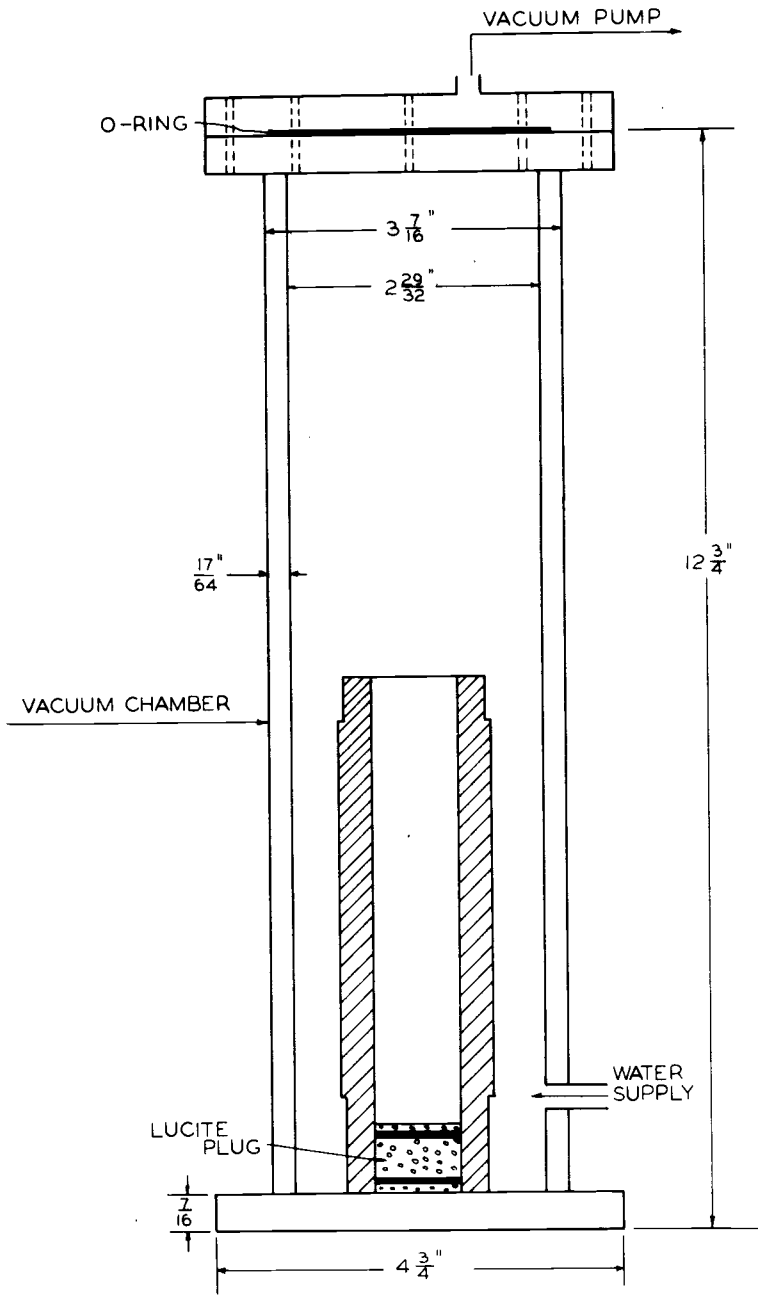

Figure 5. Vacuum chamber in which the glass beads were saturated with water.

2,4-Dichlorophenoxyacetic acid in powder form was obtained from New England Nuclear, Boston, Massachusetts. The compound weighed 4.5 milligrams and had an activity of 0.05 millicuries. This was dissolved in a 1-liter volumetric flask containing 10 ml of A.R. grade acetone and 5.5 mg of non-radioactive 2,4-Dichlorophenoxyacetic acid. The flask was filled with about 600 ml of distilled water. Air was passed through the flask for 24 hours to remove the acetone. Another 200 ml of distilled water was added and again air was passed through for 24 hours to remove remaining traces of the acetone. Distilled water was added to bring the final volume to 1 liter. The resulting solution contained 10 ppm of 2,4-Dichlorophenoxyacetic acid.

Procedure

Vacuum grease was applied on the outside of the sample rings, lucite plug, and on the inside surface of the sample column. The lucite plug was inserted from the top of the column followed by the sample rings ordered by size with large rings following the plug and the smaller rings inserted last. The sample column was then filled halfway with the glass bead sample. The column was packed using an electric vibrator and inserted in the vacuum chamber. After the chamber was evacuated water was admitted to the chamber and the sample was allowed to saturate under vacuum for two hours. Extra water on the sample was removed by pipetting. This procedure was repeated to fill the sample column.

The sample column was brought in contact with the reservoir after both surfaces were lubricated with vacuum grease. Pressing tightly sealed the contact surfaces. The 2, 4-Dichlorophenoxyacetic acid solution was slowly poured into the reservoir to a predetermined height. The chemical was allowed to diffuse into the sample for 4 days. The solution in the reservoir was stirred at 4-hour intervals with a thin lucite rod attached to a circular brass screen 11/16 in. in diameter. This was done to avoid formation of a concentration gradient near the boundary between the reservoir and porous bed. After 4 days, the remaining 2, 4-Dichlorophenoxyacetic acid solution was pipetted out and the reservoir was removed from the sample column.

The sample column was then fixed to the stand and the scoop holder was placed in position. Sample rings were raised one by one with the handle on the stand and removed with the scoop.

Treatment of Samples

Samples obtained with the scoop were washed out of the rings and into graduated centrifuge tubes with water. The volume (10 cc) was made up with water and the tubes were centrifuged for 1 hour at a speed of 10,000 rpm (acceleration x gravity).

A 0.1 ml aliquot of supernatant was pipetted from the centrifuge tube to a counting vial. Ten ml of fluor solution was added to each vial. Fresh fluor solution was prepared from stock solution for each experiment.

The vials were refrigerated overnight and then the activity was determined by counting the samples with a liquid scintillation counter.

Scintillation Fluid

This solution was prepared by mixing 640 ml of A.R. grade Toluene and 450 ml of Triton X-100. The mixture was filtered through a pad of silica gel (Grade 4, 28-200 mesh) which had been activated by heating in a vacuum oven at 80°C for at least 12 hours. The solution was stored in a refrigerator.

Fluor Solution

Fifty gm of Omnifluor (obtained from New England Nuclear, Boston, Massachusetts) was dissolved in 500 ml of A.R. grade Toluene. This served as a stock solution and was stored in a refrigerator. To make the fluor solution, 50 ml of stock solution was mixed with 950 ml of scintillation fluid. Ten ml of this fluor solution was used per sample for liquid scintillation counting purposes.

Results and Discussion

Analysis of the results was based on a mathematical model proposed by Lindstrom et al. (1968). Equation 3 was used to calculate the diffusion coefficient of 2,4-Dichlorophenoxyacetic acid in the various glass bead fractions.

$$c(x,t) = c_0 \, \mathrm{erfc}\left[\frac{x}{2\sqrt{Kt}}\right], \qquad (3)$$

where $c(x,t)$ is chemical concentration in the soil voids ($\mu g/cm^3$), c_0 is the initial concentration of chemical in the reservoir ($\mu g/cm^3$), x is the length of the column (cm), t is the time of diffusion (days), K is the porous medium diffusion coefficient, and erfc is error function complement defined as

$$\mathrm{erfc}[W] = \frac{2}{\sqrt{\pi}} \int_W^\infty e^{-V^2} dV$$

Plots were made of the relative concentration (c/c_0) as a function of distance along the column. Figures 6, 7, 8 and 9 show these for the size fractions <10, 10-20, 30-40 and 40-50 microns, respectively. Theoretical curves based on Equation 3 were fitted to the experimental data obtained for the various size fractions of glass beads. Different values of K were chosen to obtain the best fit to the experimental data. Chi-square tests run simultaneously were used to assure getting the best fit values for K. The computer analysis for this procedure is given in Appendix 2. The experimental data values of c/c_0 represent an average of the chemical concentration present in 0.1 in. long sections of the column. These points were plotted at the mid-point of each section, but may actually lie within a distance of 0.1 in. of this point. The experimental and theoretical curves agree

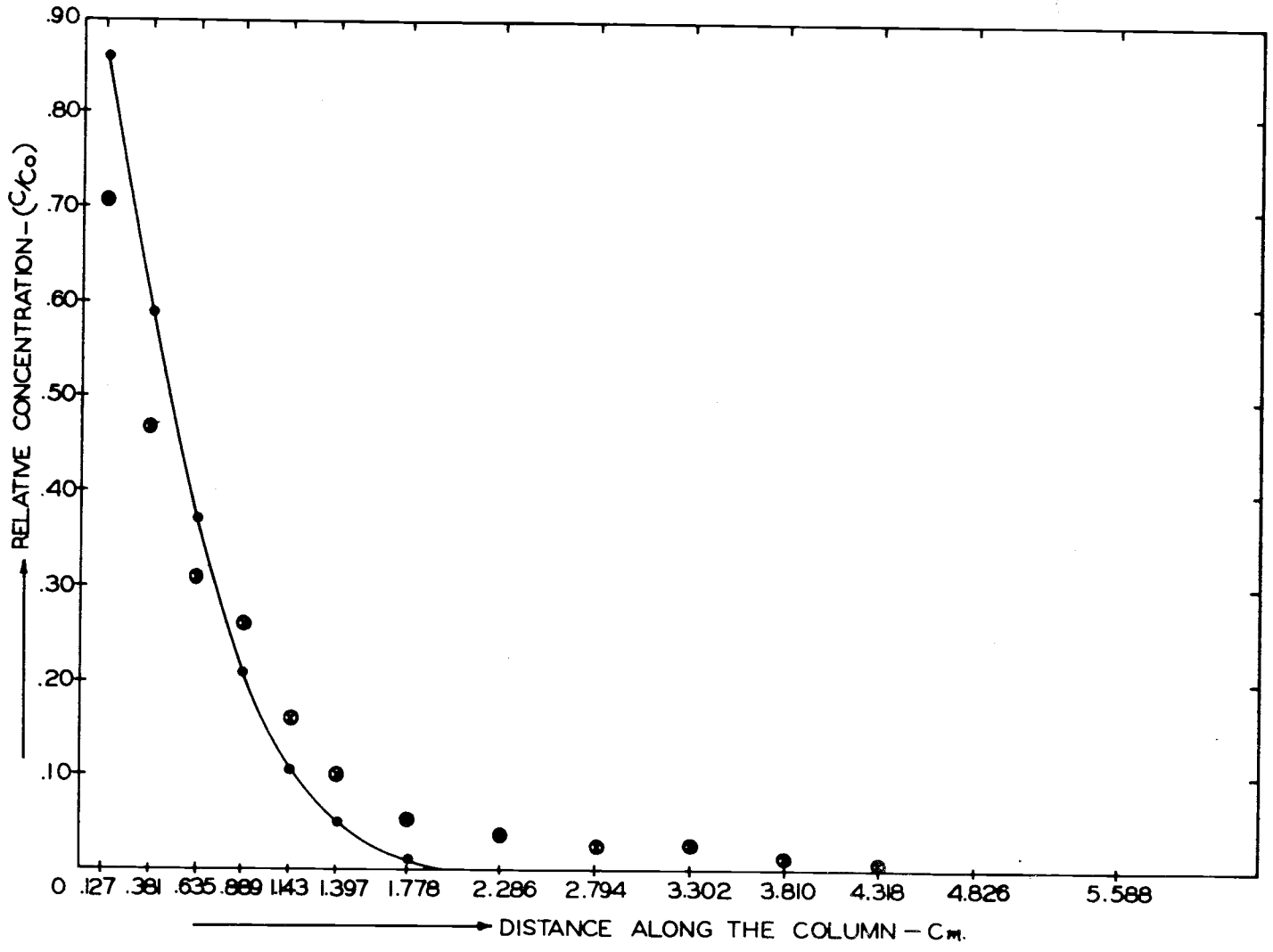

Figure 6. Void concentration of 2,4-D plotted as a function of sample depth (t = 4 days) for <10 microns glass beads. ⊗ experimental; ⊙ theoretical.

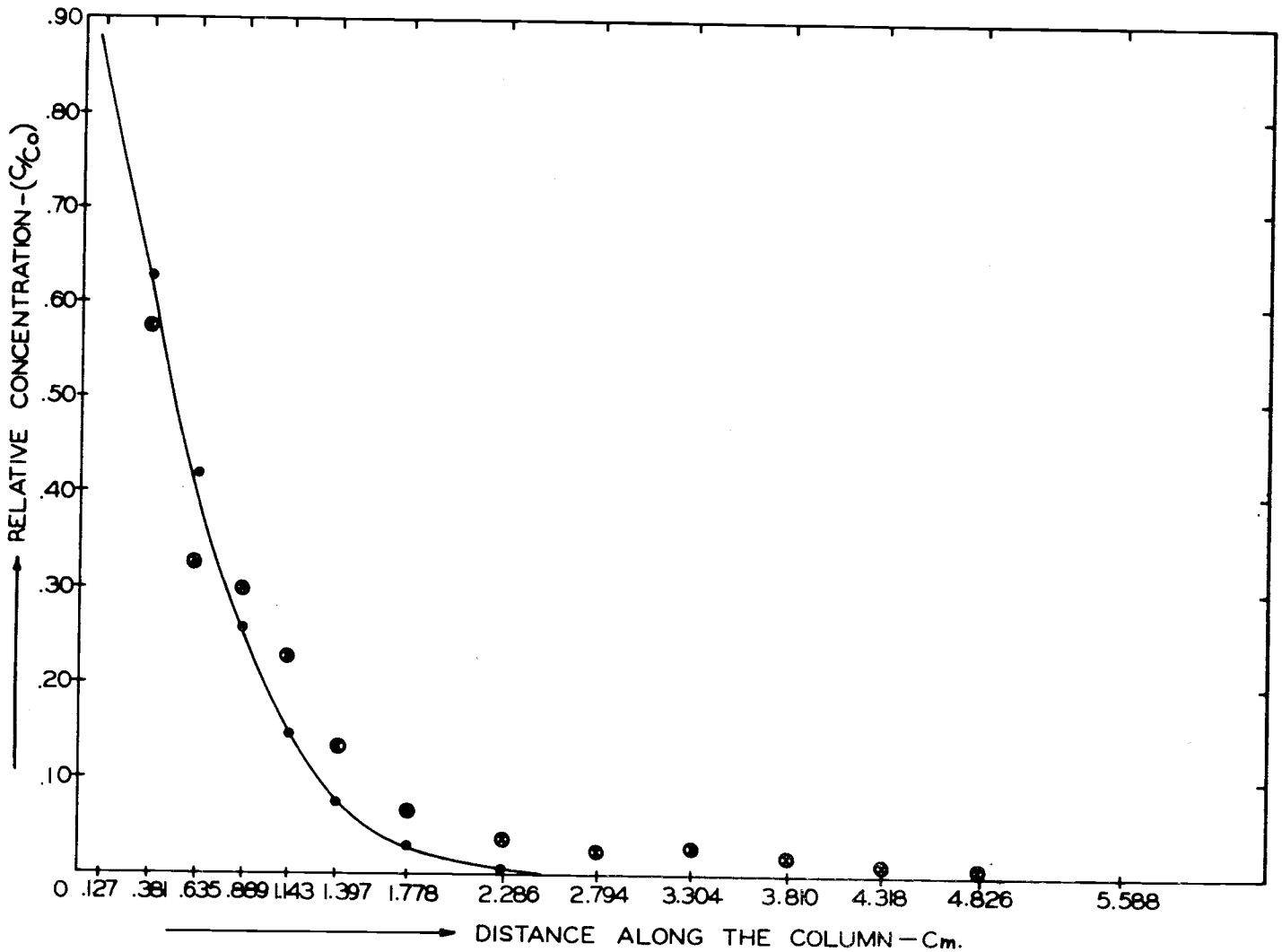

Figure 7. Void concentration of 2,4-D plotted as a function of sample depth (t = 4 days) for 10-20 microns glass beads. ⊗ experimental; ⊙ theoretical.

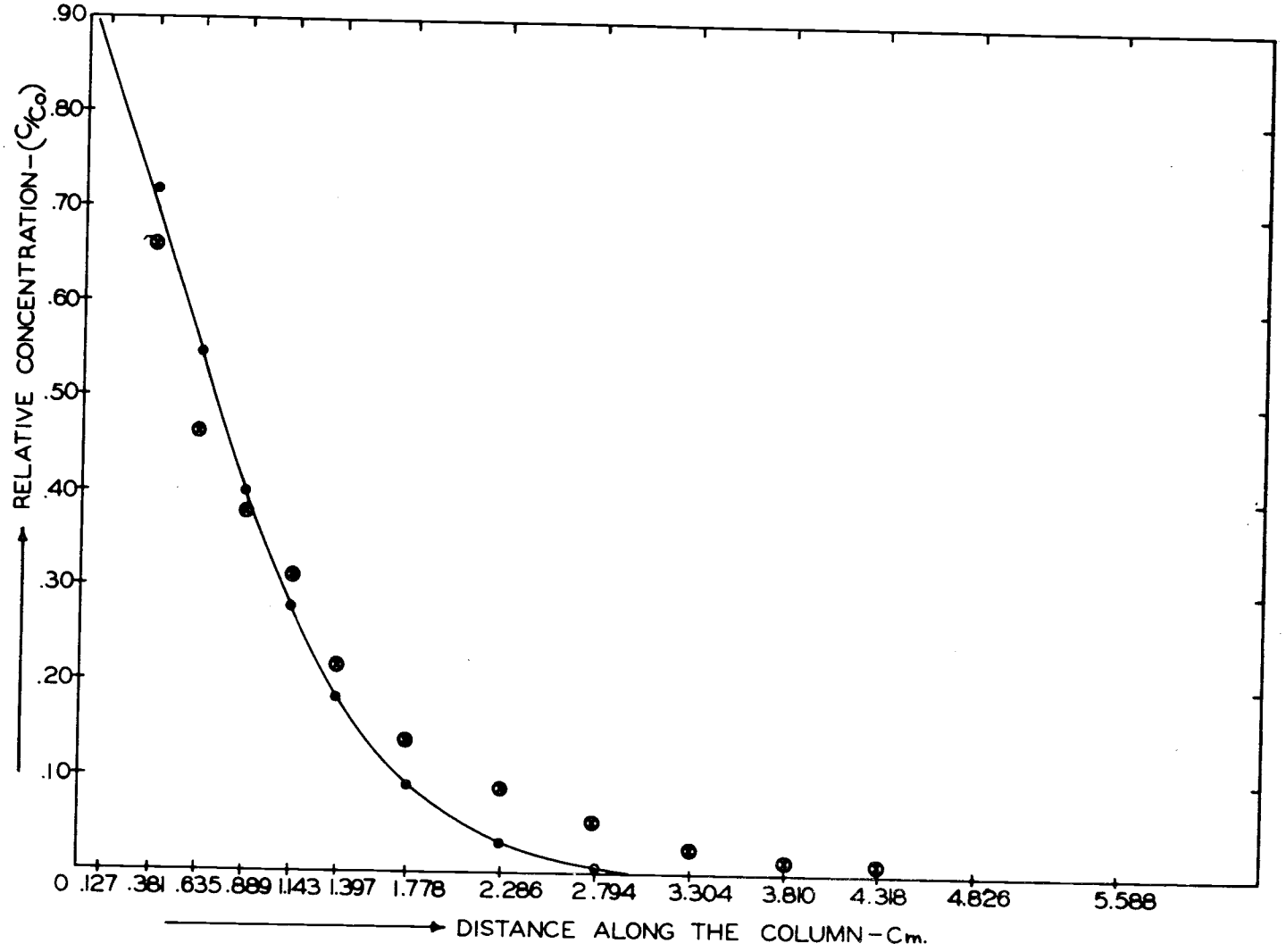

Figure 8. Void concentration of 2,4-D plotted as a function of sample depth (t = 4 days) for 30-40 microns glass beads. ⊗ experimental; ⊙ theoretical.

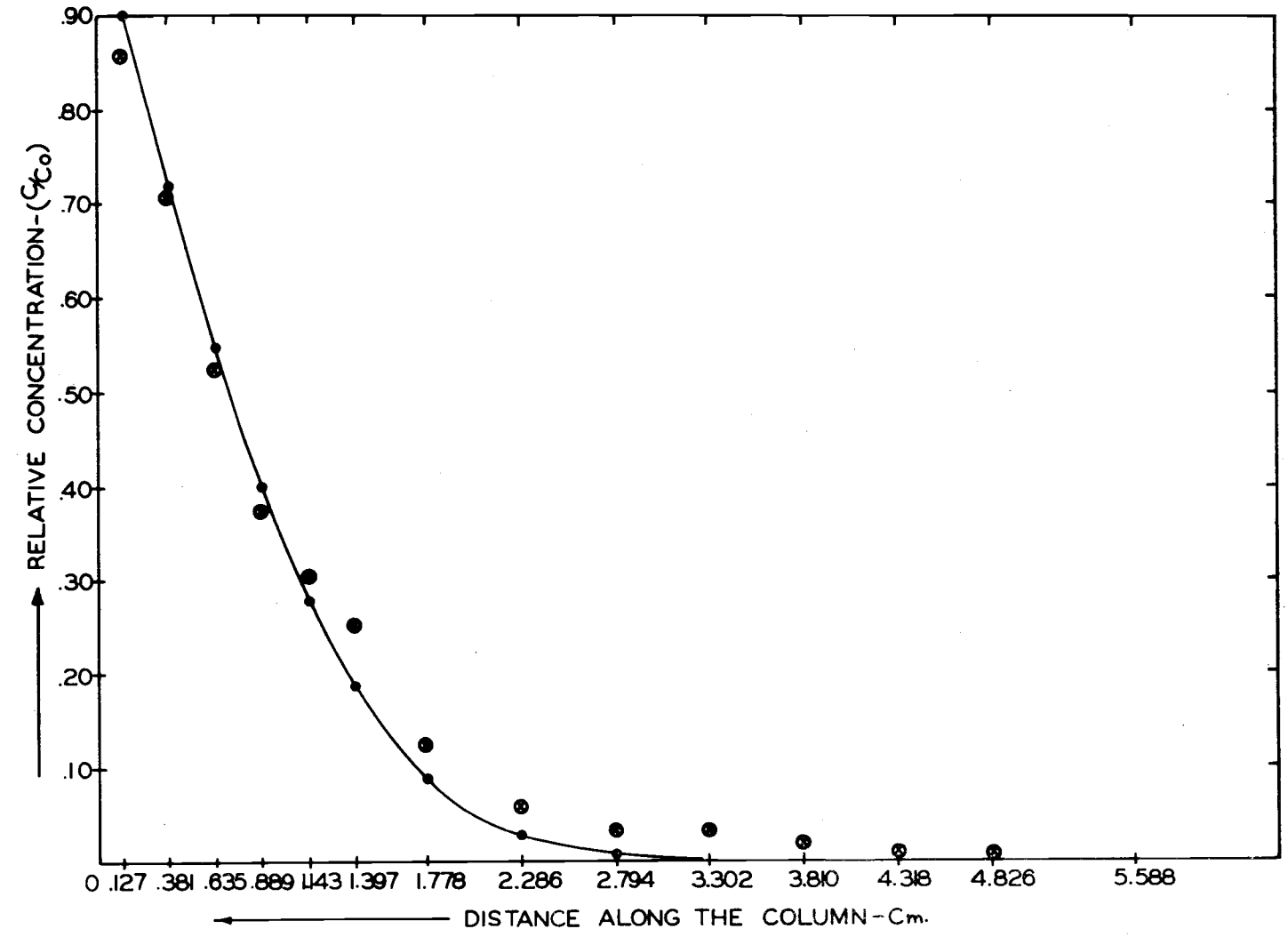

Figure 9. Void concentration of 2,4-D plotted as a function of sample depth (t = 4 days) for 40-50 microns glass beads. ⊗ experimental; ⊙ theoretical.

well within this plotting interval. Thus the values of the diffusion coefficients obtained by the curve fitting technique represent a good estimate of the experimental values. Results are shown in Table 10 for the four fractions used. Pore size distributions of these fractions determined with the mercury intrusion porosimeter were shown earlier in Tables 1 through 4. The contribution of individual pore size increments (A_j) of varying radii was calculated by dividing each pore volume present in a given size interval by the total pore volume. Tables 11, 12, 13, and 14 show the calculated values of A_j for the various pore size increments used. For the particle size fraction <10 microns the pore radius interval centered on 2.20 microns has an A_j value of .605 (Table 11). Table 12 shows that the pore size interval centered on 2.50 microns has an A_j value of .650 (average of two fractions) for the 10-20 microns fraction. For the fraction 30-40 microns the pore size interval centered on 6.80 microns has a value of $A_j = .457$ (Table 13) and for the fraction 40-50 microns $A_j = .619$ was obtained for the interval centered on 8.00 microns. As the particle size increased the radius of pore size increment contributing most also increased. Values of pore radii of these increments for the various glass bead samples used are given in Table 10.

To inspect the relationship between pore radius and measured diffusion coefficients for the various glass bead fractions, diffusion coefficient values were corrected for tortuosity, porosity and effective

porosity. The values of these parameters and the calculations are shown in Table 15. Groton and Frazer (1935) showed that the maximum value of tortuosity is $\sqrt{2} = 1.41$. This value was used to make corrections as shown in column 5 of Table 15. Column 7 was obtained by multiplying column 5 and 6. The values of K obtained in column 7 still do not provide an accurate measure of the diffusion coefficient since not all pores contribute towards the movement of the chemical. Tables 11 through 14 show that about 80% of the pore space for the various fractions was occupied by a very narrow pore size increment. The values of the diffusion coefficient shown in column 7 were further corrected for this with the resulting coefficients shown in column 8. The adjusted diffusion coefficient was plotted as a function of pore radius (Figure 10).

A relationship was obtained between pore radius and K'/K_0 by fitting the standard exponential relation

$$K'/K_0 = 1 - e^{-Ar^2}$$

to the data, where A is a constant. A chi-square test was performed to obtain the value of A. For a minimum value of $\chi^2 = 0.04$, a value of 0.096 was obtained for A. The experimental data points and the fitted curve from above exponential relation fit well within the experimental error. As the pore radius, (r) increases,

the value of the diffusion coefficient increases also and approaches the value of free chemical diffusion coefficient for pore radii greater than 10 microns.

Table 10. Values of the diffusion coefficient (K) for <10, 10-20, 30-40 and 40-50 microns glass beads calculated by Equation (3).

Particle Size (Diameter)	Average Particle Radius	Pore Radius	Porosity (ϵ)	K
microns	microns	microns		cm^2/day
<10	2.50	2.20	.370	0.0633
10-20	7.50	2.50	.370	0.0780
30-40	17.50	6.80	.370	0.1393
40-50	22.50	8.00	.370	0.1399

Table 11. Calculations of fraction of pore volume present in pore size increments for <10 microns glass beads.

Radius	Pore Volume	Range	Average Radius	Each Volume	A_j
microns	%	microns	microns	%	
90.10	100.0				
44.10	98.8	90.10-44.10	67.10	1.20	0.012
29.30	98.8	44.10-29.30	36.70	0.00	0.000
21.95	98.8	29.30-21.95	25.63	0.00	0.000
17.55	98.8	21.95-17.55	19.75	0.00	0.000
14.60	98.8	17.55-14.60	16.08	0.00	0.000
12.55	98.8	14.60-12.55	13.58	0.00	0.000
10.95	97.7	12.55-10.95	11.75	1.10	0.011
9.70	97.7	10.95- 9.70	10.33	0.00	0.000
9.00	96.5	9.70- 9.00	9.35	1.20	0.012
7.45	93.0	9.00- 7.45	8.23	3.50	0.035
6.35	91.9	7.45- 5.35	6.90	1.10	0.011
5.55	89.5	6.35- 5.55	5.95	2.40	0.024
4.40	88.4	5.55- 4.40	4.98	1.10	0.011
2.95	82.6	4.40- 2.95	3.68	5.80	0.058
1.45	22.1	2.95- 1.45	2.20	60.50	0.605
0.80	4.7	1.45- 0.80	1.13	17.40	0.174
0.34	2.3	0.80- 0.34	0.57	2.40	0.024
0.17	1.2	0.34- 0.17	0.26	1.10	0.011
0.09	1.2	0.17- 0.09	0.13	0.00	0.000
0.05	1.2	0.09- 0.05	0.07	0.00	0.000
0.02	0.0	0.05- 0.02	0.04	1.20	0.012

Table 12. Calculations of fraction of pore volume present in pore size increments for 10-20 microns glass beads.

Radius	Pore Volume	Range	Average Radius	Each Volume	A_j
microns	%	microns	microns	%	
90.10	100.0				
44.40	100.0	90.10-44.40	67.25	0.00	0.000
29.45	100.0	44.40-29.45	36.93	0.00	0.000
22.05	100.0	29.45-22.05	25.75	0.00	0.000
17.55	98.7	22.05-17.55	19.80	1.30	0.013
14.60	98.7	17.55-14.60	16.08	0.00	0.000
12.55	98.7	14.60-12.55	13.58	0.00	0.000
10.95	98.7	12.55-10.95	11.75	0.00	0.000
9.75	98.7	10.95- 9.75	10.35	0.00	0.000
9.00	96.2	9.75- 9.00	9.38	2.50	0.025
7.45	94.9	9.00- 7.45	8.23	1.30	0.013
6.40	94.9	7.45- 6.40	6.93	0.00	0.000
5.55	94.9	6.40- 5.55	5.98	0.00	0.000
4.45	93.6	5.55- 4.45	5.00	1.30	0.013
2.90	66.7	4.45- 2.90	3.68	26.90	0.273
1.45	7.7	2.90- 1.45	2.18	59.00	0.598
0.80	2.6	1.45- 0.80	1.13	5.10	0.052
0.34	1.3	0.80- 0.34	0.57	1.30	0.013
0.17	1.3	0.34- 0.17	0.26	0.00	0.000
0.09	1.3	0.17- 0.09	0.13	0.00	0.000
0.05	1.3	0.09- 0.05	0.07	0.00	0.000
0.02	1.3	0.05- 0.02	0.04	0.00	0.000

Table 13. Calculations of fraction of pore volume present in pore size increments for 30-40 microns glass beads.

Radius	Pore Volume	Range	Average Radius	Each Volume	A_j
microns	%	microns	microns	%	
90.10	100.0				
44.40	100.0	90.10-44.40	67.25	0.00	0.000
29.45	100.0	44.40-29.45	36.93	0.00	0.000
22.05	100.0	29.45-22.05	25.75	0.00	0.000
17.60	100.0	22.05-17.60	19.83	0.00	0.000
14.65	100.0	17.60-14.65	16.13	0.00	0.000
12.55	98.3	14.65-12.55	13.60	1.70	0.017
10.95	98.3	12.55-10.95	11.75	0.00	0 000
9.75	98.3	10.95- 9.75	10.35	0.00	0.000
9.00	94.9	9.75- 9.00	9.38	3.40	0.034
7.40	84.7	9.00 7.40	8.20	10.20	0.102
6.20	39.0	7.40- 6.20	6.80	45.70	0.457
5.35	20.3	6.20- 5.35	5.78	18.70	0.187
4.30	10.2	5.35- 4.30	4.83	10.10	0.101
2.90	5.1	4.30- 2.90	3.60	5.10	0.051
1.45	1.7	2.90 1.45	2.18	3.40	0.034
0.80	1.7	1.45- 0.80	1.13	0 00	0.000
0.34	1.7	0.80- 0.34	0.57	0.00	0.000
0.17	1.7	0.34- 0.17	0.26	0.00	0 000
0.09	0.0	0.17 0.09	0.13	1.70	0.017
0.05	0.0	0.09 0.05	0.07	0.00	0.000
0.02	0.0	0.05- 0.02	0.04	0.00	0.000

Table 14. Calculations of fraction of pore volume present in pore size increments for 40-50 microns glass beads.

Radius	Pore Volume	Range	Average Radius	Each Volume	A_j
microns	%	microns	microns	%	
90.10	100.0				
44.10	98.8	90.10-44.10	67.10	1.20	0.012
29.30	98.8	44.10-29.30	36.70	0.00	0.000
21.95	98.8	29.30-21.95	25.63	0.00	0.000
17.55	98.8	21.95-17.55	19.75	0.00	0.000
14.60	98.8	17.55-14.60	16.08	0.00	0.000
12.50	97.6	14.60-12.50	13.55	1.20	0.012
10.95	97.6	12.50-10.95	11.73	0.00	0.000
9.70	97.6	10.95- 9.70	10.33	0.00	0.000
8.95	91.7	9.70- 8.95	9.33	5.90	0.059
7.05	29.8	8.95- 7.05	8.00	61.90	0.619
6.00	15.5	7.05- 6.00	6.53	14.30	0.143
5.25	11.9	6.00- 5.25	5.63	3.60	0.036
4.25	7.1	5.25- 4.25	4.75	4.80	0.048
2.85	3.6	4.25- 2.85	3.55	3.50	0.035
1.45	2.4	2.85- 1.45	2.15	1.20	0.012
0.80	1.2	1.45- 0.80	1.13	1.20	0.012
0.34	1.2	0.80- 0.34	0.57	0.00	0.000
0.17	1.2	0.34- 0.17	0.26	0.00	0.000
0.09	1.2	0.17- 0.09	0.13	0.00	0.000
0.05	1.2	0.09- 0.05	0.07	0.00	0.000
0.02	0.0	0.05- 0.02	0.04	1.20	0.012

Table 15. Calculations of porosity and tortuosity corrections of the diffusion coefficients for the four fractions of glass beads.

Particle Size (Diameter) (1)	Pore Radius (2)	Porosity (3)	$\frac{1}{\text{Porosity}}$ (4)	$\frac{\text{Tortuosity}^*}{\text{Porosity}}$ (5)	$K_{measured}$ (6)	$K_{corrected}$ (7)	$\frac{K_{corrected}}{0.80}$ (K') (8)	$\frac{K'}{K_0}^{**}$ (9)
microns	microns				cm^2/day	cm^2/day	cm^2/day	
<10	2.2	0.37	2.70	3.81	0.063	0.240	0.300	0.44
10-20	2.5	0.37	2.70	3.81	0.078	0.297	0.371	0.54
30-40	6.8	0.37	2.70	3.81	0.139	0.530	0.663	0.97
40.50	8.0	0.37	2.70	3.81	0.140	0.533	0.667	0.98

* Tortuosity correction = 1.41.

** K_0 = 0.683 cm^2/day, measured experimentally.

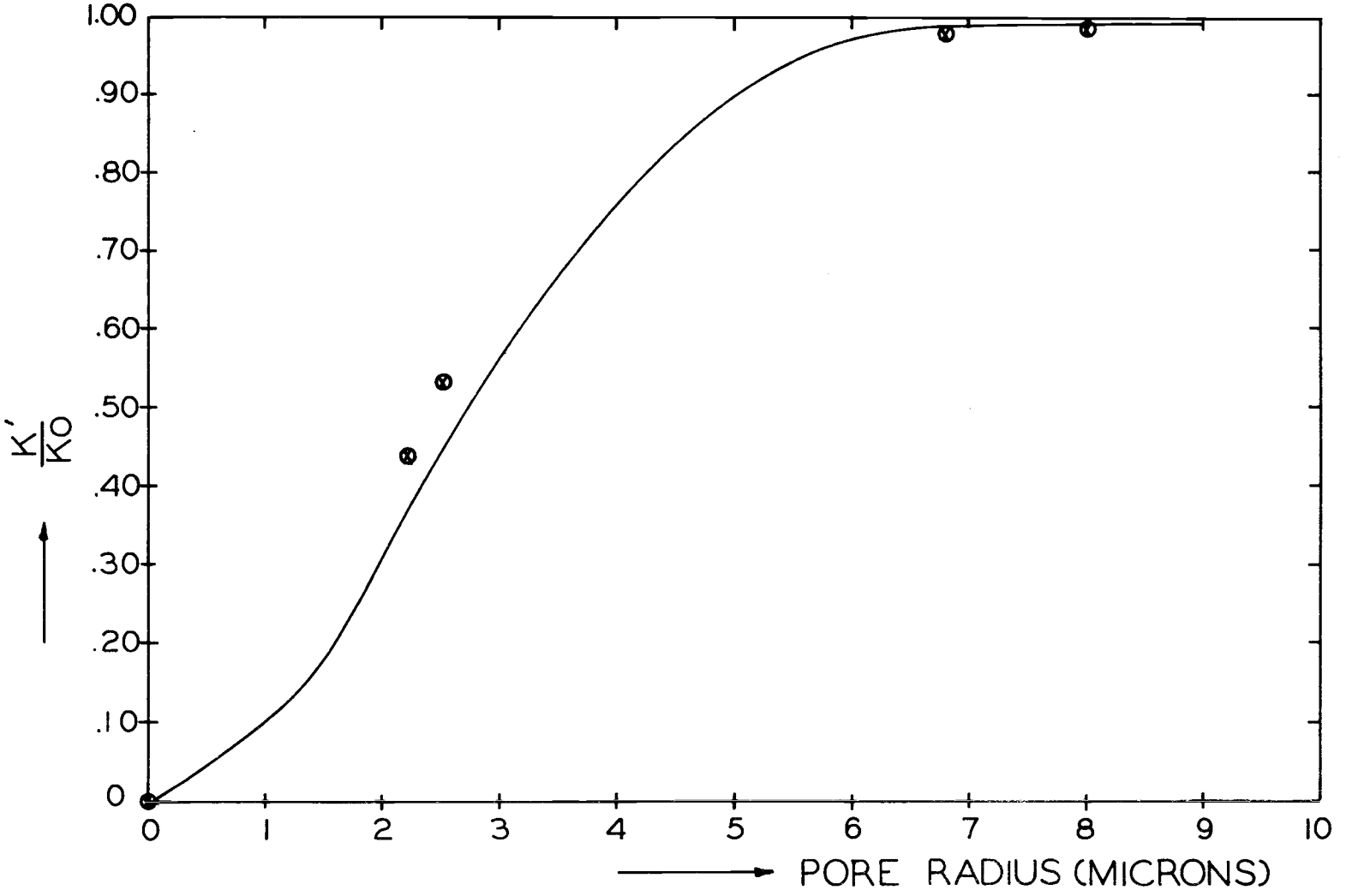

Figure 10. Relationship between pore radius and K'/K_0. Experimental results are shown as open circles. The solid line represents the equation $K'/K_0 = 1 - e^{-0.96r^2}$.

SELF DIFFUSION

Introduction

The movement of ions from soil to plant roots has been a subject of great interest and importance to research workers. The importance of diffusion in the movement of ions to plant roots has been studied and confirmed by many investigators (Husted and Low, 1954; Bouldin, 1961; Lai and Mortland, 1961; Barber, 1962; Olsen et al., 1962; and Graham-Bryce, 1963). A quantitative evaluation of ion movement in soil via diffusion cannot be made without the knowledge of diffusion coefficients of ions in soil.

The ease with which radioisotopes can be determined quantitatively led many research workers to make use of these in their research about diffusion of ions. By labelling an ion, its movement into a solution of the same ion (unlabelled) or a solution of other ions can be followed by radioactive assay. This led to the definition of a self-diffusion coefficient which occurs as an interchange of labelled and unlabelled ions such that no net transfer of charge takes place. Employing this technique many mathematical models were proposed and used to determine self-diffusion coefficients of various ions (Wang and Kennedy, 1950; Wang, 1951, 1952; Wang et al., 1953; Schofield and Graham-Bryce, 1960; Kunze and Kirkham, 1961; Graham-Bryce, 1963; Olsen et al., 1965; Farmer and Jensen, 1970). These models

are summarized in Appendix 3.

Nakayama and Jackson (1963) used agar gel media to determine the self-diffusion coefficient of tritiated water in low concentrations of the gel. The value of the self-diffusion coefficient was obtained by extrapolating the values to infinite dilution of the gel. The same technique was employed by Elgawhary et al. (1970) to determine self-diffusion coefficients of Zn and Zn EDTA.

However in practical applications of diffusion, such as transport of ions to plant roots, one does not deal with self-diffusion but with bulk diffusion. Nye (1966) proposed a relation between self-diffusion and bulk diffusion thereby mentioning that the quantitative determination of self-diffusion coefficients is equally important. To estimate quantitatively the value of the bulk diffusion coefficient for 2,4-D (carbon-14), experiments were conducted to determine self-diffusion coefficients of 2,4-D (carbon-14) by agar gel and diffusion cell methods. Also the self-diffusion coefficient of Ca^{45} was determined using $CaCl_2$. These two different chemicals and methods were used to compare and check the accuracy, reliability and reproducibility of the results.

Measurement by the Agar Method

A transient state system was used to measure the self diffusion coefficient of calcium and 2,4-Dichlorophenoxyacetic acid. Schofield

and Graham-Bryce (1960) described a method and its theoretical basis for measuring self-diffusion coefficients of ions in soils. The principle of the procedure is as follows: two columns of soil having the same concentration of the ion under investigation, but with one column having part of its ions labelled are brought together. Ions will diffuse freely across the face where the two columns were brought together. The amount of diffusion taking place in a given time can be measured by determining the concentration of the labelled ions with respect to distance from the interface. The coefficient of self-diffusion can be calculated from this distribution.

Nakayama and Jackson (1963) determined the self-diffusion coefficient of tritiated water by extrapolating the values of self-diffusion coefficients obtained for various agar concentrations to infinite dilution of zero concentration of the agar. This concept was used in the present investigation.

Chemicals Preparation

The Calcium Chloride solution was prepared by dissolving 1.11 gm of anhydrous Calcium Chloride in one liter of double distilled water. This gave a solution of 0.01 M $CaCl_2$. Then 0.555 gm of anhydrous calcium chloride was weighed and dissolved in 300 ml of double distilled water in a 500 ml volumetric flask. Two ml of labelled Calcium Chloride (calcium - 45) was added. The flask was well shaken and mae up to volume. This gave a solution of

0.01 M $CaCl_2$ (calcium - 45) with an activity of 5000 dpm. The solution of 2,4-Dichlorophenoxyacetic acid was prepared by dissolving 10 mg according to the procedure given in the previous chapter.

Agar media were prepared with ion agar obtained from Colab Laboratories Incorporated, Chicago. Sample columns were made up with the rings described earlier as follows:

7 rings 0.2 in. thick agar and labelled chemical	8 rings 0.1 in. thick	8 rings 0.1 in. thick agar and non-labelled chemical	7 rings 0.2 in. thick

boundary

Scintillation fluid, fluor solution, and sampling tools described earlier were used.

Procedure

The determination of the activity in agar samples by a G.M. thin window counter is not absolute and reproducible because of self-absorption. To overcome this complication, the agar must be transferred to a liquid form so that the activity can be determined by a liquid scintillation counter. Mahin and Lofberg (1966) described a safe procedure to determine carbon-14, sulfur-35 and tritium in blood or tissue samples by the liquid scintillation method. This method was modified to suit the analysis of calcium-45 and carbon-14 contained in the agar. Agar samples were put into the counting vials and 0.2 ml

of perchloric acid was added to each vial followed by the addition of 0.2 ml of hydrogen peroxide. Instead of digesting the samples for 30 minutes in a water bath at 70°C as suggested by Mahim and Lofberg, the vials were heated for 30 minutes in an oven at 50°C. The vials were cooled and 10 ml of fluor solution was added. The samples were refrigerated overnight and then counted by a liquid scintillation counter.

In order to check the reproducibility of this procedure, an experiment was conducted. Vacuum grease was applied on the outside of the sample rings, lucite plug, and on the inside surface of the sample column. The lucite plug was inserted from the top of the column followed by five rings of 0.2 in. height and five rings of 0.1 in. height. The agar solution was prepared by weighing out 0.125 gm of agar which was put into a 250 ml beaker containing 25 ml of 0.01 M Calcium Chloride (calcium-45). It was heated to 90°C with continuous stirring. When the temperature reached 90°C, the beaker was allowed to cool to 55°C. The material was then poured into the sample column. After 24 hours, the sample column was fixed to the stand and the scoop holder was placed in position. Sample rings were raised one by one with the handle on the stand and removed with the scoop. The samples were put into weighed counting vials. The vials were weighed again and the weight of agar was noted. Perchloric acid (0.2 ml) was added to each vial followed by the addition of 0.2 ml of hydrogen peroxide. The samples were heated in an oven for 30

minutes at 50°C. The vials were cooled and 10 ml of fluor solution was added. The samples were refrigerated overnight and then counted by a liquid scintillation counter. The results are tabulated in Table 16. These results indicate that the procedure was satisfactory. The actual experiments were conducted in the same manner with agar solutions of 0.65, 0.75, 0.85, 1.0, 1.1, and 1.25 percent. The agar solutions were heated and poured into the sample column as described above. After solidification of agar, eight rings of 0.1 in. height and then seven rings of 0.2 in. height were inserted into the sample column from the top. The above preparation of agar solution was repeated except that this time 0.01 M Calcium Chloride (calcium-45) was used. The agar solution was poured into the sample column. The system was allowed to remain in contact for 24 hours. After the required period, sampling and counting was done as described above.

The experiment was repeated with 2,4-Dichlorophenoxyacetic acid, only now a total of 16 rings (0.1" height) were used instead of 30 rings, and the contact time was reduced to three hours.

Results and Discussion

Daniels and Alberty (1967) using the term tracer diffusion coefficient for the self-diffusion coefficient gave the following mathematical relation to determine its value:

Table 16. Activity determination of calcium-45 as a function of distance along the column.

Distance From Top	Weight of Vial	Weight of Vial + Agar	Weight of Agar	Activity #1	Activity #2	Mean Activity	Corrected Activity	cpm gm
inches	gm	gm	gm	cp5m*	cp5m*	cpm**	cpm	
0.05	16.4551	17.1943	0.7392	12626	12563	2519	2491	3370
0.15	16.5239	17.2202	0.6963	12953	12924	2588	2560	3677
0.25	16.4984	17.1951	0.6967	11917	11859	2378	2350	3373
0.35	16.5146	17.2352	0.7206	12308	12238	2455	2427	3368
0.45	16.3789	17.0784	0.6995	11713	11678	2339	2311	3304
0.60	16.4997	17.8578	1.3581	22804	22783	4559	4531	3336
0.80	16.5240	17.9306	1.4066	23913	23820	4773	4745	3373
1.00	16.3879	17.7587	1.3708	23111	---	4622	4594	3351
1.20	16.4685	17.8704	1.4019	23637	23576	4721	4693	3348
1.40	16.4576	17.8625	1.4049	23883	23761	4764	4736	3371
		Background		140	142	28		

* Means counts per five minutes.

** Means counts per one minute.

$$D = \frac{uRT}{zF} \qquad (4)$$

where: u is the ionic mobility ($cm^2 volt^{-1} sec^{-1}$), R is the gas constant (ergs $deg^{-1} mole^{-1}$), T is the Kelvin temperature (degree), z is the number of elemental charges, and F is the Faraday number. The relation based on ionic mobilities considering an infinitely dilute solution gives the maximum value of the self-diffusion coefficient. The values of parameters in the equation for calcium are: $u = 61.6 \times 10^{-5}$ $cm^2 volt^{-1} sec^{-1}$, $R = 8.31 \times 10^7$ ergs $deg^{-1} mole^{-1}$, $T = 298°$, $F = 23060.9$ cal $volt^{-1}$ $equivalent^{-1}$, and $z = 2$. Substituting these values in Equation (4), yields $D = 0.787 \times 10^{-5}$ cm^2/sec. This is the theoretical maximum value of the self-diffusion coefficient of calcium-45.

The Self-Diffusion Coefficient of Calcium-45 Using 0.01 M $CaCl_2$. Distributions of calcium-45 from 0.01 M $CaCl_2$ as a function of distance in columns made up of different agar concentrations are shown in Table 17. Equation (5) developed by Porter et al. (1960) and used by Olsen et al. (1965) and Elgawhary, et al. (1970) was used to calculate the self-diffusion coefficient Dp.

$$Dp = \frac{(b+\theta)\pi\ell^2}{t} \left(\frac{q}{q_0}\right)^2 \qquad (5)$$

where: Dp is the porous system self-diffusion coefficient (cm^2/sec), b is the slope of the linear regression between the amount of absorbed

Table 17. Calcium Chloride (calcium-45) distribution as a function of distance along the column in various agar concentrations.

Distance Along the Column	Activity of Ca-45 in Various Agar Concentrations					
	0.5%	0.65%	0.75%	0.85%	1.00%	1.25%
inches	cpm	cpm	cpm	cpm	cpm	cpm
2.10	16436	44385	46790	41921	48515	45640
1.90	43666	41706	46401	42493	42653	44969
1.70	43093	42845	44407	39838	44049	44904
1.50	43169	41894	46139	41820	42851	43925
1.30	43015	42787	45563	40947	43975	44515
1.10	42642	42550	45084	40970	44014	43955
0.90	42209	42615	44239	40555	44395	43469
0.75	21565	21246	23176	18936	20099	20499
0.65	20894	20297	21596	20384	20839	20390
0.55	20159	20455	20620	18275	20282	20165
0.45	19666	17789	21046	18118	18155	19264
0.35	19070	18430	19442	15925	18352	17525
0.25	16545	15813	17177	16061	17023	16410
0.15	15152	15247	15257	13294	14273	13147
0.05	13425	13392	13414	12191	13494	12568
0.05	10354	10668	11679	10408	10180	11025
0.15	10120	9005	9734	7671	8578	8249
0.25	7832	6842	7454	6588	7025	6497
0.35	6032	5648	5479	4679	5103	5021
0.45	4610	3822	4129	3491	3625	2729
0.55	3375	2849	2999	2353	2634	2522
0.65	2220	1911	1908	1501	1740	1617
0.75	1414	1172	1266	1005	1029	1007
0.90	1515	1199	1228	956	1022	978
1.10	529	419	403	301	329	294
1.30	157	132	114	77	82	79
1.50	37	46	27	23	26	20
1.70	18	10	8	5	0	11
1.90	6	9	6	0	0	13
2.10	8	3	0	0	0	3

Ca per cc of soil and the amount of soluble Ca per cc of solution (assumed to be zero), θ is the volumetric moisture content in soil or agar-agar (cm^3/cm^3), t is the time during which two blocks of soil or agar-agar remain in contact (sec), q is the amount of Ca^{45} that diffuses from one block to the other in time t (gr/gr), q_0 is the total amount of Ca^{45} in the system, and ℓ is the length of each block (cm).

Table 18 shows the calculated values of Dp for various agar concentrations. Elgawhary, et al. (1970) extrapolated results of similar measurements for Zn^{65} to zero percent agar to obtain Dp without using a statistical procedure. Moreover, they based this extrapolation on only three points which does not seem to be sufficient to obtain an accurate estimate of the extrapolated values. Also, the interval between zero and one percent agar was much too great to make such an estimate. More observations for agar concentrations less than one percent and at least one point between one and two percent agar could give more reliable results. Though they were able to obtain the value of Dp for Zn^{65} well within the theoretical maximum value, their procedure causes doubt about the accuracy of their reported value.

To avoid this problem, the present study was conducted with concentrations of 0.50, 0.65, 0.75, 0.85, 1.00, and 1.25 percent in the agar solutions. It was found that by increasing the agar

Table 18. Values of Dp for Calcium Chloride (calcium-45) for 0.50, 0.65, 0.75, 0.85, 1.00 and 1.25 percent agar media calculated according to Equation (5).

Concentration of Agar, c	Moisture Content, θ	Activity Present in the Column		Time, t	Length, ℓ	Self-Diffusion Coefficient, Dp
		Lower Half q*	Total q**			
%		cpm	cpm	sec	cm	$cm^2/sec \times 10^5$
0.50	0.9950	48207	478913	86400	5.588	1.1441
0.65	0.9935	43735	485186	86400	5.588	0.9161
0.75	0.9927	46434	516785	86400	5.588	0.9093
0.85	0.9915	39058	460786	86400	5.588	0.8084
1.00	0.9900	41373	494343	86400	5.588	0.7869
1.25	0.9875	40065	491410	86400	5.588	0.7449

* q is the sum of corrected cpm of last 15 rings in Table 17.

** q_0 is the total sum of corrected cpm in Table 17.

concentrations beyond 2.5 percent, the solution solidified before cooling to 55°C and the experiment could not be conducted. The calculated values of Dp plotted as a function of the agar concentration are shown in Figure 11. Various non-linear equations were tried to fit a curve through these data points without satisfactory results. Hall, Wishaw, and Stokes (1953) determined diffusion coefficients of calcium and ammonium chlorides in concentrated aqueous solutions. They plotted the values of D as a function of $\sqrt{c}$, (concentration), and found that at concentrations of less than 0.01 M, Equation (6) best fit the data.

$$Dp = a\, e^{b\sqrt{c}}, \qquad (6)$$

where a and b are constants and c is the agar concentration. This equation was used. The graph obtained is shown in Figure 11 as a solid line. The correlation coefficient (r) was 0.94 and the extrapolated value for the self-diffusion coefficient was $Dp = 2.16 \times 10^{-5}$ cm^2/sec. Comparing this value with the theoretical maximum value for self-diffusion coefficient of calcium-45, $D = 0.787 \times 10^{-5}$ cm^2/sec, it appears quite high. This disagreement between experimental and theoretical values can be attributed to several factors.

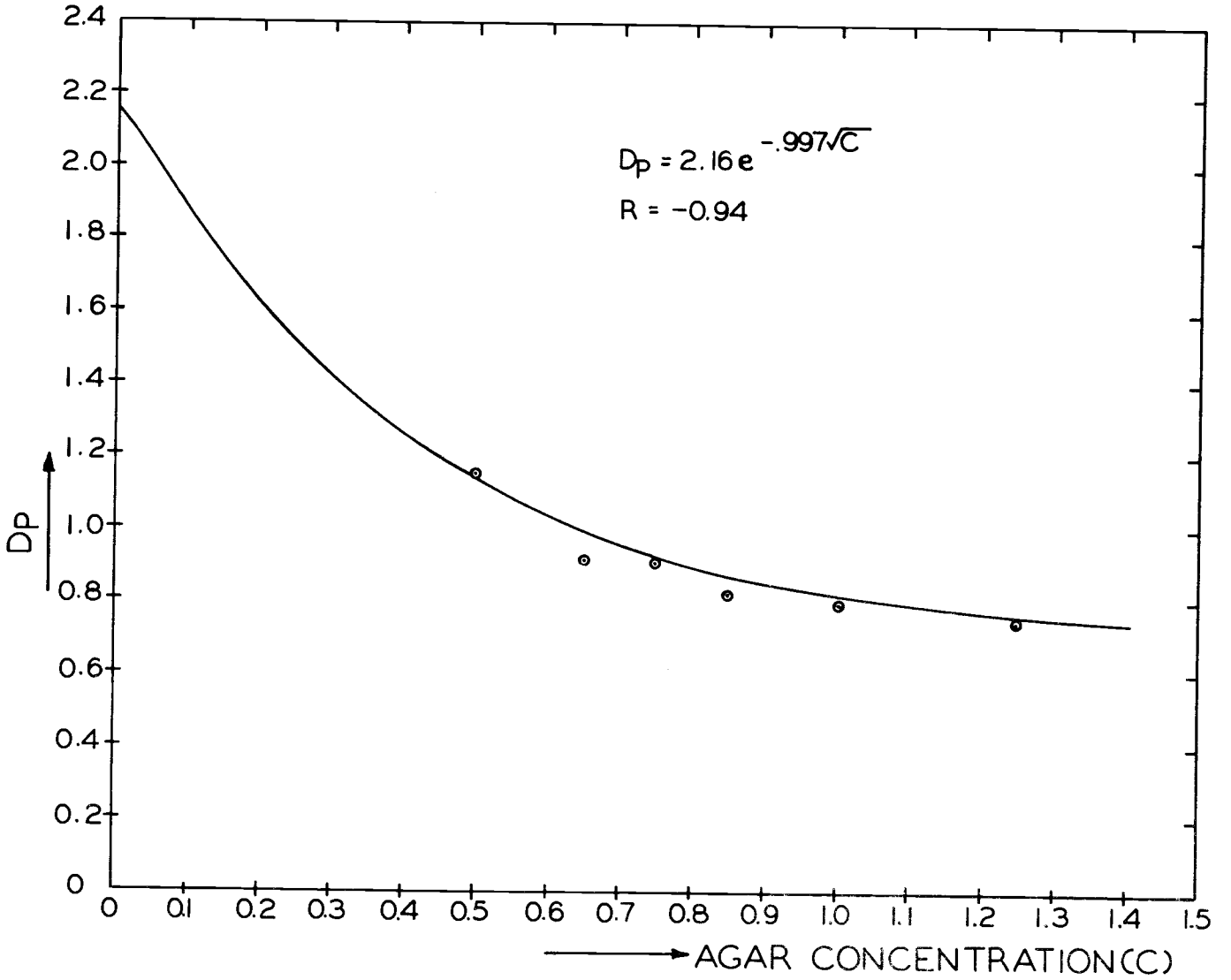

Figure 11. Relationship between Dp and agar concentrations for 0.01 M Calcium Chloride (calcium-45).

Tortuosity. Porter et al. (1960) while developing Equation 5 mentioned that the effect of tortuosity must be considered to calculate the value of the diffusion coefficient. They thus described the term "effective diffusivity" which included a correction for tortuosity and a factor which takes into account ionic interaction and the increased viscosity of water in the porous system. Olsen et al. (1965) combined the factor of tortuosity with the diffusion coefficient in bulk solution and defined a term called porous system self-diffusion coefficient according to Equation (7)

$$Dp = D\alpha\gamma\left(\frac{L}{Le}\right)^2\theta \qquad (7)$$

where Dp is the porous system self diffusion coefficient (cm^2/sec), D is the diffusion coefficient in bulk solution (cm^2/sec), α is a viscosity factor, γ is the negative adsorption term, $\left(\frac{Le}{L}\right)^2$ is the tortuosity correction, and θ is the volumetric moisture content (cm^3/cm^3). Thus, the value of Dp, as obtained by Elgawhary et al. (1970). is not the value of self-diffusion coefficient as claimed by them but an "effective" or "porous system" self-diffusion coefficient.

Agar solution on solidification does provide a tortuous path for the movement of ions. Bloksma (1957) while working with clay gels calculated values of "labyrinth factors" to account for tortuosity. He demonstrated, on the basis of theoretical and experimental considerations, the importance of this factor. The value of the labyrinth

factor varied between 0.41 and 0.49 for montmorillonite and kaolinite gels. Slabaugh[1] mentioned that a tortuosity factor must be included for calculations of self-diffusion coefficients while working with agar media.

The literature does not provide values for tortuosity in agar solutions. The value of 0.39 for soils with a water content corresponding to a suction of one atmosphere and 0.04 for very dry soils was given by Porter et al. (1960).

Capacity Factor. While calculating the value of Dp from Equation (5), the value of the capacity factor (b) was assumed to be zero. This assumption was not experimentally verified. Even if there is a slight adsorption of ions by the agar, the value of b cannot be taken as zero.

Viscosity Gradients. Aladjem et al. (1959) found that the extrapolation to zero percent agar resulted in an appreciable increase in the value of the diffusion coefficient. They found that by decreasing the agar concentration from 5.0% to 0.5% or less, an abrupt discontinuous change in viscosity occurred. Also, during the solidification of the agar, density and viscosity gradients occur.

Considering the above factors, extrapolation to zero percent agar concentration is not expected to yield a reliable estimate of the

---

[1] Personal communication, Dr. W.H. Slabaugh, Colloid Chemist, Oregon State University, Corvallis.

self-diffusion coefficient. To allow for the effect of the factors discussed, correction factors need to be introduced. Assuming a value of 0.35 or less for these factors, the value of Dp gives a value which is less than the theoretical maximum value of the self-diffusion coefficient. Since there is no way to find out the exact value of the correction factor, the agar method does not provide an accurate estimate of the quantitative value of the self-diffusion coefficient.

The Self-Diffusion Coefficient of 2,4-D (Carbon-14). Distribution of carbon-14 from the 2,4-D solution as a function of distance in columns made up of different agar concentrations is shown in Table 19. Equation (5) was used to calculate the values of Dp for different agar concentrations (Table 20). Equation (6) was used to fit a graph (Figure 12) through the data points to get the best fit. A correlation coefficient $r = 0.98$ was obtained. The extrapolated value of Dp was 2.42×10^{-5} cm^2/sec. This value of Dp is quite high compared to the theoretical maximum value. As per above discussion, this value of Dp does not represent the self-diffusion coefficient and to obtain its true value a correction needs to be applied.

Measurement by the Cell Diffusion Method

Anderson and Saddington (1949) proposed a method to determine the self-diffusion coefficient of an ion. Their method involved the immersion of a short capillary tube filled with a solution containing a

Table 19. 2,4-D (carbon-14) distribution as a function of distance along the column in various agar concentrations.

Distance Along the Column	Activity of Carbon-14 in Various Agar Concentrations					
	0.5%	0.6%	0.7%	0.8%	0.9%	1.0%
inches	cpm	cpm	cpm	cpm	cpm	cpm
.75	42219	45885	45794	50382	10940	58950
.65	51326	48522	56178	49124	60984	59296
.55	52474	50632	52420	52426	61423	60958
.45	50498	49517	55284	48937	59043	58963
.35	52269	50167	53033	48068	56679	59573
.25	48513	48224	54454	46262	58059	57650
.15	45993	44139	46470	42390	52789	50119
.05	36216	34447	33591	31861	39844	38711
.05	20352	19845	20589	19833	22688	22408
.15	8894	10485	10588	8446	10656	10111
.25	4689	3602	3533	2755	3494	3052
.35	903	883	936	586	846	765
.45	163	145	194	103	131	121
.55	33	21	48	26	5	12
.65	12	25	31	8	5	3
.75	8	25	16	12	6	6

Table 20. Values of Dp for 2,4-D (carbon-14) for 0.5, 0.6, 0.7, 0.8, 0.9 and 1.0 percent agar media calculated according to Equation (5).

Concentration of Agar, c	Moisture Content, θ	Activity Present in the Column		Time, t	Length, ℓ	Self-Diffusion Coefficient, Dp
		Lower Half q*	Total q**			
%		cpm	cpm	sec	cm	$cm^2/sec \times 10^5$
0.50	0.995	39954	419462	10080	2.032	1.1000
0.60	0.994	35031	406529	10800	2.032	0.8861
0.70	0.993	35935	433159	10800	2.032	0.8204
0.80	0.992	31769	401219	10800	2.032	0.7466
0.90	0.991	37586	477431	10800	2.032	0.7373
1.00	0.990	36472	480692	10800	2.032	0.6842

* q is the sum of corrected cpm of last 8 rings in Table 19

** q_0 is the total sum of corrected cpm in Table 19.

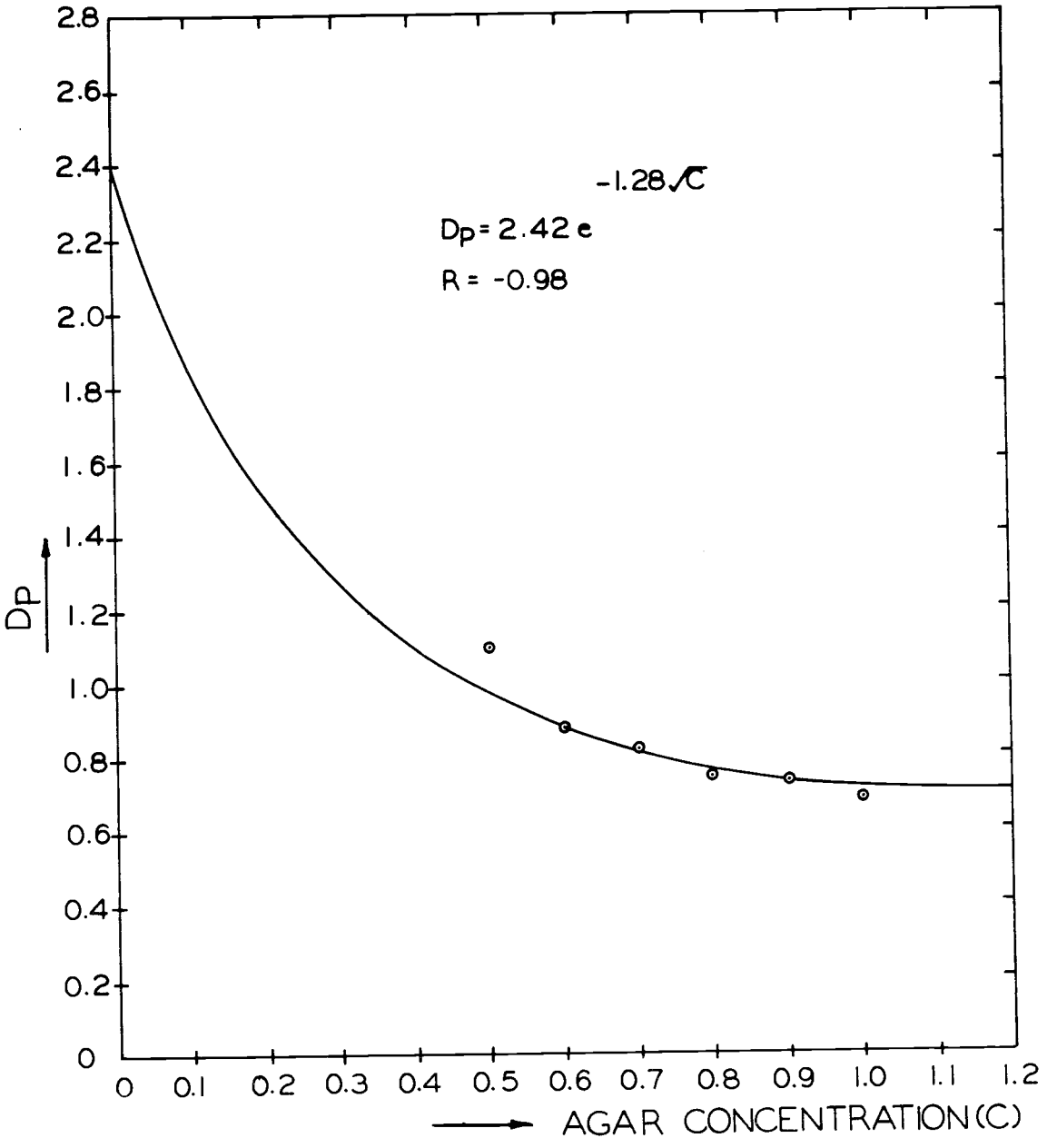

Figure 12. Relationship between Dp and agar concentrations for 2,4-D (carbon-14).

labelled ion in a bath containing a solution of the same concentration, but not labelled, for a known period of time. Wang (1951) modified the procedure by using a circulating bath of one liter. This was done to maintain a negligible concentration of the labelled ion in the outside solution at the interface with the capillary, which was necessary to justify the boundary conditions for calculation of the value of the diffusion coefficient. An experiment was set up based on this procedure to determine the self-diffusion coefficient of calcium by using 0.01 M Calcium Chloride (active and inactive).

Equipment

Cells. Diffusion cells were made of glass tubing with uniform bore. These cells were 2.0 cm long, had an inside diameter of 0.1 cm and an outside diameter of 0.75 cm (Figure 13). A ground glass cover was fused to the bottom. These cells were filled or emptied by means of a micro-liter syringe.

Cell Stand. To hold the cells in position, a cell stand was made of lucite. It was 4.0 cm long, 2.75 cm wide and had a thickness of 1 1/8 cm. A hole of 0.75 cm was drilled in the middle of this stand. A lucite rod, 16 cm long was attached in one of the corners to give support to this stand.

Bath Cover. To avoid evaporation of the solution during the experiment, a cover was made of lucite to fit the solution bath (1

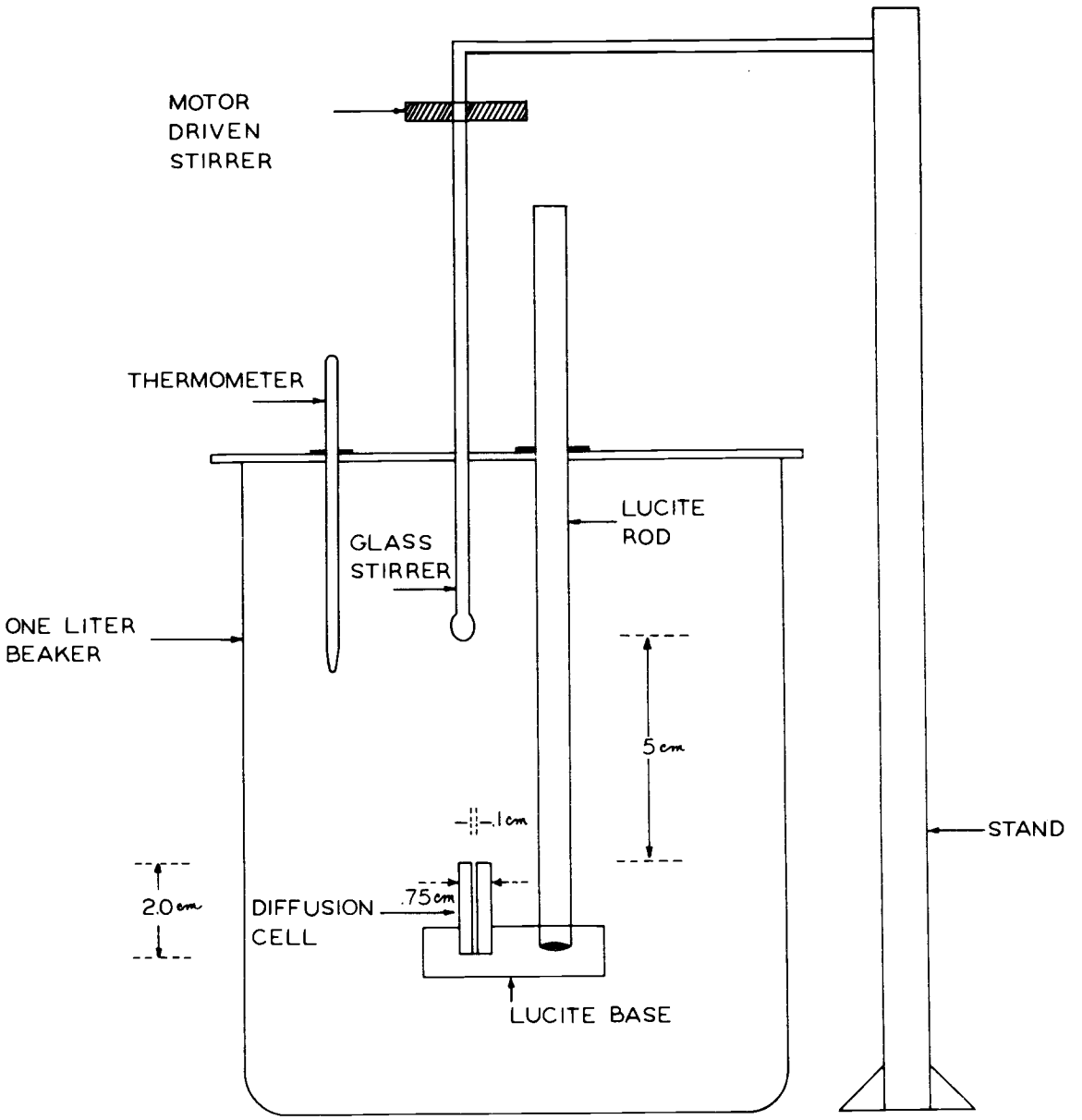

Figure 13. Cell diffusion apparatus.

liter pyrex beaker). This cover had holes to fit a thermometer, lucite rod of the cell stand, and a glass rod stirrer attached to a motor and a control device.

Chemical Preparation

The details of 0.01 M Calcium Chloride solution (active and inactive), scintillation fluid, and fluor solution used in this experiment have been described earlier.

Procedure

The diffusion cell was rinsed four times with 0.01 M Calcium Chloride (calcium-45) and then filled by means of a micro-liter syringe. The cell was fixed in position in the lucite stand with the help of a rubber band. A one liter beaker, serving as the bath, was filled with 0.01 M Calcium Chloride (non-radioactive) solution such that the lower portion of the cell stand touched the solution. It was kept like that for two hours to attain a thermal equilibrium. More 0.01 M Calcium Chloride (non-radioactive) was poured into the beaker till it was full. The diffusion cell and the glass rod stirrer were kept in such a way that the bottom of the cell stand was at a distance of 3.0 cm from the bottom of the beaker and the end of the glass rod stirrer was at a distance of 4.0 cm from the top of the cell. The stirrer was started at a rate of 50 r.p.m. The diffusion was allowed

to take place for 8 hours. At the end of this period the stirrer was stopped and the diffusion cell was taken out of the beaker. The cell was emptied and rinsed with fluor solution into a counting vial. Ten ml of fluor solution was then added. The cell was rinsed again with 0.01 M Calcium Chloride (calcium-45) and then filled. The cell was emptied and rinsed with fluor solution into a counting vial. Ten ml of fluor solution was added. Both the samples were refrigerated overnight and the activity was determined by liquid scintillation counting. The first sample gave the activity after the experiment whereas the second sample gave the initial activity of calcium-45.

Results and Discussion

Self-Diffusion Coefficient Determinations. The Self-Diffusion Coefficient for Calcium-45. The cell diffusion procedure of Anderson and Saddington (1949) as described above was based on Fick's Law. Considering the above mentioned boundary conditions, they outlined

$$\gamma = \frac{8}{\pi^2}\left[e^{-\theta} + \frac{e^{-9\theta}}{9} + \frac{e^{-25\theta}}{25} + \ldots\right] \qquad (8)$$

Where, γ is the fraction of the original amount of radioactive isotope which is left in the capillary cell at the end of the diffusion period, and θ is

$$\theta = \frac{\pi^2 Dt}{4\ell^2}, \tag{9}$$

with D being the self-diffusion coefficient (cm^2/sec), t the time of diffusion (sec), and ℓ the length of the capillary cell (cm). For large value of θ Equation (8) becomes

$$\gamma = \frac{8}{\pi} e^{-\theta} \tag{10}$$

or

$$D = \frac{4\ell^2}{t\pi^2} \ln\left[\frac{8}{\pi\gamma}\right] . \tag{11}$$

Results of the experiments are given in Table 21. Experiments number 1 and 2 were conducted for 3 days whereas the experiment number 3 was conducted for 1 day. The length of the capillary cell was 2.04 cm. The table provides the original amount of radioactive isotope in the cell (c_0) and the amount of radioactive isotope which was left in the capillary cell after the diffusion had taken place (c). These values of c and c_0 along with the values of ℓ and t were substituted in Equation (11) to calculate the value of self-diffusion coefficient for calcium-45. Calculated values of the self-diffusion coefficient obtained for three experiments are also shown in Table 21. An average of three values was taken and the value of self-diffusion coefficient of calcium-45, thus obtained was 0.747×10^{-5} cm^2/sec.

Table 21. Values of Dp for Calcium Chloride (calcium-45) calculated according to Equation (11).

Experiment Number	Time	Activity of Calcium-45 c_0	Activity of Calcium-45 c	Self-Diffusion Coefficient, Dp
	sec	cpm	cpm	$cm^2/sec \times 10^5$
1	259200	2080	487	0.81
2	259200	1902	546	0.67
3	86400	2912	1379	0.76
			Average	0.747

The theoretical maximum value according to Equation (4) is 0.787×10^{-5} cm^2/sec. The literature does not report quantitative values for the self-diffusion coefficient of calcium-45. The value obtained from the experiment which was less than the maximum value, was assumed to be the correct one for the 0.01 M $CaCl_2$ (calcium-45) solution.

The Self-Diffusion Coefficient for 2,4-D (Carbon-14). The values of the original amount of radioactive isotope (c_0) and the amount of radioactive isotope which was left in the capillary cell after the diffusion had taken place (c) of 2,4-D (carbon-14) are shown in Table 22. Three experiments were conducted, each for one day. The values of c, c_0, t, and ℓ were substituted in Equation (11). Table 22 shows the values of the self-diffusion coefficient obtained for three experiments. An average of the three values was taken and the value of the self-diffusion coefficient for 2,4-D (carbon-14), thus obtained was 0.79×10^{-5} cm^2/sec.

Table 22. Values of Dp of 2,4-D (carbon-14) calculated according to Equation (11).

Experiment Number	Time	Activity of Carbon-14 c_0	Activity of Carbon-14 c	Self-Diffusion Coefficient, Dp
	sec	cpm	cpm	$cm^2/sec \times 10^5$
1	86400	3886	2031	0.8212
2	86400	3966	2061	0.8265
3	86444	4055	2217	0.7224
			Average	0.7900

No quantitative value of self-diffusion coefficient of 2,4-D (carbon-14) has been reported in literature. The estimation of self-diffusion coefficient for calcium-45 was well within the maximum value and was assumed to be correct. Since the same procedure was followed to determine self-diffusion coefficient of 2,4-D (carbon-14), its measured value of 0.79×10^{-5} was assumed to be correct.

TRANSPORT OF 2,4-DICHLOROPHENOXYACETIC ACID IN WATER SATURATED NON-SORBING POROUS MEDIA

Introduction

No soil is homogeneous in the sense that all pores are of the same size. A soil can be nearly homogeneous in the microscopic sense if the range of its pore size distribution is extremely narrow. However in the macroscopic sense a soil may be homogeneous, that is, each given element of volume of soil, if chosen large enough, will be identical with every other element of volume in that pore size distributions of these elements will be the same. Soils represent a medium of various interconnecting pores. Several models have been proposed to study the transport of chemicals through such media. Gardner and Brooks (1957) derived equations to describe the leaching of soluble salts from soils. They showed that the flow process itself, rather than diffusion is the important factor in the redistribution of salts in soils. Their assumption, that the flow process is responsible for the diffusion boundary between the soil solution and the leaching water and for the subsequent removal of initially bypassed salt, gave satisfactory agreement between their theoretical equation and laboratory and field data.

Nielsen and Biggar (1961, 1962, 1963) and Biggar and Nielsen (1962, 1963) showed the effects of diffusion coefficient, bulk density and

average intervoid flow rate with miscible displacement studies. Lindstrom and Boersma (1971) improved dispersion equations by considering the actual pore size distribution. Since the previous models considered soil as a uniform medium, an average pore size was assumed to describe the transport of chemicals. Mathematical theory presented by Lindstrom and Boersma (1971) allows for the contribution of each pore present in the soil and thus gives a better description of mass transport of chemicals in water saturated porous media. Experiments were conducted to evaluate the theoretical model presented by Lindstrom and Boersma (1971) for the transport of 2,4-D (carbon-14) in various glass bead columns, representing the porous media.

Materials and Methods

Equipment was designed to study the transport of a chemical through a water saturated non-sorbing porous medium. The method used consisted of introducing chemicals into the pores of a saturated column and displacing the chemical "plug" down the column with water. The apparatus used is shown in Figure 14. It consisted of sample column, sliding plates, and sampling tools. Separate components are shown in Figure 15.

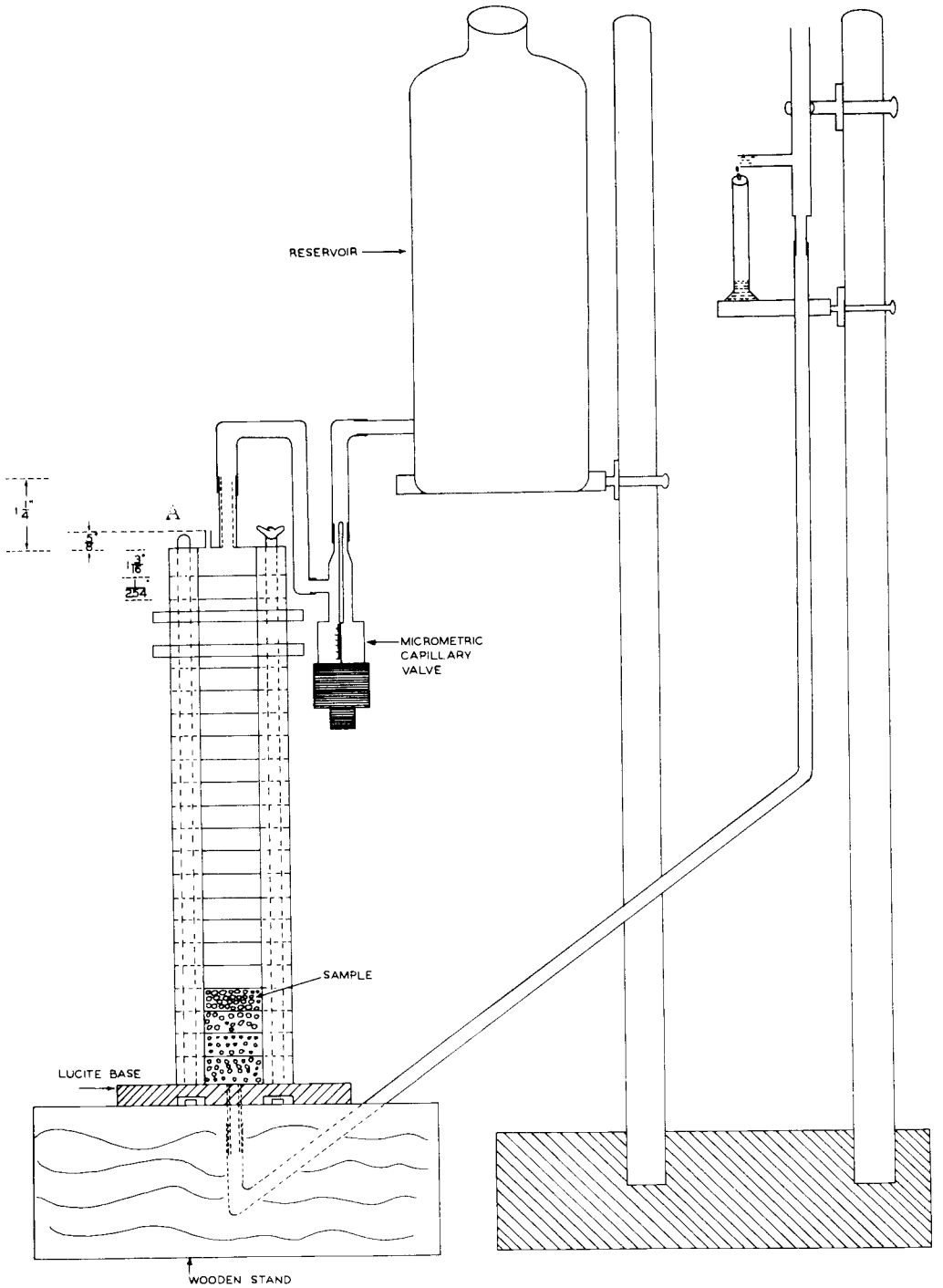

Figure 14. Equipment used to study the transport of chemicals in porous media.

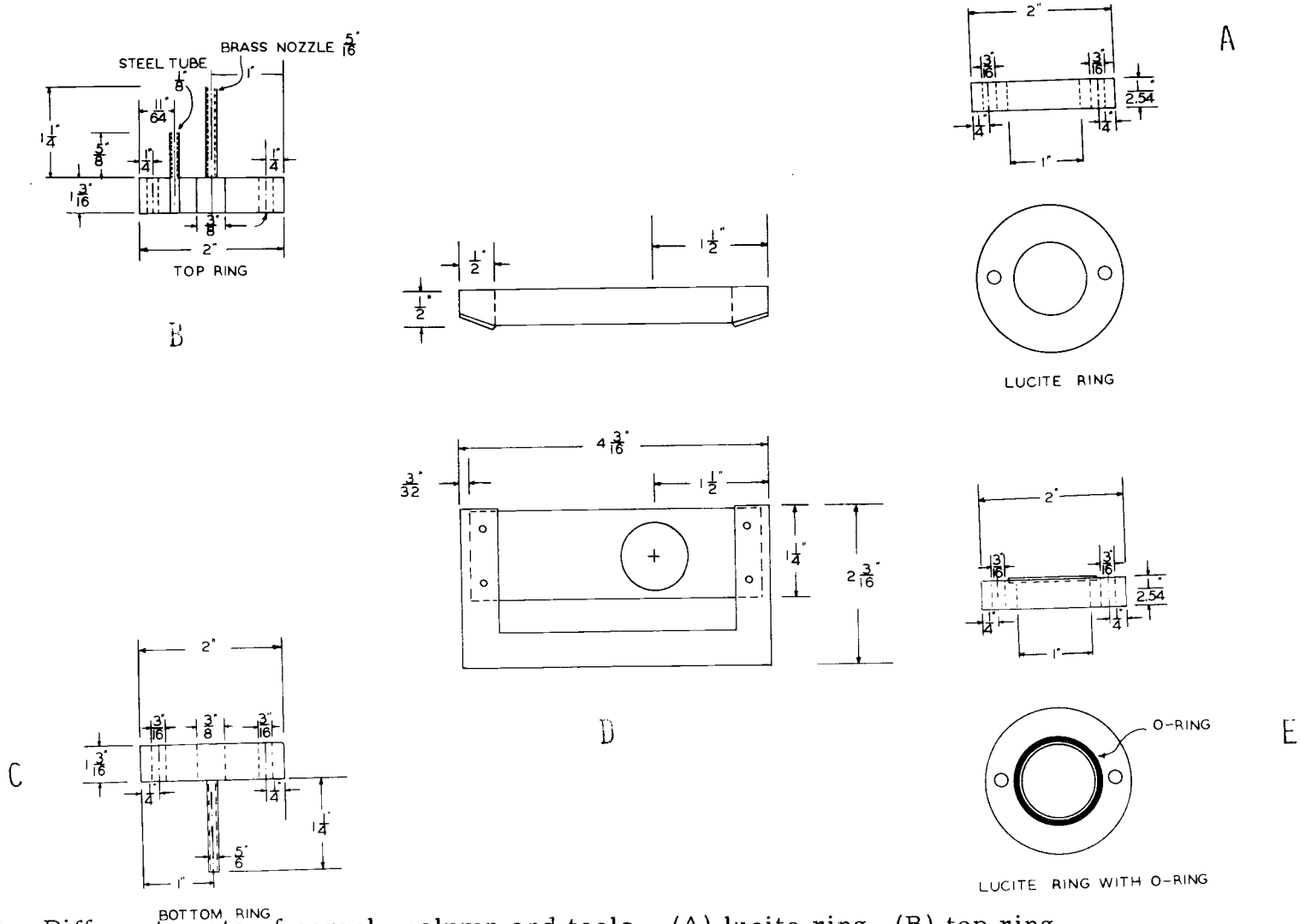

Figure 15. Different parts of sample column and tools. (A) lucite ring, (B) top ring (C) bottom ring, (D) steel plate, (E) lucite ring with 0-ring.

Sample Column

The sample column holding the material making up the porous medium consisted of a stack of lucite rings (Figure 15A) held together by means of two rods. The top and bottom lucite rings had brass nozzles 1 1/4 in. long. The top ring had a stainless steel tube 1/8 in. O.D., and 1/16 in. I.D., 5/8 in. long which served as an air vent (Figure 15B). All rings except those on top (Figure 15B) and bottom (Figure 15C) had a 2.0 in. outside diameter, 1.0 in. inside diameter and a height of 1.0 cm. The top and bottom rings had a 2.0 in. outside diameter, 3/8 in. inside diameter and a height of 13/16 in. Each ring had two holes, 3/16 in. in diameter, 5/32 in. away from the outside of the ring on opposite sides which were drilled to receive the rods holding the assembly together. A base of lucite plate (3.0 in. x 3.0 in. x 1/4 in.) was provided to support the column. A hole, 1/2 in. I.D. was cut in the center of the plate to pass the brass nozzle of the bottom ring of the column through. Two holes (3/16 in. I.D.) were drilled to fit the threaded rods.

Introducing the Sample in the Column

The chemical to be leached down the column was introduced into the pores of the sample contained by one of the top rings.

In order to isolate the material in the lucite ring to be saturated

with the chemical, from the rest of the rings, sliding plates were made. These consisted of a rectangular steel plate (4 1/4 in. x 1 1/4 in.), 1/64 in. thick held in U-shaped clamp (Figure 15D). A gap was provided between the base of the U-shaped clamp and the steel plate so that the plate could slide between the rings with one threaded rod in its way. A circular hole 1.0 in. diameter was cut 9/16 in. away from one of the sides of the clamp. This hole was cut in such a way that by sliding the plate between the rings it could completely close or open the rings.

To obtain adequate seals between the plate and the lucite rings 0-rings were provided. The column had one lucite ring with an 0-ring on each side. These were 1/16 in. thick and were placed 1/40 in. from the inside diameter of the lucite ring (Figure 15E). The lucite rings facing this one each had one 0-ring facing the two just mentioned. The height of the 0-rings in the grooves was so adjusted that by pressing the two, it made a perfect seal and during the experiment, there was no effect on the volume of the sample.

Chemical Preparation

Details of 2,4-Dichlorophenoxyacetic acid (carbon-14) preparation, scintillation fluid and fluor solution were described earlier.

Procedure

Vacuum grease was applied on one of the sides of each lucite ring. The grease was applied to the outside edge of the rings only to avoid sticking of the sample grains to the grease when the column was disassembled. A threaded rod was passed through each hole in the lucite plate and then the bottom ring having a nozzle was put in place. A circular screen of nitex cloth with a pore diameter of 10 μ and 1 3/16 in. diameter was placed on it (Tobler-Ernest, Corporation, New York). Then rings were stacked one by one with greased face down through the threaded rods. Each ring was pressed down by hand after each stacking to make a good seal with the preceding one. Seventeen rings were placed in this manner. The eighteenth ring had an 0-ring which was placed facing up. The stack of rings was then secured by means of wing nuts, and the column was filled with glass beads. After adding about 30 g of the sample it was packed by an electric vibrator to insure uniform packing. A total of about 120 g filled the column. After it was full, the wing nuts were removed. A circular screen similar to the one placed on the bottom was placed over the sample. The top ring with brass nozzle and air vent was then placed on top of the column and the wing nuts were tightened again.

To avoid air pockets in the porous bed, the sample was saturated under vacuum. The top nozzle was connected to a one liter conical

flask which was further connected to a vacuum pump and mercury manometer. The bottom nozzle was connected through a stop cock to a reservoir with double distilled water. The vacuum pump was started with this stop cock and the air vent closed. After 8 hours, the stock cock was opened and the sample was allowed to wet with water. The extra water being released at the top was collected in the conical flask. The sample was saturated in this manner for 1 hour. The column was then removed from the vacuum pump and the top nitex screen was removed. The column along with the tube attached to the bottom nozzle was moved to a constant temperature room. The top nozzle was connected through a micrometric capillary valve to a reservoir containing double distilled water (Figure 14). The bottom tube having a stock cock was connected to a wide glass tube with an outlet projecting on one side. The micrometric capillary valve and the stop cock were opened to allow flow. The leachate was collected in a graduated cylinder. The flow rate was adjusted as per the requirement of the experiment.

Introducing the Chemical

The chemical was to be introduced into the solution contained in one of the lucite rings at the end of the column where the leaching water entered. To assure uniform leaching across the column, two lucite rings were deemed necessary between the nozzle through which

the water entered the column and the ring containing the chemical. These three rings were prepared separately and added to the column after the initial packing.

Vacuum grease was applied on both sides of a sliding plate and on one side of a lucite ring which had 0-rings on both sides. The sliding plate and ring were placed on another ring to give support and then the assembly was secured with threaded rods by means of wing nuts. The sliding plate was so adjusted that it completely closed the bottom of the top ring. Two ml of 2,4-D (carbon-14) was put into the ring which was then filled with the sample. The sample was stirred well by means of a thin wire to remove air pockets, covered with Saran wrap, and kept overnight. Another column was prepared in a similar way except that instead of one ring, two rings were kept above the sliding plate. The ring next to the sliding plate had an 0-ring which was facing it. These two rings were packed and saturated with water and kept overnight.

After adjusting the flow rate in the column, the stop cock and the micrometric capillary valve were closed and the top ring was removed. The ring containing the chemical and the sliding plate was put on top of the column. Next, the two rings containing the water saturated sample were inserted with a sliding plate between these and the one containing the labelled chemical. Top ring and wing nuts were put back in position and the nuts were tightened well to avoid leakage.

The top nozzle was connected to the reservoir as described earlier. The air vent was now plugged. The lower and upper plates were moved in such a way that the hole in the plate coincided with the hole in the column. The stop cock and micrometric capillary valve were opened and the leachate was collected.

After a specified period of time, the stop cock and micrometric capillary valve were closed. The plates were slid back to isolate the original sample ring again. The bottom nozzle was closed and the column was moved to a wooden support with a hole in it. One of the threaded rods was pushed down through this hole. The rings were lifted one by one after applying a gentle horizontal push to separate them from the ring below. A volumetric flask with funnel was brought near the column. The ring was lifted up through the second threaded rod and transferred to the funnel immediately. Though the sample was wet, it was held firmly in the ring and no scoop was needed to separate the rings. Occasionally a scoop was needed to separate the top one or two rings. The contents of the rings were washed with water into a 50 ml volumetric flask and made to volume. The flasks were well shaken and the sample was allowed to settle. One ml of the supernatant was pipetted into a counting vial and the activity was determined as described earlier.

Results and Discussion

Hydrodynamic Flow Velocity

In their paper on mass transport of previously distributed chemicals in porous media, Lindstrom and Boersma (1971) used the standard Hagen-Poiseuille flow law which follows from Newtonian viscous flow theory (their Equation 5, page 193), to estimate the average hydrodynamic flow velocity, v_j. Here the averaging is done over a larger number of pore sizes and the subscript j refers to the jth pore size increment.

In attempting to use this equation to estimate the average hydrodynamic flow velocity in various glass bead-water-chemical systems, values of v_j (Equation 5, page 193, Lindstrom and Boersma, 1971) were calculated for each value of the pressure gradient on the dispersion cell. Values were obtained which were much higher than might logically have been exptected. It was suggested (Lindstrom, private communication)[2] that a non-linear Darcy flow model such as the one presented by Narasimhan and Sra (1969) be tried. Their non-linear flow theory follows from the non-Newtonian visco-inelastic fluid flow theory. Hence, assume for a given pore size increment

---

[2]Dr. F. T. Lindstrom, Research Mathematician, Dept. of Agriculture Chemistry, Oregon State University, Corvallis.

$$Q_j = K_j A_j \left(\frac{\Delta H}{L}\right)^{1/n_j} \qquad (12)$$

where Q_j is the flow rate (cm^3/hr), K_j is the saturated hydraulic conductivity (cm/hr), A_j is the cross sectional area normal to average direction of flow (cm^2), ΔH is the pressure head (cm), L is the length of packed column, j is a subscript making reference to the pore size increment considered, and n is a constant.

It can be seen immediately that if $n_j = 1$ and $K_j \propto r_j^2$, where r_j is the pore radius of the jth pore size fraction, Equation (12) reduces to the Hagen-Poiseuille flow law. Results obtained here indicate that this law may not hold in porous media made up of very fine micron size particles. Evidence in support of a non-Newtonian visco-inelastic theory for water flowing in fine pores and capillaries will be presented. The evidence is based on obtaining the value of n_j according to Equation (13) for each pore size increment j, by a least square fit.

$$\ln Q_j = \ln(K_j A_j) + \frac{1}{n_j} \ln\left(\frac{\Delta H}{L}\right), \qquad (13)$$

Table 23 summarizes hydraulic heads, ΔH, used in the flow experiments for four glass bead size fractions. Table 24 summarizes the results from the least square fit of Equation (13) to these data. In all cases considered L, the length of the packed column was

Table 23. Hydraulic heads, flow rates and size fractions used in the experiments.

< 20 Microns		<30 Microns		28-53 Microns		105-149 Microns		149-210 Microns	
Hydraulic Gradient, ΔH	Flow Rate, Q	Hydraulic Gradient, ΔH	Flow Rate, Q	Hydraulic Gradient ΔH	Flow Rate, Q	Hydraulic Gradient, ΔH	Flow Rate, Q	Hydraulic Gradient, ΔH	Flow Rate, Q
cm	cm^3/hr	cm	cm^3/hr	cm	cm^3/hr	cm	cm^3/hr	cm	cm^3/hr
4.3	8.3	6.2	6.0	4.2	8.1	0.50	36.8	0.80	144.0
8.0	14.6	13.1	11.7	8.0	14.5	0.90	63.2	1.25	223.0
15.3	25.4	25.0	20.8	15.4	25.9	1.60	110.2	2.10	370.0
30.0	45.3	48.3	37.2	31.1	50.2	2.90	195.8	3.35	584.0

18 cm for <30 and 28-53 microns glass beads and 3 cm for the rest of the samples. The correlation coefficient for the least square line was 0.99 or better for each size fraction considered. This lends strong support to the non-Newtonian hypothesis of Narasimhan and Sra (1969).

Table 24. Values of hydraulic conductivity and 1/n for various glass beads as obtained from Equation (13).

Particle Size (Diameter)	Pore Radius, r	ln r	1/n	Hydraulic Conductivity K	ln K
microns	microns			cm/hr	
<20	2.35	0.85	0.871	1.2087	0.1895
<30	4.28	1.45	0.889	3.0576	1.1176
28-53	8.03	2.08	0.909	5.9716	1.7870
105-149	18.36	2.91	0.952	39.6749	3.6807
149-210	31.03	3.44	0.978	103.4581	4.6392

It can be seen in Table 24 that as the pore radius increases the value of 1/n approach 1. This agrees with Narasimhan and Sra (1969), and shows that as the pore radius increases the flow fields undergo a change from non-Newtonian to Newtonian flow fields. Recent data (Wissler, 1971) support this hypothesis.

Hydraulic Conductivity

The saturated conductivity K, was calculated and listed in Table 24 for the five samples used. Its value increases rapidly with increasing pore radius as expected. It is instructive to observe the results of efforts to numerically fit three standard empirical equations giving K as a function of r, the pore radius. These three

empirical forms, with the pertinent numerically fit parameters are listed in Tables 25, 26 and 27.

Table 25. Difference between calculated and measured hydraulic conductivity as determined by model number 1.

Model number 1: $K = \alpha r + \beta r^2$

where $\alpha = 0.2203$

$\beta = 0.1008$

r = correlation coefficient = 0.99

Average Pore Radius, r	Hydraulic Conductivity: Calculated K, Model 1	Hydraulic Conductivity: Measured, K	Difference Between Calculated and Measured Values of K
microns	cm/hr	cm/hr	cm/hr
2.35	1.0744	1.2087	-0.1343
4.28	2.7894	3.0576	-0.2682
8.03	8.2687	5.9716	2.2971
18.36	38.0233	39.6749	-1.6516
31.03	103.8923	103.4581	0.4342

Table 26. Difference between calculated and measured hydraulic conductivity as determined by model number 2.

Model number 2: $K = \alpha e^{\beta r}$

$\alpha = 1.4440$

$\beta = 0.1495$

r = correlation coefficient = 0.97

Average Pore Radius, r	Hydraulic Conductivity: Calculated K, Model 2	Hydraulic Conductivity: Measured, K	Difference Between Calculated and Measured Values of K
microns	cm/hr	cm/hr	cm/hr
2.35	2.0518	1.2087	0.8431
4.28	2.7381	3.0576	-0.3195
8.03	4.7965	5.9716	-1.1751
18.36	22.4709	39.6749	-17.2040
31.03	149.3638	103.4581	45.9057

Table 27. Difference between calculated and measured hydraulic conductivity as determined by model number 3.

Model number 3: $K = \alpha^{\beta r}$

where $\alpha = 1.6198$

$\beta = 1.0899$

r = correlation coefficient = 0.81

Average Pore Radius, r	Hydraulic Conductivity Calculated, K Model 3	Measured, K	Difference Between Calculated and Measured Values of K
2.35	1.8048	1.2087	0.5961
4.28	2.0081	3.0576	-1.0495
8.03	2.6193	5.9716	-3.3523
18.36	10.4164	39.6749	-29.2585
31.03	1070.6819	103.4581	967.2238

The model shown in Table 25 deserves special attention because it contains as a limiting case (for large r) the Hagen-Poiseuille saturated conductivity. Figure 16 shows a log-log plot of the conductivity vs pore radius. For small values of r the slope is almost 1, i.e., $K \propto r$ whereas, for large r values the slope is about 2, i.e., $K \propto r^2$. The empirical form stated in Table 25 was based on this observation. Table 26 compares the experimental values of K with those computed from the naturally occurring exponential function. Table 27 compares the values of K with the Gompertz empirical form (Davis, 1962). Correlation coefficients for models 1, 2 and 3 were 0.99, 0.97 and 0.81 respectively. Model numbers 1 and 2 thus give a better estimate of hydraulic conductivity. Model number 1 provides a case of large pore radius and can be considered as a better

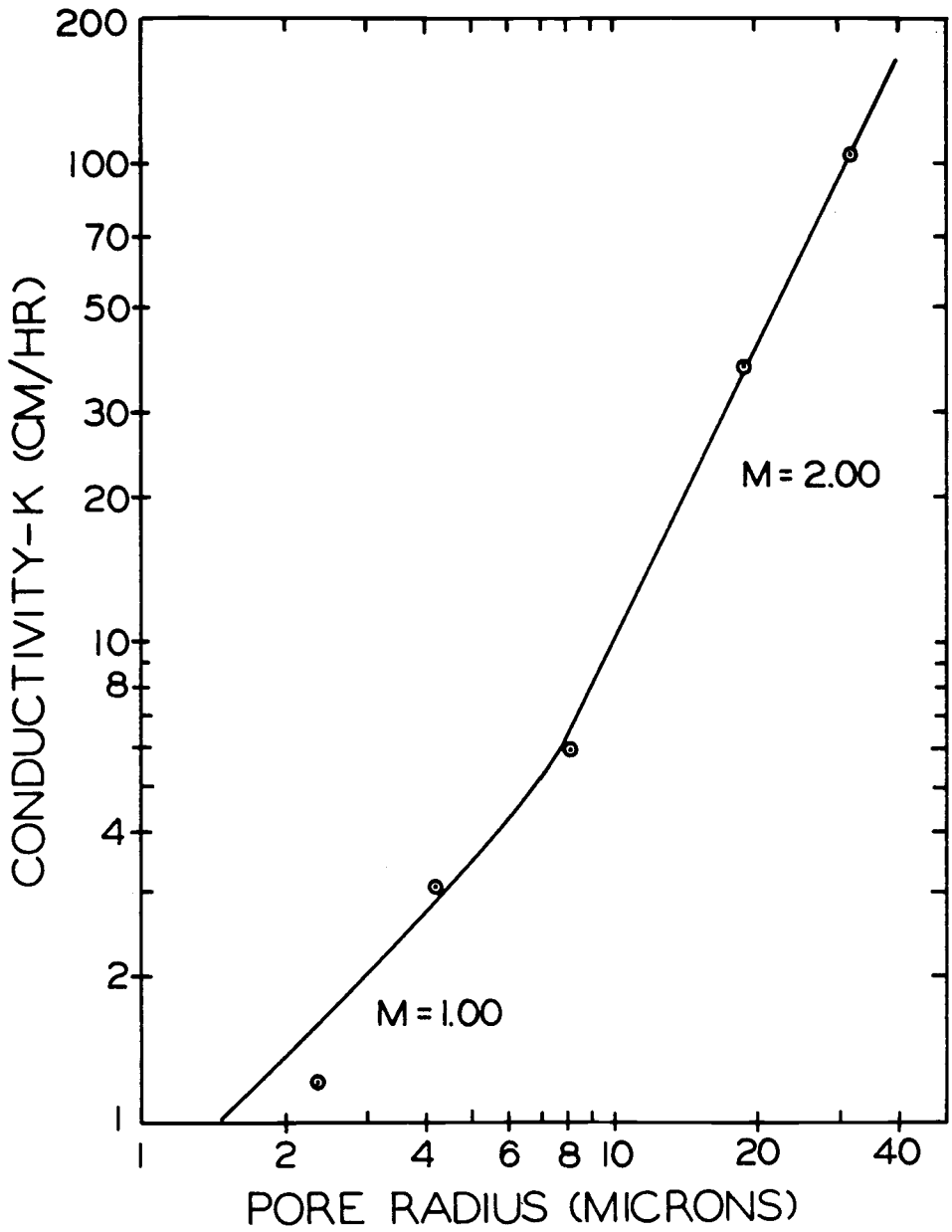

Figure 16. Log-log plot of pore radius and experimentally measured hydraulic conductivity.

model as compared to the other two models.

Relative Contribution of Various Pore Sizes

The pore size distributions of the glass bead fractions <30, 28-53, 105-149 and 149-210 microns are shown in Tables 5 through 8. The volumes of each pore fraction in small pore size increments was calculated for all glass bead fractions and are shown in Tables 28 through 31. The contribution of each pore was obtained by taking the difference of pore volume of two successive pore fractions and the fractional volume of each pore size increment (A_j) was calculated by dividing each pore volume by the total pore volume. Table 28 shows that for the fraction <30 microns, 47 percent of the pore volume is occupied by pores of radius 4.95 microns and 32 percent of the pore volume is occupied by pores of radius 3.62 microns. In the fraction 28-53 microns, 84 percent of the pore volume is occupied by pores of radius 8.03 microns (Table 29). Table 30 shows that for the fraction 105-149 microns, 80 percent of the pore volume is occupied by pores of radius 18.36 microns whereas for the fraction 149-210 microns, 71 percent of the pore volume is occupied by pores of radius 31.03 microns (Table 31). In each fraction of glass beads one pore size increment occupies most of the total pore volume except in the case of the fraction <30 microns where two fractions occupy 47 and 32 percent respectively of the total pore volume. In these media only

Table 28. Calculations of pore volume present in pore size increments for <30 microns glass beads.

Radius	Pore Volume	Range	Average Radius	Each Volume	Fraction of Each Volume, A_j
microns	%	microns	microns	%	
90.10	100.0				
43.51	94.91	90.10-43.51	66.81	5.09	.0509
28.81	91.53	43.51-28.81	36.16	3.38	.0338
21.59	89.83	28.81-21.59	25.20	1.70	.0170
17.33	89.83	21.59-17.33	19.46	0.00	.0000
14.14	89.83	17.33-14.14	15.74	0.00	.0000
12.41	89.83	14.14-12.41	13.28	0.00	.0000
10.87	89.83	12.41-10.87	11.64	0.00	.0000
9.67	89.83	10.87- 9.67	10.27	0.00	.0000
8.96	88.14	9.67- 8.96	9.32	1.69	.0169
7.44	88.14	8.96- 7.44	8.20	0.00	.0000
6.36	88.14	7.44- 6.36	6.90	0.00	.0000
5.54	86.44	6.36- 5.54	5.95	1.70	.0170
4.35	38.98	5.54- 4.35	4.95	47.46	.4747
2.88	6.78	4.35- 2.88	3.62	32.18	.3219
1.45	1.69	2.88- 1.45	2.17	5.09	.0509
.79	1.69	1.45- .79	1.12	0.00	.0000
.34	1.69	.79- .34	0.57	0.00	.0000
.17	0.00	.34- .17	0.26	1.69	.0169
.09	0.00	.17- .09	0.13	0.00	.0000
.04	0.00	.09- .04	0.07	0.00	.0000
.02	0.00	.04- .02	0.03	0.00	.0000

Table 29. Calculations of pore volume present in pore size increments for 28-53 microns glass beads.

Radius	Pore Volume	Range	Average Radius	Each Volume	Fraction of Each Volume, A_j
microns	%	microns	microns	%	
90.10	100.0				
44.40	100.0	90.10-44.40	67.25	0.00	.0000
29.45	100.0	44.40-29.45	36.93	0.00	.0000
22.04	100.0	29.45 22.04	25.75	0.00	.0000
17.60	100.0	22.04-17.60	19.82	0.00	.0000
14.64	99.25	17.60-14.64	16.12	0.75	.0075
12.54	99.25	14.64-12.54	13.59	0.00	.0000
10.97	99.25	12.54-10.97	11.76	0.00	.0000
9.74	98.50	10.97- 9.74	10.34	0.75	.0075
9.02	97.01	9.74- 9.02	9.38	1.49	.0149
7.04	13.43	9.02- 7.04	8.03	83.58	.8358
6.05	8.96	7.04- 6.05	6.55	4.47	.0447
5.31	7.46	6.05- 5.31	5.68	1.50	.0150
4.77	4.48	5.31- 4.77	5.04	2.98	.0298
2.87	2.99	4.77- 2.87	3.82	1.49	.0149
1.45	1.49	2.87- 1.45	2.16	1.50	.0150
0.79	0.00	1.45 0.79	0.76	1.49	.0149
0.34	0.00	0.79- 0.34	0.57	0.00	.0000
0.17	0.00	0.34- 0.17	0.26	0.00	.0000
0.09	0.00	0.17- 0.09	0.13	0.00	.0000
0.04	0.00	0.09- 0.04	0.07	0.00	.0000
0.02	0.00	0.04 0.02	0.03	0.00	.0000

Table 30. Calculations of pore volume present in pore size increments for 105-149 microns glass beads.

Radius	Pore Volume	Range	Average Radius	Each Volume	Fraction of Each Volume, A_j
microns	%	microns	microns	%	
90.11	100.0				
43.80	97.30	90.11 43.80	66.96	2.70	.0270
29.06	95.95	43.80-29.06	36.43	1.35	.0135
21.68	93.24	29.06-21.68	25.37	2.71	.0271
15.04	13.51	21.68-15.04	18.36	79.73	.7974
12.74	8.11	15.04-12.74	13.89	5.40	.0540
11.10	6.75	12.74-11.10	11.92	1.36	.0136
9.82	4.05	11.10- 9.82	10.46	2.70	.0270
8.83	4.05	9.82- 8.83	9.33	0.00	.0000
8.25	4.05	8.83- 8.25	8.54	0.00	.0000
6.93	2.70	8.25- 6.93	7.59	1.35	.0135
5.98	2.70	6.93- 5.98	6.46	0.00	.0000
5.26	1.35	5.98- 5.26	5.62	1.35	.0135
4.24	1.35	5.26- 4.24	4.75	0.00	.0000
2.86	1.35	4.24- 2.86	3.55	0.00	.0000
1.45	1.35	2.86- 1.45	2.16	0.00	.0000
0.79	1.35	1.45- 0.79	1.12	0.00	.0000
0.34	1.35	0.79- 0.34	0.57	0.00	.0000
0.17	1.35	0.34- 0.17	0.26	0.00	.0000
0.09	1.35	0.17- 0.09	0.13	0.00	.0000
0.04	1.35	0.09- 0.04	0.07	0.00	.0000
0.02	0.00	0.04 0.02	0.03	1.35	.0135

Table 31. Calculations of pore volume present in pore size increments for 149-210 microns glass beads.

Radius	Pore Volume	Range	Average Radius	Each Volume	Fraction of Each Volume, A_i
microns	%	microns	microns	%	
91.10	100.0				
39.55	96.38	91.10-39.55	65.33	3.62	.0362
22.50	25.30	39.55-22.50	31.03	71.08	.7108
17.75	13.25	22.50-17.75	20.13	12.05	.1205
14.65	9.64	17.75-14.65	16.20	3.61	.0361
12.50	7.23	14.65-12.50	13.58	2.41	.0241
10.95	6.02	12.50-10.95	11.73	1.21	.0121
9.70	6.02	10.95- 9.70	10.33	0.00	.0000
8.75	4.82	9.70 8.75	9.23	1.20	.0120
8.15	3.61	8.75- 8.15	8.45	1.21	.0121
6.85	2.41	8.15- 6.85	7.50	1.20	.0120
5.95	2.41	6.85- 5.95	6.40	0.00	.0000
5.25	2.41	5.95- 5.25	5.60	0.00	.0000
4.20	2.41	5.25- 4.20	4.73	0.00	.0000
2.85	2.41	4.20- 2.85	3.53	0.00	.0000
1.45	1.21	2.85- 1.45	2.15	1.20	.0120
0.80	1.21	1.45- 0.80	1.13	0.00	.0000
0.30	1.21	0.80- 0.30	0.55	0.00	.0000
0.15	1.21	0.30- 0.15	0.23	0.00	.0000
0.09	1.21	0.15 0.09	0.12	0.00	.0000
0.04	1.21	0.09- 0.04	0.07	0.00	.0000
0.02	0.00	0.04- 0.02	0.03	1.21	.0121

one pore size increment contributed most of the flow path.

Dispersion Profiles

Results of the dispersion experiments are shown in Figures 17, 18, 19 and 20. These experiments were carried out to evaluate models proposed by Lindstrom and Boersma (1971) for dispersion in soils. These were based on allowing for the contributions of each pore size increment present in the medium. Since only one pore size increment occupied most of the pore space in the glass bead porous media it was decided to base the calculations of flow rate and flow velocity on the modified Darcy equation established previously.

$$Q = KA\left(\frac{\Delta H}{L}\right)^{1/n} \tag{14}$$

and

$$v = \frac{Q}{\epsilon A} \tag{15}$$

where ϵ is the porosity and $\epsilon = .37$ (Table 32). The dispersion models proposed by Lindstrom et al. (1967) and Lindstrom and Boersma (1971) were modified accordingly to calculate the theoretical dispersion profiles. Details of the theory and the computer analysis are given in Appendix 4. Values of the parameters used to generate the theoretical curves are shown in Table 32. Values of the dispersion coefficients D were determined as shown in Appendix 4.

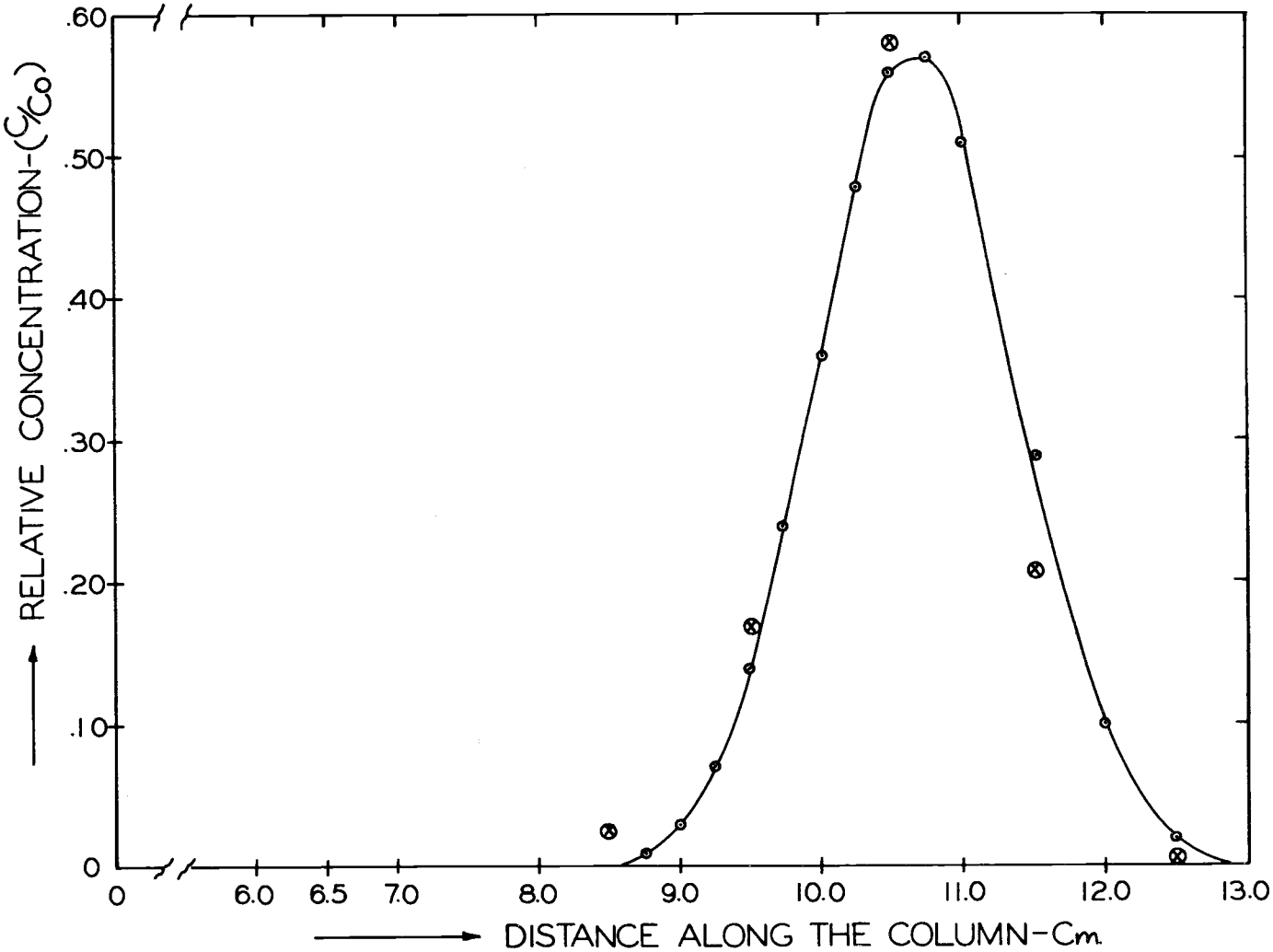

Figure 17. Experimental and theoretical distribution of 2,4-D (carbon-14) in water saturated glass beads (<30 microns) as a function of distance along the column.
⊗ experimental; ⊙ theoretical.

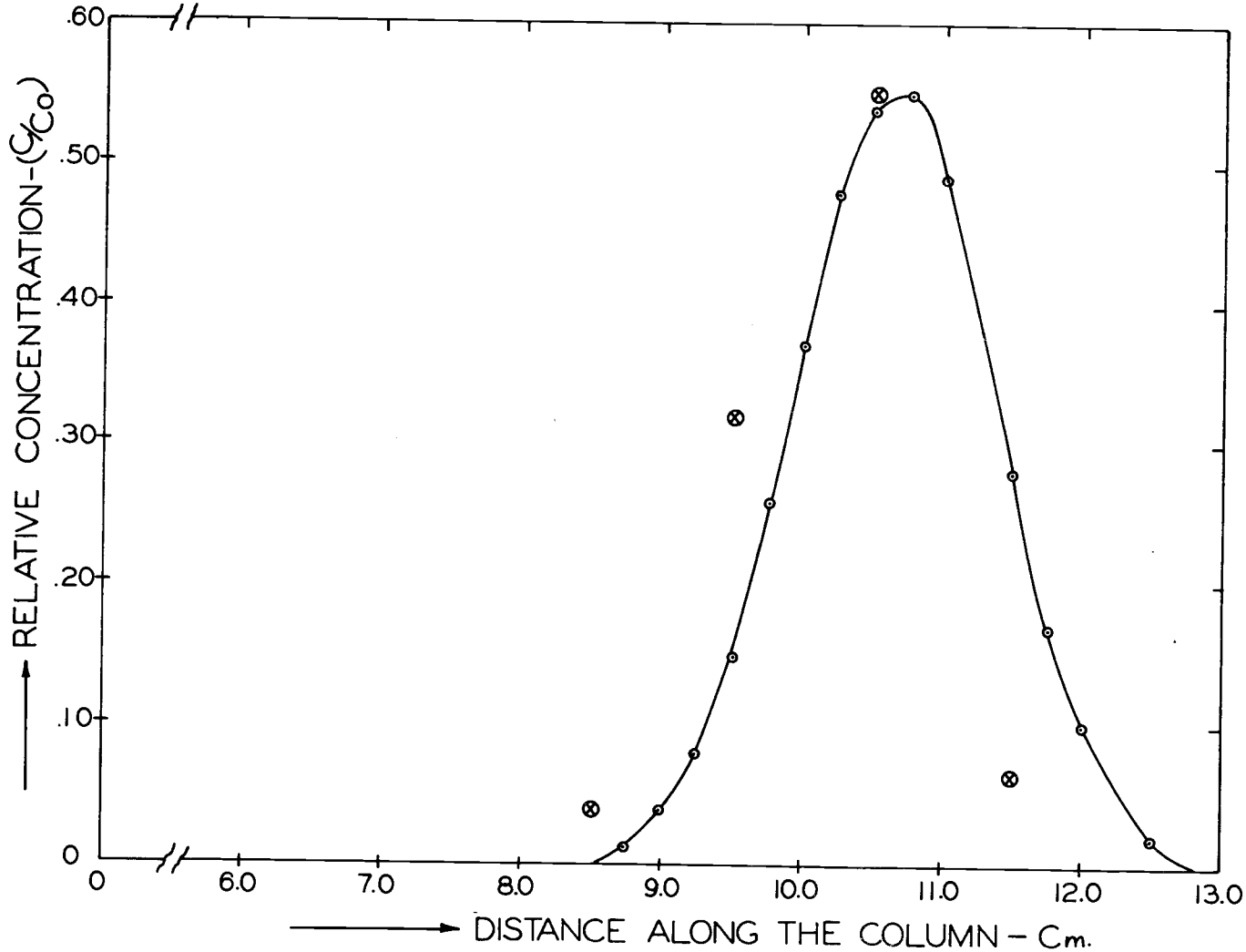

Figure 18. Experimental and theoretical distribution of 2,4-D (carbon-14) in water saturated glass beads (28-53 microns) as a function of distance along the column.
⊗ experimental; ⊙ theoretical.

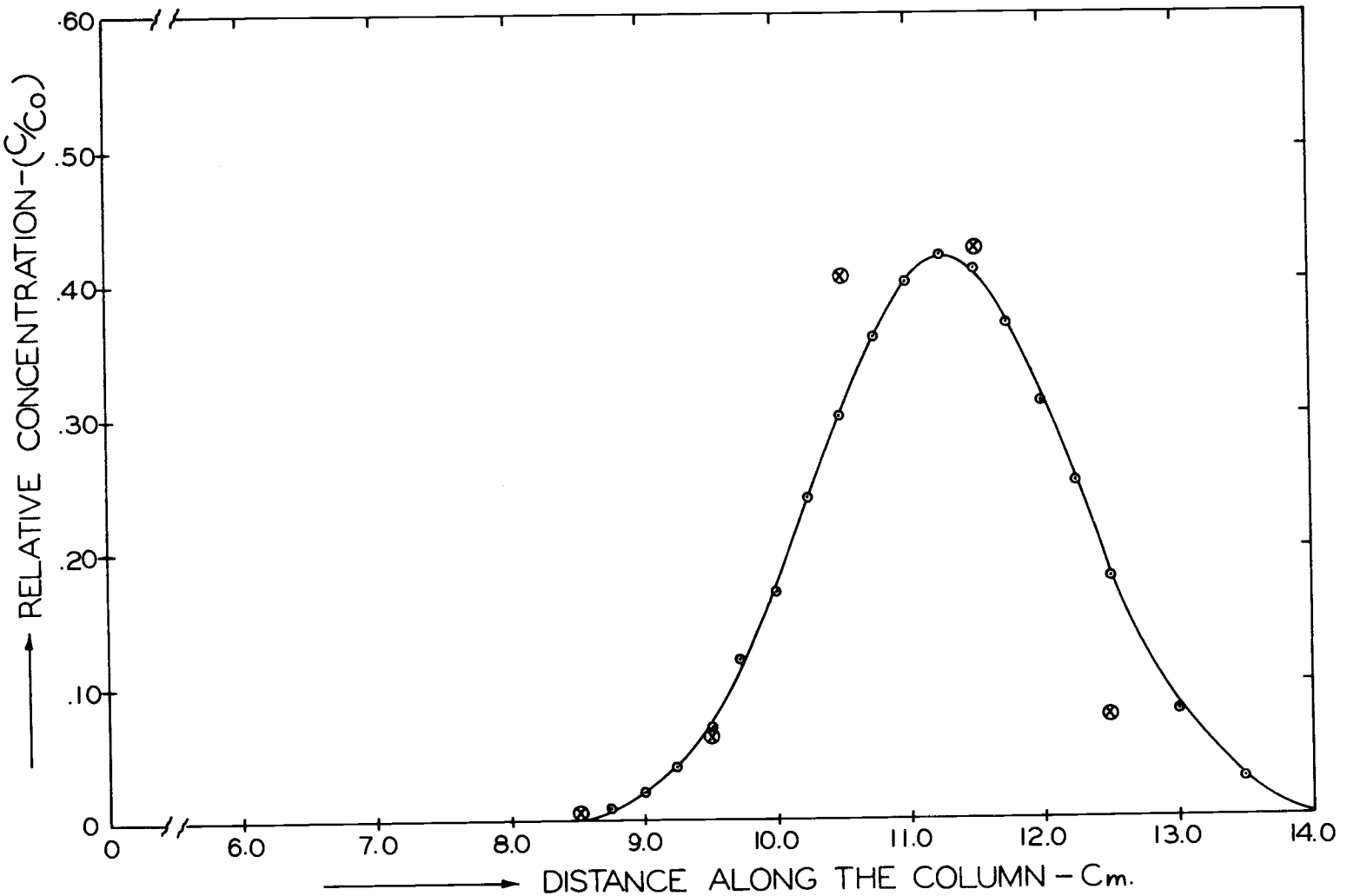

Figure 19. Experimental and theoretical distribution of 2,4-D (carbon-14) in water saturated glass beads (105-149 microns) as a function of distance along the column.
⊗ experimental; ⊙ theoretical.

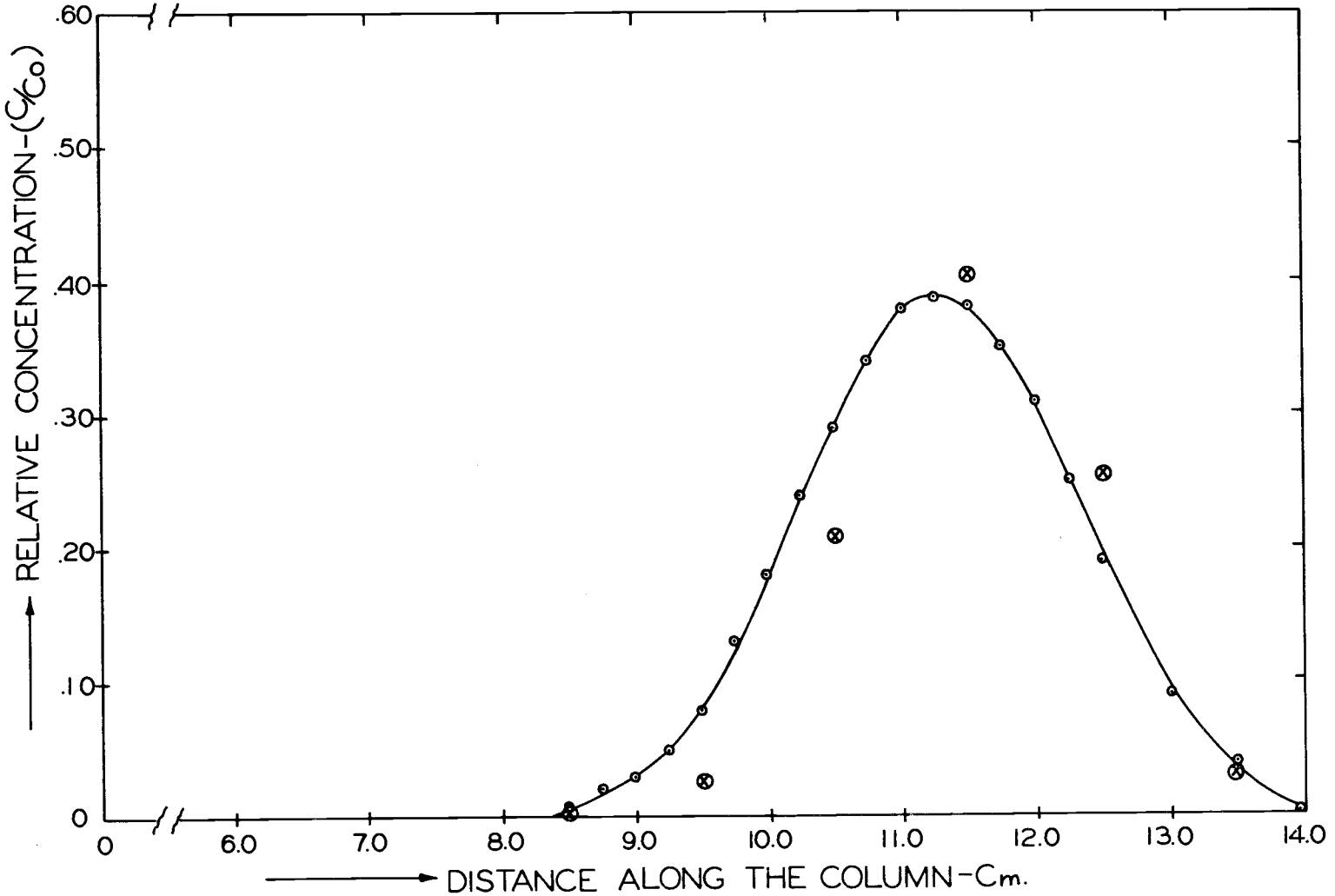

Figure 20. Experimental and theoretical distribution of 2,4-D (carbon-14) in water saturated glass beads (149-210 microns) as a function of distance along the column.
⊗ experimental; ⊙ theoretical.

Table 32. Values of parameters used to generate the theoretical dispersion profiles.

Particle Size (Diameter)	Average Radius	Porosity, ϵ	Velocity, v	Dispersion Coefficient, D
microns	microns		cm/day	cm^2/day
<30	7.50	0.370	40.92	1.01
28-53	20.25	0.370	42.27	1.36
105-149	63.50	0.370	45.20	2.08
149-210	78.75	0.370	45.38	2.08

The theoretical curves are shown in Figures 17, 18, 19 and 20. The experimental data points represent an average value of the relative concentration over an increment of 1 cm along the column and were plotted at the center of each increment. The actual value may have fallen at any point near this range. Thus the theoretical and experimental curves agree well within the limits of experimental error confirming the theoretical model.

The relative concentration (c/c_0) for the smallest size fraction of glass beads (<30 microns) has a maximum value of 58 percent. The maximum value decreases as the size of glass beads increases. This shows how the pore size affects the dispersion of the chemical. For smaller size fraction of <30 microns, pore radii of the order of 3 to 5 microns (Table 28) are responsible for the passage of the chemical and retain most of the chemical to give a high value of c/c_0. For the largest size fraction of 149-210 microns,

a pore radius of 30 microns (Table 31) is responsible for the passage of the chemical. The maximum value of c/c_0 was 38 percent for this fraction. As the particle size increases, and hence pore radius, there is more spreading of the chemical, reducing the maximum (peak) value of c/c_0.

The relative concentration, c/c_0, for the smallest size fraction of beads used (<30 microns) had a maximum value of 58 percent. This maximum value decreased as the size of the glass beads increased, to become 38 percent for the largest size fraction (149-210 microns). At the same time the curve describing the chemical distribution became broader as the particle size increased.

TRANSPORT OF 2,4-DICHLOROPHENOXYACETIC ACID IN WATER SATURATED SORBING POROUS MEDIA

Introduction

An experiment was conceived to study the effect of adsorption and desorption on the movement of a chemical through a porous medium. In the previous experiment, glass beads were used as the material to form the porous media. The same size fractions of glass beads were used in this experiment. Being an inert material, glass beads have no adsorption sites. In order to determine adsorption and desorption effects on the movement of 2,4-D it was necessary to create adsorption sites on the glass beads.

Chao et al. (1964) studied the effect of hydrous Fe- and Al-oxides on SO_4 adsorption in relation to pH when present as surface coatings on soil samples. They succeeded in coating soil particles with the oxides because of the presence of negative adsorption sites on the clay particles. Their procedure was tried to coat the glass beads with hydrous Fe-oxides. To see if adsorption sites were created or not, 3 g of the sample so treated was transferred to a 50 ml volumetric flask. To this, 2 ml of labelled 2,4-D was added and the volume was made up with distilled water. Separately 3 g of the untreated sample was prepared in the same way. The flasks were shaken intermittently. After 5 hours, 1 ml of the aliquot was

transferred to a counting vial and the activity was determined. Table 33 shows that no adsorption had taken place. The procedure adopted by Chao et al. was then modified to create adsorption sites by coating glass beads with ferric hydroxide precipitate. To obtain this 150 g of glass beads were put in a 2 liter beaker. Boiling distilled water (600 ml) was added to the beaker which was then heated for 10 minutes with continuous stirring with a glass rod. Three grams of anhydrous ferric chloride was dissolved in 25 ml of distilled water and the solution was added to the beaker. The contents were heated for 5 minutes and then cooled for 10 minutes.

Table 33. Determination of adsorption of 2,4-D (carbon-14) by glass beads (28-53 microns) coated by the method of Chao et al. (1964).

Sample	Activity #1	Activity #2	Activity	Corrected Activity
	cp10m	cp10m	cpm	cpm
Blank	338	361	35	---
Untreated glass beads	5825	6666	625	590*
Treated glass beads	5639	6481	606	571*

*These counts are the same within statistical error of radioactivity counting.

Enough ammonium hydroxide was added to precipitate ferric hydroxide. The precipitate along with glass beads was transferred to a Buchner funnel and washed with acetone until free of water. Three washings, 100 ml each, were found to be sufficient to

remove the last traces of water. The material was then washed with acetone into a flash evaporator flask which was connected to the flash evaporator. After all acetone was removed, a coating on the beads was obtained. The above described procedure was repeated to check if adsorption had taken place. Table 34 shows that again no adsorption took place.

Table 34. Determination of adsorption of 2,4-D (carbon-14) by glass beads (28-53 microns) coated by the modified method of Chao et al. (1964).

Sample	Activity #1	Activity #2	Activity	Corrected Activity
	cp10m	cp10m	cpm	cpm
Blank	315	348	33	---
Untreated glass beads	5779	6506	614	581*
Treated glass beads	5680	6391	604	571*

*These counts are the same within statistical error of radioactivity counting.

Another alternative was to mix anion exchange resin with the glass beads. But the concentration of 2,4-D was so low (total 20 μg) that only 26 mg of the resin (assuming resin has 3.5 meq/g exchange capacity on a dry weight basis and is one hundred percent efficient in adsorption) would be sufficient to adsorb all of the 2,4-D. The capacity of the column was about 150 g of glass beads and it was quite impossible to mix 26 mg of the resin uniformly with 150 g of the sample. Thus, a combination of anion exchange resin (Dowex 1-X4;

chloride form; 3.5 meq/g total exchange capacity on a dry weight basis) and ferric hydroxide was employed to coat the glass beads. The resin was powdered in a ball mill and passed through a 50-micron sieve. A mixture of 150 g of glass beads and 10 mg of powdered resin was prepared in a two liter beaker. The above procedure using a flash evaporator was employed to coat the glass beads. The sample was passed through appropriate sieves and checked under a microscope to inspect the coating. It was found that the glass bead surfaces were coated with a thin layer of ferric hydroxide and resin and that no cementing of particles had taken place. This procedure produced the proper number of adsorption sites on the glass beads for the present experiment in which the concentration of 2,4-D used was 10 ppm. If a chemical of higher concentration is used, a greater amount of resin and/or ferric chloride would be required. In the present experiment different amounts of resin (1, 5, 10 and 100 mgm) were tried. Ten mg of resin was found to be optimum and the same amount was used to coat the rest of the samples.

Pore size distributions of the samples were also determined (Tables 35, 36, 37 and 38). A comparison of the pore size distributions of uncoated and coated glass beads indicated that no appreciable change in pore size distribution occurred by coating the glass beads.

Table 35. Pore size distribution determination of coated glass beads (<30 microns) with the mercury intrusion porosimeter.

Mercury Head (1)	0-15 Gauge (2)	Pressure Gauge (3)	Absolute Pressure (4)	Stem Reading (5)	Cumulative Pore Volume (6)	Pore Diameter (7)	Pore Volume (8)
psia	psia	psia	psia	cm^3	cm^3	microns	percent
5.029	6.0	0.0	.971	.000	.059	180.20	100.00
4.989	7.0	0.0	2.011	.003	.056	87.02	94.91
4.963	8.0	0.0	3.037	.005	.054	57.62	91.53
4.949	9.0	0.0	4.051	.006	.053	43.19	87.83
4.949	10.0	0.0	5.051	.006	.053	34.65	89.83
4.949	11.0	0.0	6.051	.006	.053	28.92	89.83
4.949	12.0	0.0	7.051	.006	.053	24.82	89.83
4.949	13.0	0.0	8.051	.006	.053	21.74	89.83
4.936	14.0	0.0	9.064	.007	.052	19.31	88.14
4.936	14.7	0.0	9.764	.007	.052	17.92	88.14
4.936	14.7	2.0	11.764	.007	.052	14.88	88.14
4.936	14.7	4.0	13.764	.007	.052	12.71	88.14
4.764	14.7	6.0	15.936	.020	.039	10.98	66.10
4.499	14.7	10.0	20.201	.040	.019	8.66	32.20
4.287	14.7	20.0	30.413	.056	.003	5.75	5.08
4.260	14.7	50.0	60.440	.058	.001	2.90	1.69
4.260	14.7	100.0	110.440	.058	.001	1.58	1.69
4.260	14.7	250.0	260.440	.058	.001	0.67	1.69
4.247	14.7	500.0	510.453	.059	.000	0.34	.00
4.247	14.7	1000.0	1010.453	.059	.000	0.17	.00
4.247	14.7	2000.0	2101.453	.059	.000	.087	.00
4.247	14.7	4000.0	4010.453	.059	.000	.044	.00

Table 36. Pore size distribution determination of coated glass beads (28-53 microns) with the mercury intrusion porosimeter.

Mercury Head (1)	0-15 Gauge (2)	Pressure Gauge (3)	Absolute Pressure (4)	Stem Reading (5)	Cumulative Pore Volume (6)	Pore Diameter (7)	Pore Volume (8)
psia	psia	psia	psia	cm^3	cm^3	microns	percent
5.029	6.0	0.0	.971	.000	.067	180.2	100.00
5.029	7.0	0.0	1.971	.000	.067	88.79	100.00
5.029	8.0	0.0	2.971	.000	.067	58.90	100.00
5.029	9.0	0.0	3.971	.000	.067	44.07	100.00
5.029	10.0	0.0	4.971	.000	.067	35.20	100.00
5.029	11.0	0.0	5.971	.000	.067	29.28	100.00
5.029	12.0	0.0	6.971	.000	.067	25.08	100.00
5.029	13.0	0.0	7.971	.000	.067	21.94	100.00
5.016	14.0	0.0	8.984	.001	.066	19.48	98.51
5.002	14.7	0.0	9.698	.002	.065	18.04	97.01
4.274	14.7	2.0	12.426	.057	.009	14.08	13.43
4.221	14.7	4.0	14.479	.061	.006	12.09	8.96
4.207	14.7	6.0	16.493	.062	.005	10.61	7.46
4.207	14.7	10.0	20.493	.062	.005	8.53	7.46
4.168	14.7	20.0	30.532	.065	.002	5.73	2.99
4.168	14.7	50.0	60.532	.065	.002	2.89	2.99
4.154	14.7	100.0	110.546	.066	.001	1.58	1.49
4.141	14.7	250.0	260.559	.067	.000	.67	0.00
4.141	14.7	500.0	510.559	.067	.000	.34	0.00
4.141	14.7	1000.0	1010.559	.067	.000	.17	0.00
4.141	14.7	2000.0	2010.559	.067	.000	.09	0.00
4.141	14.7	4000.0	4010.559	.067	.000	.04	0.00

Table 37. Pore size distribution determination of coated glass beads (105-149 microns) with the mercury intrusion porosimeter.

Mercury Head (1)	0-15 Gauge (2)	Pressure Gauge (3)	Absolute Pressure (4)	Stem Reading (5)	Cumulative Pore Volume (6)	Pore Diameter (7)	Pore Volume (8)
psia	psia	psia	psia	cm^3	cm^3	microns	percent
5.029	6.0	0.0	.971	.000	.074	180.22	100.00
5.002	7.0	0.0	1.998	.002	.072	87.59	97.30
4.989	8.0	0.0	3.011	.003	.071	58.12	95.95
4.963	9.0	0.0	4.037	.005	.069	43.35	93.24
4.181	10.0	0.0	5.819	.064	.010	30.07	13.51
4.128	11.0	0.0	6.872	.068	.006	25.47	8.11
4.115	12.0	0.0	7.885	.069	.005	22.19	6.75
4.008	13.0	0.0	8.992	.071	.003	19.46	4.05
4.008	14.0	0.0	9.992	.071	.003	17.51	4.05
4.075	14.7	0.0	10.625	.072	.002	16.47	2.70
4.075	14.7	2.0	12.625	.072	.002	13.86	2.70
4.075	14.7	4.0	14.625	.072	.002	11.96	2.70
4.062	14.7	6.0	16.638	.073	.001	10.52	1.35
4.062	14.7	10.0	20.638	.073	.001	8.48	1.35
4.062	14.7	20.0	30.638	.073	.001	5.71	1.35
4.062	14.7	50.0	60.638	.073	.001	2.89	1.35
4.062	14.7	100.0	110.638	.073	.001	1.58	1.35
4.062	14.7	250.0	260.638	.073	.001	.67	1.35
4.062	14.7	500.0	510.638	.073	.001	.34	1.35
4.062	14.7	1000.0	1010.638	.073	.001	.17	1.35
4.062	14.7	2000.0	2010.638	.073	.001	.087	1.35
4.048	14.7	4000.0	4010.652	.074	.000	.044	0.00

Table 38. Pore size distribution determination of coated glass beads (149-210 microns) with the mercury intrusion porosimeter.

Mercury Head (1)	0-15 Gauge (2)	Pressure Gauge (3)	Absolute Pressure (4)	Stem Reading (5)	Cumulative Pore Volume (6)	Pore Diameter (7)	Pore Volume (8)
psia	psia	psia	psia	cm^3	cm^3	microns	percent
5.029	6.0	0.0	.971	.000	.083	180.2	100.00
4.989	7.0	0.0	2.210	.003	.080	79.1	96.38
4.207	8.0	0.0	2.893	.062	.021	45.6	25.30
4.075	9.0	0.0	4.925	.072	.011	35.5	13.25
4.035	10.0	0.0	5.965	.075	.008	29.3	9.64
4.009	11.0	0.0	6.991	.077	.006	25.0	7.23
3.995	12.0	0.0	8.005	.078	.005	21.9	6.02
3.995	13.0	0.0	9.005	.078	.005	19.4	6.02
3.995	14.0	0.0	10.005	.078	.005	17.5	6.02
3.982	14.7	0.0	10.718	.079	.004	16.3	4.82
3.956	14.7	2.0	12.744	.081	.002	13.7	2.41
3.956	14.7	4.0	14.744	.081	.002	11.9	2.41
3.956	14.7	6.0	16.744	.081	.002	10.5	2.41
3.956	14.7	10.0	20.744	.081	.002	8.4	2.41
3.956	14.7	20.0	30.744	.081	.002	5.7	2.41
3.942	14.7	50.0	60.758	.082	.001	2.9	1.21
3.942	14.7	100.0	110.758	.082	.001	1.6	1.21
3.942	14.7	250.0	260.758	.082	.001	.7	1.21
3.942	14.7	500.0	510.758	.082	.001	.3	1.21
3.942	14.7	1000.0	1010.758	.082	.001	.17	1.21
3.942	14.7	2000.0	2010.758	.082	.001	.087	1.21
3.929	14.7	4000.0	4010.771	.083	.000	.044	0.00

Apparatus

The columns made up of lucite rings described previously were used in this experiment, but the sample was saturated with 0.01 M NH_4Cl and not water. A solution of 0.01 M ammonium chloride was used to leach the sample to obtain desorption of the chemical. After the adsorption had taken place, the chloride anion from the ammonium chloride could exchange with the 2-4, D on the adsorption site on the resin and bring it into the free phase again. This was necessary to simulate the adsorption-desorption characteristics incorporated in the model.

Analysis

After sampling was completed according to previously described procedures, the sample volume was made up with distilled water in 50 ml volumetric flasks. One ml of aliquot was used to rinse the pipette and one ml of the aliquot was transferred into vials to determine activity by liquid scintillation. Thus, the activity present in free phase was obtained.

Results and Discussion

Results of the experiments are shown in Figures 21, 22, 23, and 24 for the size fractions <30, 28-53, 105-149, and 149-210 microns,

respectively.

In the previous experiment theoretical curves were generated to compare with the experimental curves. Those theoretical curves were generated assuming that no adsorption of the chemical took place and the values of ϕ and γ were chosen to be zero (Appendix 4). In the present experiment the glass beads were coated with resin and ferric hydroxide and thus the value of ϕ and γ were not zero. Since ϕ and γ occur as a product, an estimate was made of its value by using the following relation suggested by Lindstrom[3]

$$X_p \cong \frac{\ell}{2} + \frac{vt}{1+\phi\gamma}$$

where X_p is the distance along the column where the peak occurs (cm), ℓ is the length of each ring along the column (cm), v is the apparent average flow velocity (cm/day), t is the time (day), and $\phi\gamma$ is a parameter which estimates the amount of adsorption of the chemical on the glass beads. The values of X_p were estimated from the experimental curves. The values of the flow velocities and dispersion coefficients used to generate the theoretical curves for the 4 size fractions are shown in Table 39. The dispersion coefficients were calculated according to the procedure outlined in Appendix 4.

---

[3]Dr. F.T. Lindstrom, Research Mathematician, Dept. of Agricultural Chemistry, Oregon State University, Corvallis.

Table 39. Values of average flow velocity and dispersion coefficients employed to generate the theoretical curves for four fractions of coated glass beads.

Particle Size (Diameter)	Average Flow Velocity, v	Dispersion Coefficient, D
microns	cm/day	cm^2/day
<30	48.68	1.01
28-53	48.50	1.10
105-149	51.30	2.08
149-210	51.30	2.40

Figures 21 through 24 show the theoretical and experimental curves. The experimental data points represent an average value of the chemical concentration present in 1 cm length of the column. The points are plotted at the mid-point and thus can lie within a distance of 1 cm from the indicated position. The theoretical and experimental curves agree well within the experimental error. This indicates the validity of the theoretical model.

In a second set of experiments, the amount of the adsorption per unit site was doubled by coating the glass beads with twice the amount of resin used previously. To generate the theoretical model for this set, the value of the product $\phi\gamma$ was also doubled ($\phi\gamma = 0.86$). Theoretical and experimental curves for this experiment are shown in Figure 25. These curves also agree well within the experimental error confirming the theoretical model.

A third set of experiments was conducted to see if the tailing

effect in the experimental curves of coated glass beads was due to trapping of the chemical in dead pores or to the adsorption of the chemical. Experiments were conducted for various time periods at a constant flow rate of 4 ml/hr with coated and non-coated glass beads. Results of these experiments are shown in Figure 26. As the time periods increased, the coated glass beads show a pronounced tailing effect indicating that the tailing is either due to adsorption or due to dead pores present in the medium. For the experiments with non-coated glass beads (28-53 microns) for the same time periods as with coated glass beads, no tailing was observed. This suggests that the tailing effect in coated glass beads is due to adsorption and not to trapping in dead pores.

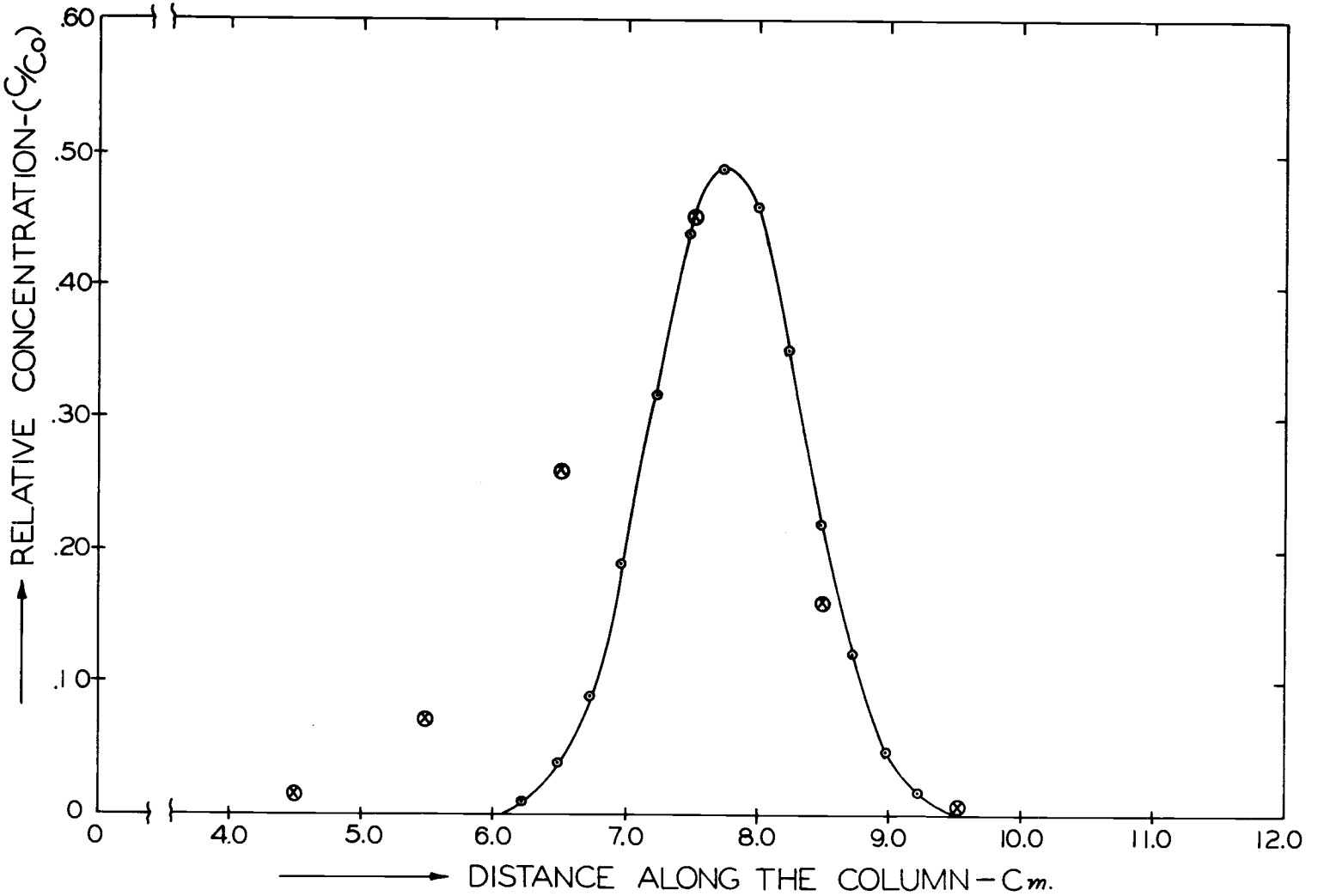

Figure 21. Experimental and theoretical distribution of 2,4-D (carbon-14) in water saturated coated glass beads (<30 microns) as a function of distance along the column.
⊗ experimental; ⊙ theoretical.

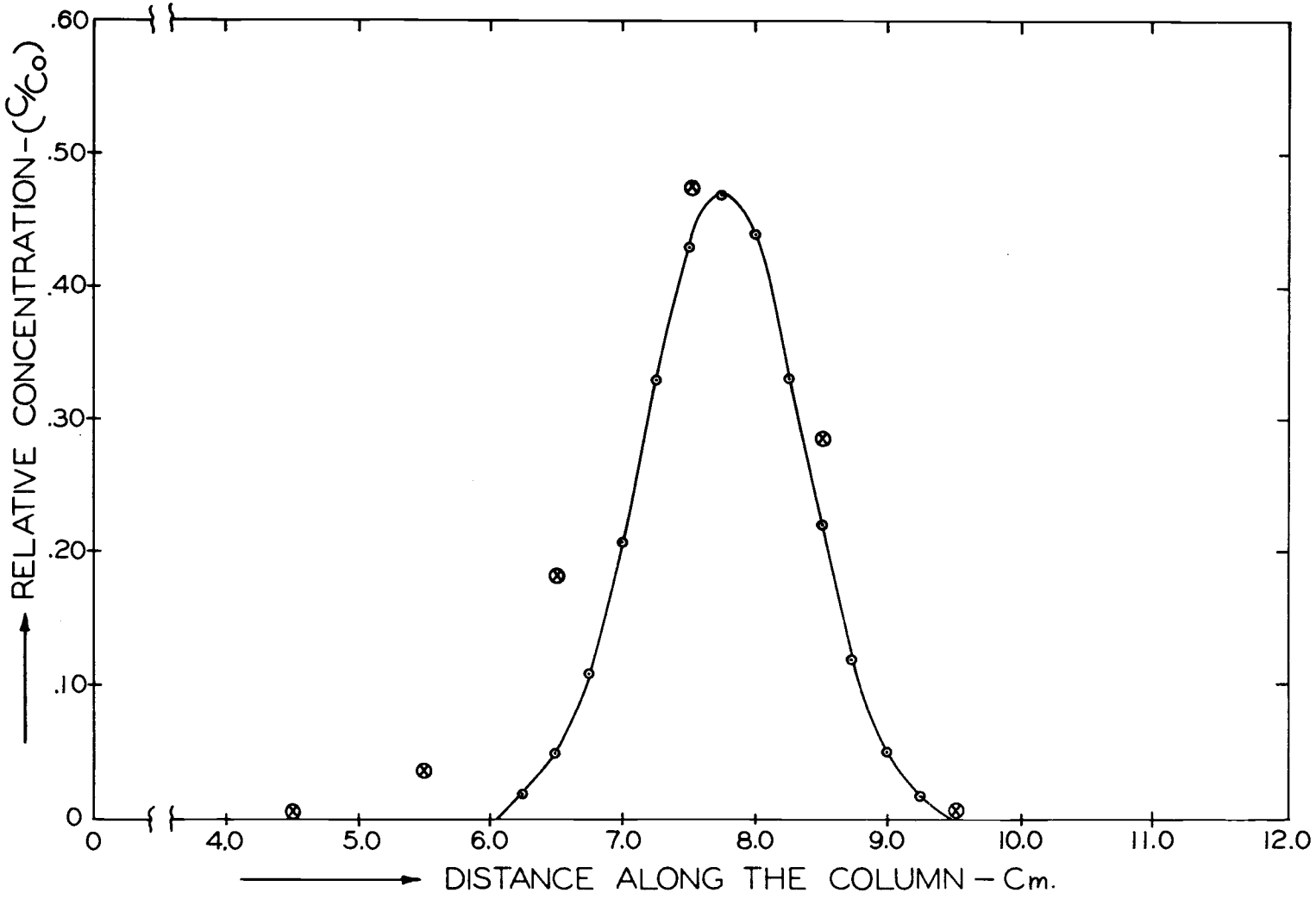

Figure 22. Experimental and theoretical distribution of 2, 4-D (carbon-14) in water saturated coated glass beads (28-53 microns) as a function of distance along the column. ⊗ experimental; ⊙ theoretical.

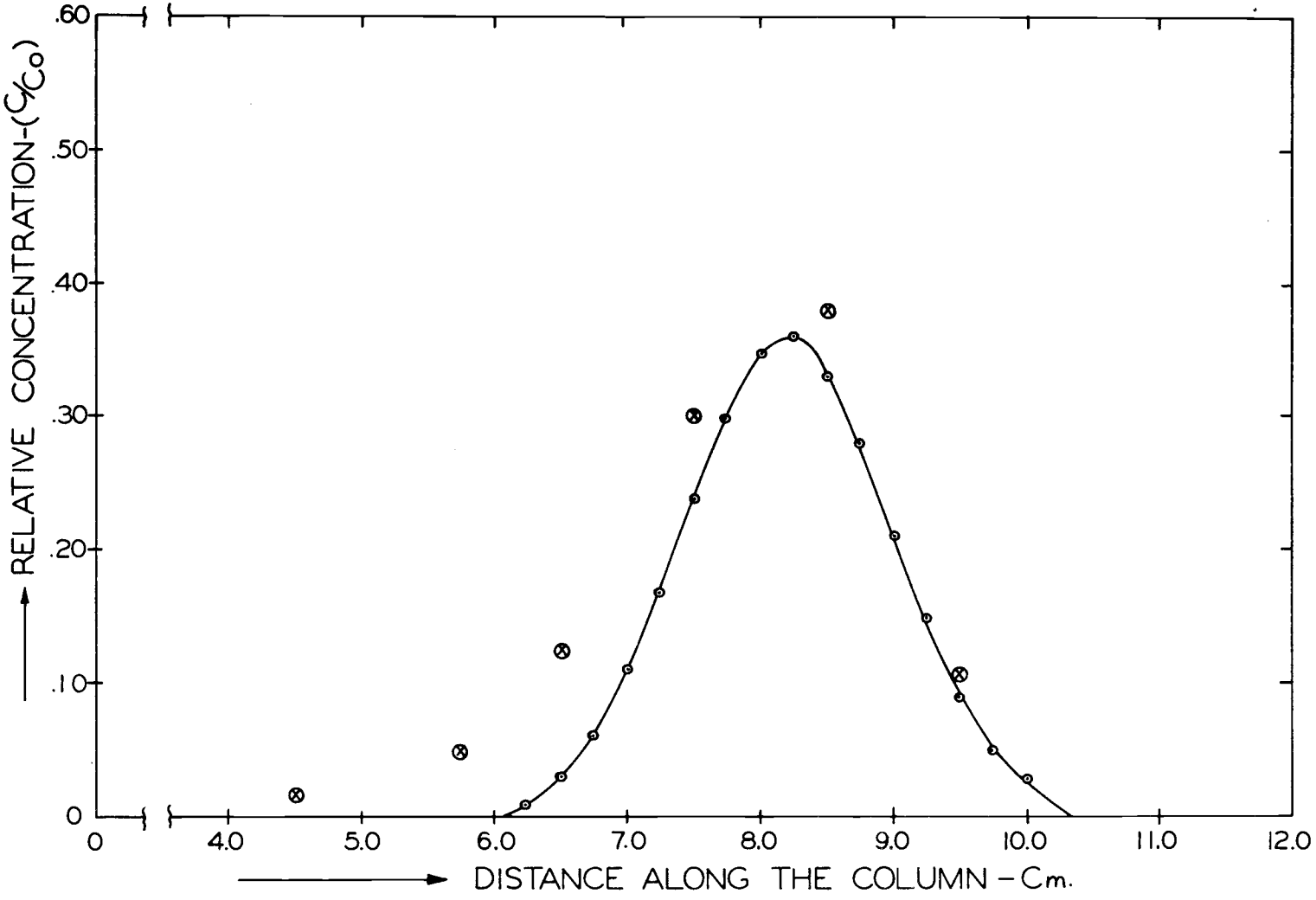

Figure 23. Experimental and theoretical distribution of 2,4-D (carbon-14) in water saturated coated glass beads (105-149 microns) as a function of distance along the column. ⊗ experimental; ⊙ theoretical.

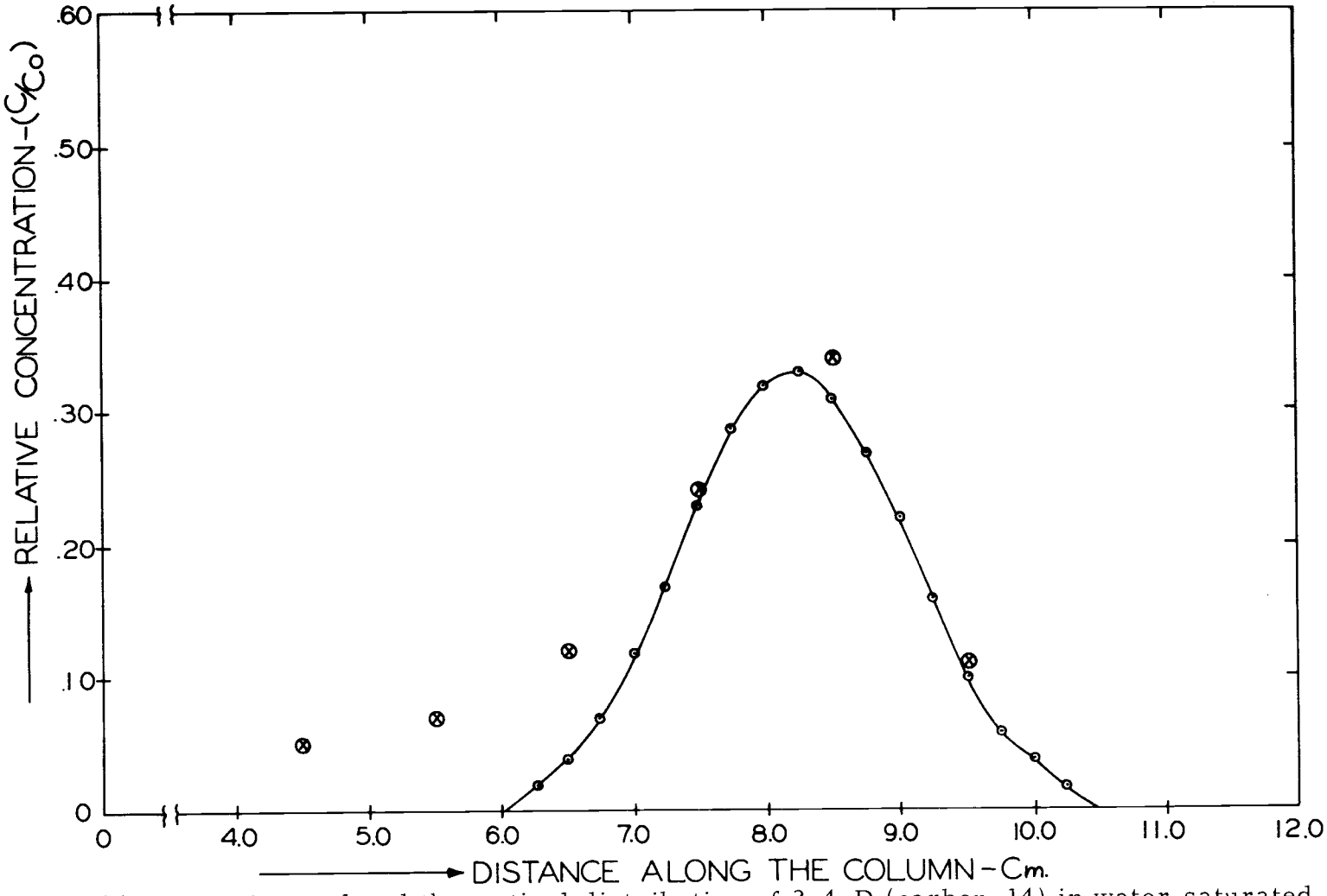

Figure 24. Experimental and theoretical distribution of 2,4-D (carbon-14) in water saturated coated glass beads (149-210 microns) as a function of distance along the column. ⊗ experimental; ⊙ theoretical.

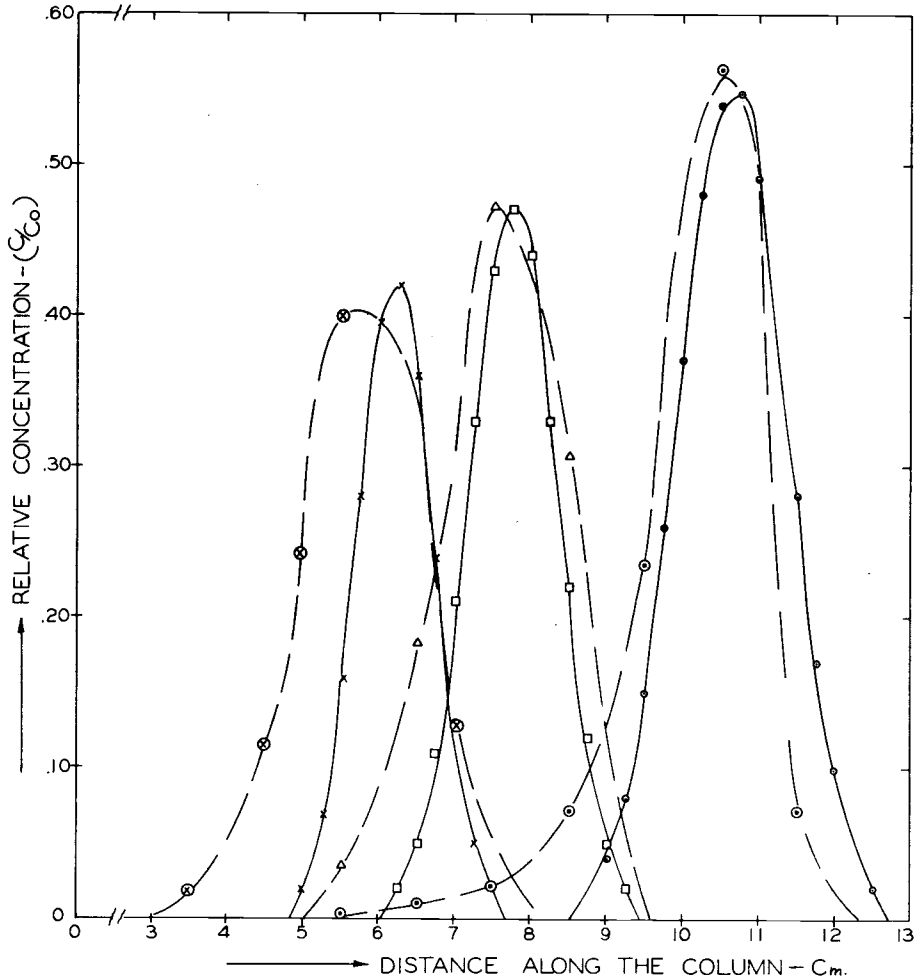

Figure 25. Comparison of theoretical (solid line) and experimental (broken line) curves for different amounts of adsorption for 28-53 microns glass beads. ⊙ no adsorption; ◉ no adsorption; □ $\phi\gamma = 0.43$; △ 6.67 mg of powdered resin/100 g of glass beads; × $\phi\gamma = 0.86$; ⊗ 13.34 mg of powdered resin/100 g of glass beads.

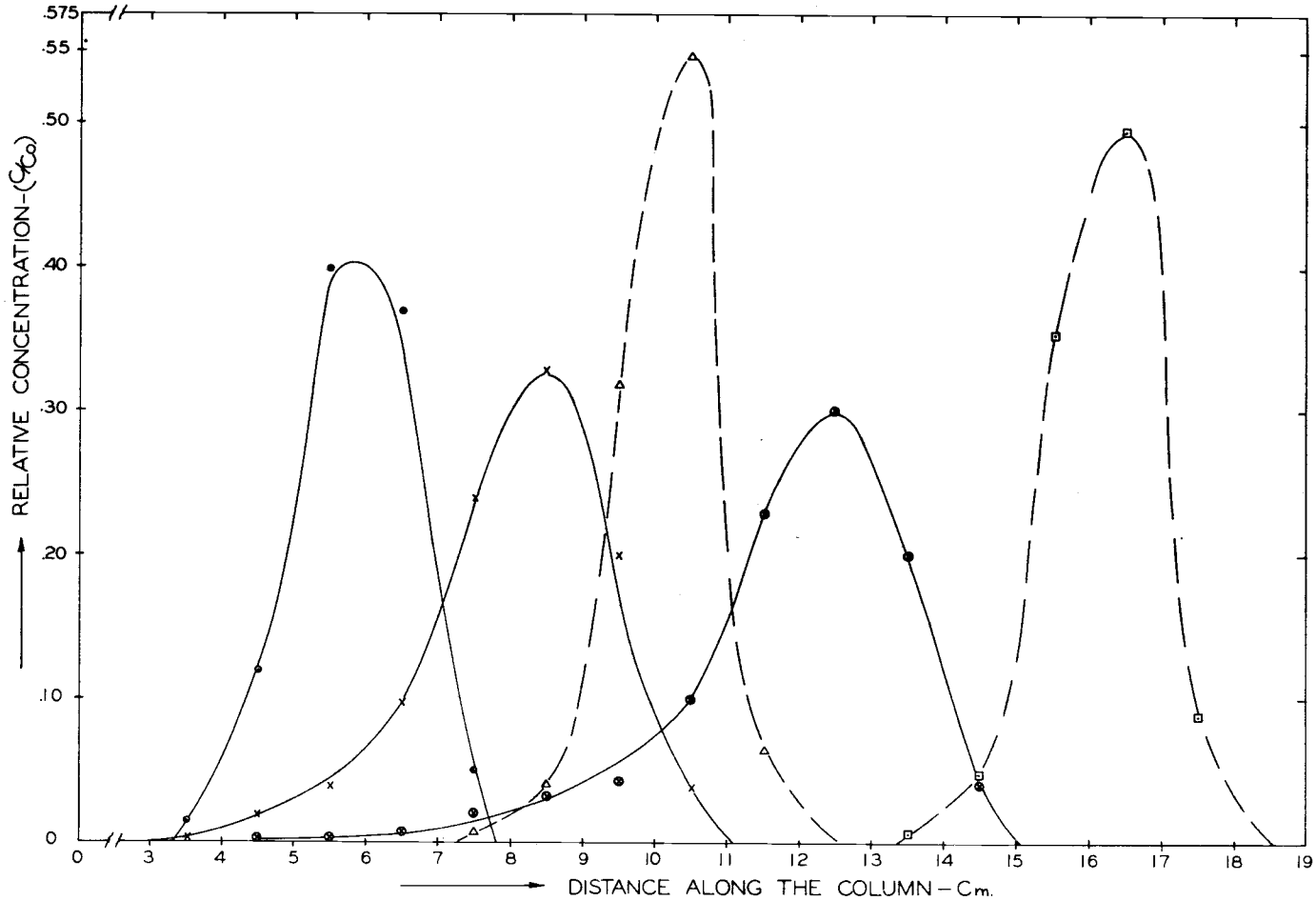

Figure 26. Effect of adsorption and dead pores for coated (solid line) and non-coated (broken line) glass beads (28-53 microns) for various periods of time at a flow rate of 4 ml/hr. ⊙ 5.0 hours; × 7.5 hours; ⊗ 10.0 hours; △ 5.0 hours; ⊡ 7.5 hours.

SUMMARY AND CONCLUSION

Pore size distributions of glass bead materials varying in size were obtained with a mercury intrusion porosimeter. Results of these measurements were used in subsequent chapters where effects of pore size on the diffusion and transport of 2,4-D (carbon-14) through water saturated porous media (glass beads) were considered.

The diffusion coefficients of 2,4-D (carbon-14) for glass bead fractions with particle sizes <10, 10-20, 30-40 and 40-50 microns were obtained experimentally. It was found that as the average particle size, and hence the pore radius, increased, the value of the diffusion coefficient also increased. A relation of the type $K'/K = 1 - e^{-Ar^2}$ was obtained between pore radius and the ratio of the porous material diffusion coefficient and the free chemical diffusion coefficient, where A is a constant. These results suggest that porous system diffusion coefficients of various chemicals can be obtained from the self-diffusion coefficient.

Self-diffusion coefficients for 2,4-D (carbon-14) and Calcium Chloride (calcium-45) were obtained by agar and cell diffusion methods. The agar method gave higher values of the self-diffusion coefficient than the theoretical maximum value. The deviations encountered may be due to: (1) Tortuosity. The equation employed to calculate the self-diffusion coefficient gives a value of "effective or porous

system diffusion coefficient" with no allowance made for tortuosity. Yet tortuosity is known to play a part and adjustment for it is necessary. (2) Capacity Factor. In the calculations the capacity factor was assumed to be zero. This assumption was not experimentally verified. (3) Viscosity and Density Gradients. During solidification of agar a gradient in viscosity and density occurs and a correction needs to be applied for this. The agar method was not considered to be a reliable method to determine the self-diffusion coefficients of ions. The cell diffusion method gave more reliable values compared to the theoretical maximum value of the self-diffusion coefficient for Calcium Chloride (calcium-45) and was also used to determine the self-diffusion coefficient for 2,4-D (carbon-14).

Experiments were designed to evaluate dispersion models developed by Lindstrom et al. (1967) and Lindstrom and Boersma (1971). Transport of 2,4-D (carbon-14) was studied for glass beads with particles <30, 28-53, 105-149 and 149-210 microns in diameter. Theoretical dispersion curves were generated and compared with experimental curves. The theoretical curves agreed well with the experimental results. As the average particle radius, and hence pore radius, increased, the shape of the curve varied. For the small glass beads (<30 microns), the maximum value of the relative concentration of the chemical was 0.58 whereas for the large glass beads (149-210 microns), the maximum value of the relative concentration of the

chemical was 0.38. There was more spreading of the chemical in the larger than in the smaller glass beads. This was in agreement with the theoretical model. Thus the proposed mathematical theory described the movement of 2,4-D well.

Mathematical models used above were modified to include adsorption terms. Again, theoretical curves were generated for the transport of 2,4-D (carbon-14) and comparisons were made with experimental curves. Theoretical and experimental curves agreed well within experimental error suggesting that the mathematical theory is valid for sorbing porous media as well.

BIBLIOGRAPHY

Abramowitz, M. and I.A. Stegun. 1965. Handbook of Mathematical Functions. Dover, New York. 1056 p.

Aladjem, F.R.W. Jaross, R.L. Paldino, and J.A. Lackner. 1959. The Antigen-antibody reaction. III. Theoretical considerations concerning the formation, location, and curvature of the antigen-antibody precipitation zone in agar diffusion plates, and a method for the determination of diffusion coefficients of antigens and antibodies. Journal of Immunology 83:221-231.

Anderson, J.S. and K. Saddington. 1949. The use of radioactive isotopes in the study of the diffusion of ions in solution. Journal of Chemical Society 5:S381-S386.

Barber, S.A. 1962. A diffusion and mass flow concept of soil nutrient availability. Soil Science 93:39-49.

Barber, S.A., J.M. Walker, and E.H. Vasey. 1963. Mechanism for the movement of plant nutrients from the soil and fertilizer to the plant root. Journal of Agricultural and Food Chemistry 11:204-207.

Barrer, R.M. 1951. Diffusion in and through solids. Cambridge University Press, London. 464 p.

Biggar, J.W. and D.R. Nielsen. 1962. Miscible displacement: II. Behaviour of tracers. Soil Science Society of America Proceedings. 26:125-218.

Biggar, J.W. and D.R. Nielsen. 1963. Miscible displacement: V. Exchange processes. Soil Science Society of America Proceedings. 27:623-627.

Bloksma, A.H. 1957. The diffusion of sodium and iodide ions and of urea in clay pastes. Journal of Colloid Science 12:40-52.

Bouldin, D.R. 1961. Mathematical description of diffusion processes in the soil-plant system. Soil Science Society of America Proceedings 25:476-480.

Brenner, H. 1962. The diffusion model of longitudinal mixing in beds of finite length: Numerical values. Chemical Engineering Science 17:229-243.

Call, F. 1956. A new method of calculating unsteady state diffusion coefficients in porous solids. Journal of Applied Chemistry 6:298-300.

Chao, T.T., M.E. Harward, and S.C. Fang. 1964. Iron or aluminum coatings in relation to sulfate adsorption characteristics of soils. Soil Science Society of America Proceedings 28:632-635.

Childs, E.C. 1940. The use of soil moisture characteristics in soil studies. Soil Science 50:239-252.

Crank, J. 1956. The Mathematics of Diffusion. Clarendon Press, Oxford. 347 p.

Daniels, F. and R.A. Alberty. 1967. Physical Chemistry. John Wiley and Sons Incorporated, New York. 767 p.

Davis, H.T. 1962. Introduction to non-linear differential and integral equations. Dover, New York. 566 p.

Dutt, G.R. and P.F. Low. 1962. Diffusion of alkali chlorides in clay-water systems. Soil Science 93:233-240.

Elgawhary, S.M., W.L. Lindsay, and W.D. Kemper. 1970. Effect of EDTA on the self-diffusion of zinc in aqueous solution and in soil. Soil Science Society of America Proceedings 34:66-70.

Farmer, W.J. and C.R. Jensen. 1970. Diffusion and analysis of carbon-14 labeled dieldrin in soils. Soil Science Society of America Proceedings 34:28-31.

*Ficks, A. 1855. Uber Diffusion. Poggendorffs Ann. 94:59-86.

Fisher, J.C. 1951. Calculation of diffusion penetration curves for surface and grain boundary diffusion. Journal of Applied Physics 24:74-77.

Fried, M., C.E. Hagen, J.F. Saiz, J.F. del Rio, and J.E. Leggett. 1957. Kinetics of phosphate uptake in the soil-plant system. Soil Science 84:427-437.

Gardner, W. R. and R. H. Brooks. 1957. A descriptive theory of leaching. Soil Science 83:295-304.

Graham-Bryce, I. J. 1963. Effect of moisture content and soil type on self-diffusion of ^{86}Rb in soils. Journal of Agricultural Science 60:239-244.

*Graham, T. 1850. Supplementary observations on the diffusion of liquids. Philosophical Transactions of Royal Society of London. 140:805-836.

Groton, L. L. and H. Frazer. 1935. Systematic packing of spheres-with particular relation to porosity and permeability. Journal of Geology 43:758-909.

Hall, J. R., B. F. Wishaw, and R. H. Stokes. 1953. The diffusion coefficient of calcium chloride and ammonium chloride in concentrated aqueous solutions at 25°. Journal of American Chemical Society 75:1556-1560.

Husted, R. F. and P. F. Low. 1954. Ion diffusion in bentonite. Soil Science 77:343-353.

Juhola, A. J. and E. O. Wiig. 1949. Pore structure in activated charcoal. II. Determination of macro pore-size distribution. Journal of American Chemical Society 71:2078-2080.

Kemper, W. D., D. E. L. Maasland and L. K. Porter. 1964. Mobility of water adjacent to bentonite surfaces. Soil Science Society of America Proceedings 28:164-167.

Klute, A. and J. Letey. 1958. The dependence of ionic diffusion on the moisture content of nonadsorbing porous media. Soil Science Society of America Proceedings 22:213-215.

Kunze, R. J. and D. Kirkham. 1961. Deuterium and the self-diffusion coefficient of soil moisture. Soil Science Society of America Proceedings 25:9-12.

Lai, T. M., and M. M. Mortland. 1961. Diffusion of ions in bentonite and vermiculite. Soil Science Society of America Proceedings 25:353-357.

Lai, T. M. and M. M. Mortland. 1968. Cationic diffusion in clay minerals: I. Homogeneous and heterogeneous systems. Soil Science Society of America Proceedings 32:56-61.

Leamer, R. W. and J. F. Lutz. 1940. Determination of pore size distribution in soils. Soil Science 49:347-360.

Le Claire, A. D. 1963. The analysis of grain boundary diffusion measurements. British Journal of Applied Physics. 14:351-356.

Lindstrom, F. T., R. Haque, V. H. Freed and L. Boersma. 1967. Theory on the movement of some herbicides in soils: Linear diffusion and convection of chemicals in soils. Environmental Science and Technology 1:561-567.

Lindstrom, F. T., L. Boersma and H. Gardiner. 1968. 2,4-D diffusion in saturated soils: A mathematical theory. Soil Science 106:107-113.

Lindstrom, F. T. and L. Boersma. 1971. A theory on the mass transport of previously distributed chemicals in a water saturated sorbing porous medium. Soil Science 111:192-199.

Mahin, D. T. and R. T. Lofberg. 1966. A simplified method of sample preparation for determination of tritium, carbon-14, or sulfur-35 in blood or tissue by liquid scintillation counting. Analytical Biochemistry 16:500-509.

Nakayama, F. S. and R. D. Jackson. 1963. Diffusion of tritiated water (H^3 H^1 O^{16}) in agar gel and water. Journal of Physical Chemistry 67:932-933.

Narasimhan, M. N. L. and K. S. Sra. 1969. Generalized measures of deformation - rates in viscoelasticity and their applications to rectilinear and simple shearing flows. International Journal of Non-Linear Mechanics. 4:361-372.

Nielsen, D. R. and J. W. Biggar. 1961. Miscible displacement in soils: 1. Experimental information. Soil Science Society of America Proceedings. 25:1-5.

Nielsen, D. R. and J. W. Biggar. 1962. Miscible displacement: III. Theoretical considerations. Soil Science Society of America Proceedings. 26:216-222.

Nielsen, D. R. and J. W. Biggar. 1963. Miscible displacement: IV. Mixing in glass beads. Soil Science Society of America Proceedings. 27:10-13.

Nye, P. H. 1966. The measurement and mechanism of ion diffusion in soil. I. The relation between self-diffusion and bulk diffusion. Journal of Soil Science 17:16-23.

*Obermayer, A. V. 1880. Über die Abhängigkeit des Diffusionscoefficienten der Gase von der Temperatur. Sitzungsberichte der Akademie der Wissenenschaften, Wien, Mathematisch-Naturwissenschaftlichen Classe (Abteilung II). 81:1102-1127.

Olsen, S. R., W. D. Kemper and R. D. Jackson. 1962. Phosphate diffusion to plant roots. Soil Science Society of America Proceedings 26:222-227.

Olsen, S. R. and F. W. Watanabe. 1963. Diffusion of phosphorous related to soil texture and plant uptake. Soil Science Society of America Proceedings 27:648-652.

Olsen, S. R., W. D. Kemper and J. C. Van Schaik. 1965. Self-diffusion coefficients of phosphorous in soil measured by transient and steady-state methods. Soil Science Society of America Proceedings 29:154-158.

Porter, L. K., W. D. Kemper, R. D. Jackson and B. A. Stewart. 1960. Chloride diffusion in soils as influenced by moisture content. Soil Science Society of America Proceedings 24:460-463.

Purcell, W. R. 1949. Capillary pressures--their measurement using mercury and the calculation of permeability therefrom. Petroleum Branch American Institute of Mining and Metalurgical Engineers, Transactions 186:39-50.

Schofield, R. K. 1939. Pore size distribution as revealed by the dependence of suction on moisture content. In: Transactions of the First Commission of the International Society of Soil Science. Bangor, Wales, 1939, ed. by G. W. Robinson. Vol. A. Aberystwyth. p. 54-57.

Schofield, R. K. and I. J. Graham-Bryce. 1960. Diffusion of ions in soils. Nature 188:1048-1049.

Wang, J. H. and J. W. Kennedy. 1950. Self-diffusion coefficients of sodium ion and iodide ion in aqueous sodium iodide solutions. Journal of American Chemical Society 72:2080-2083.

Wang, J. H. 1951. Self-diffusion and structure of liquid water. I. Measurement of self-diffusion of liquid water with deuterium as tracer. Journal of American Chemical Society 73:510-513.

Wang, J. H. 1952. Tracer diffusion in liquids. I. Diffusion of tracer amount of sodium ion in aqueous potassium chloride solutions. Journal of American Chemical Society 74:1182-1186.

Wang, J. H., C. V. Robinson and I. S. Edelman. 1953. Self-diffusion and structure of liquid water. III. Measurement of the self diffusion of liquid water with H^2, H^3, and O^{18} as tracers. Journal of American Chemical Society 75:466-470.

Washburn, E. W. 1921. Note on a method of determining the distribution of pore sizes in a porous material. National Academy of Science, Proceedings 7:115-116.

Whipple, R. T. P. 1954. Concentration contours in grain boundary diffusion. Philosophical Magazine 45:1225-1236.

Winslow, N. M. and J. J. Shapiro. 1959. An instrument for the measurement of pore-size distribution by mercury penetration. ASTM Bulletin 49:39-44.

Wissler, E. H. 1971. Viscoelastic effect in the flow of non-Newtonian fluids through a porous medium. Industrial and Engineering Chemistry. Fundamentals. 10:411-417.

---

*Original material has not been seen.

APPENDICES

APPENDIX 1

Mathematical Models Proposed by Different Authors to Determine Diffusion Coefficients of Various Ions

F. Call (1956)

The diffusion equation

$$\frac{dc}{dt} = -D\frac{d^2c}{dx^2} \qquad (A-1.1)$$

is solved for a finite cylinder of length ℓ and unit cross-sectional area by applying the initial and boundary conditions

$c = c_s$ at $x = 0$, at all t,

$c = c_0$ at $x = \ell$, at all t,

$c = 0$ at $t = 0$, and x is between 0 and ℓ.

The solution is

$$c = c_s\left(1 - \frac{x}{\ell}\right) - \frac{2c_s}{\pi}\sum_{n=1}^{\infty}\frac{1}{n}\sin\frac{n\pi x}{\ell}\exp\left(-\frac{D'n^2\pi^2 t}{\ell^2}\right), \qquad (A-1.2)$$

where D is the diffusion coefficient, D' is the diffusion coefficient in the unsteady state, c is the concentration of vapor, t is the time, and x is the distance.

The concentration of vapor at the upper face of the soil core is

obtained by putting $x = \ell$ in this solution.

The mass of vapor (m) diffusing out of the soil core in unit time, obtained by differentiating Equation (A-1.2) with respect to x, putting $x = \ell$ and substituting in the equation

$$\frac{dm}{dt} = -D \frac{dc}{dx}$$

is

$$\frac{dm}{dt} = \frac{Dc_s}{\ell} \left[1+2 \sum_{n=1}^{\infty} (-1)^n \exp - \left(\frac{D'n^2\pi^2 t}{\ell^2} \right) \right] . \qquad (A-1.3)$$

When t becomes very large, the exponential term tends to zero and the equation reduces to that for the steady state while D' is the coefficient for the unsteady state. The diffusion flux J_t out of the cylinder at any time t is given by Equation (A-1.3) while the steady state flux J_∞ is given with very small error by

$$J_\infty = \frac{Dc_s}{\ell} . \qquad (A-1.4)$$

The ratio of these two fluxes is therefore

$$\frac{J_t}{J_\infty} = 1 + 2 \sum_{n=1}^{\infty} (-1)^n \exp - \frac{D'n^2\pi^2 t}{\ell^2} . \qquad (A-1.5)$$

If the fraction $\frac{J_t}{J_\infty}$ is chosen to have a convenient value, say 0.5, the

equation reduces to

$$0.25 = e^{-x} - e^{-4x} + e^{-9x} - e^{-16x} + \ldots ,$$

where

$$x = \frac{D'\pi^2 t}{\ell^2} .$$

This is readily solved to give

$$\frac{D'\pi^2 t}{\ell^2} = 1.371 \qquad \text{(A-1.6)}$$

from which D' can be obtained.

A. Klute and J. Letey (1958)

The ordinary differential equation of diffusion with a constant diffusion coefficient was assumed to be valid, with a modification to account for the radioactive decay of an isotope. The rate of decay of the isotope is proportional to its concentration. The diffusion equation is then:

$$\frac{\partial \mu}{\partial t} = D \frac{\partial^2 \mu}{\partial x^2} - \lambda \mu , \qquad \text{(A-1.7)}$$

where μ is the concentration of diffusing material, t is time, D is the diffusivity, and λ is the proportionality factor between the rate of decay and the concentration of the isotope.

The boundary and initial conditions which characterize the diffusion system used are as follows:

$$\left.\begin{aligned} &\frac{\partial \mu}{\partial x} = 0 \quad \text{at} \quad x = 0,\ x = 2h \\ &\left.\begin{aligned} \mu &= 0 \quad h < x < 2h \\ \mu &= \mu_0 \quad 0 < x < h \end{aligned}\right\} \quad \text{at} \quad t = 0. \end{aligned}\right. \tag{A-1.8}$$

These conditions describe a one-dimensional closed finite diffusion system in which there is initially a stepwise distribution of diffusing material. The solution of Equation (A-1.7) subject to the conditions (A-1.8) is:

$$\mu = e^{-\lambda t}\left[\frac{\mu_0}{2} + \frac{2\mu_0}{\pi}\sum_{n=1}^{\infty}\frac{1}{n}\sin\frac{n\pi}{2}\cos\frac{n\pi x}{2h}\,e^{-\frac{n^2\pi^2 Dt}{4h^2}}\right]. \tag{A-1.9}$$

The quantity of diffusing substance moved across the plane $X = h$, i.e., the midpoint of the diffusion cell, in time t, is given by:

$$Q_1 = \int_{X=h}^{X=2h} A(\mu)_{t_1}\,dx, \tag{A-1.10}$$

where A is the cross-sectional area of the diffusion cell, and $(\mu)_{t_1}$ is the concentration distribution at time t_1. Evaluation of the integral leads to

$$Q_1 = e^{-\lambda t} \mu_0 \frac{Ah}{2} \left[1 - \frac{8}{\pi^2} \sum_{n=0}^{\infty} \frac{1}{(2n+1)^2} e^{\frac{-(2n+1)^2 \pi^2 Dt}{4h^2}} \right] . \qquad (A-1.11)$$

The quantity of diffusing substance left in the region $0 < x < h$ at time t_1 is given by:

$$Q_2 = \int_{x=0}^{x=h} A(\mu)_{t_1} dx . \qquad (A-1.12)$$

Evaluation of the integral gives:

$$Q_2 = e^{-\lambda t} \mu_0 \frac{Ah}{2} \left[1 + \frac{8}{\pi^2} \sum_{n=0}^{\infty} \frac{1}{(2n+1)^2} e^{\frac{-(2n+1)^2 \pi^2 Dt}{4h^2}} \right] . \qquad (A-1.13)$$

The fraction of transfer is defined as follows:

$$F = \frac{Q_1}{Q_1 + Q_2} . \qquad (A-1.14)$$

From Equations (A-1.11), (A-1.13), and (A-1.14) it follows that:

$$F = \frac{1}{2} \left[1 - \frac{8}{\pi^2} \sum_{n=0}^{\infty} e^{\frac{-(2n+1)^2 \pi^2 Dt}{4h^2}} \right] . \qquad (A-1.15)$$

Equation (A-1.15) cannot be solved explicitly for D but it can be

solved graphically. The quantity of radioactive material in each half cell was measured, at an arbitrary time t_1 and the fraction transfer calculated. The diffusivity was evaluated from a plot of F versus $Dt/4h^2$.

D.R. Bouldin (1961)

The model adopted assumes a unit of root surface at time equal to zero in an infinite medium at some initial concentration $c = c_0$. The system will possess cylindrical symmetry with respect to the center of the root cylinder. It is assumed that the roots are so far apart that there is no interaction between adjacent roots. The diffusion equation in the medium may then be written

$$\frac{\partial c}{\partial t} = D\left(\frac{\partial^2 c}{\partial r^2} + \frac{1}{r}\frac{\partial c}{\partial r}\right), \qquad \text{(A-1.16)}$$

with the condition

$$c = c_0, \quad a < r < \infty, \quad t = 0,$$

where c is the concentration at time t, r is the distance from the center of the cylinder, D is the diffusion coefficient (assumed to be constant), and a is the radius of root cylinder.

Assume that over a restricted range of concentration, the rate of uptake is proportional to the concentration in solution. Thus, at the root surface

$$F = D\left[\frac{\partial c}{\partial r}\right]_{r=a} = Mc, \qquad \text{(A-1.17)}$$

where F is the flux across a unit of root surface area, and M is a constant of proportionality between concentration and rate of uptake.

Equation (A-1.16) has been solved subject to the stated boundary conditions for the flow of heat under the equivalent conditions of an infinite medium bounded internally by a circular cylinder with radiation at the surface into a medium at zero radiation.

T.M. Lai and M.M. Mortland (1961)

When a quantity Q of a substance is deposited as a uniform and infinitely thin layer on a surface and allowed to diffuse into an infinitely thick medium, this boundary condition can be treated as Fick's law for instantaneous sources. The following solution will be found (Barrer, 1951, p. 45):

$$c_x = \frac{Q}{\sqrt{\pi Dt}}\, e^{-x^2/4Dt}, \qquad \text{(A-1.18)}$$

where c_x is the concentration of the diffusing substance at time t at a distance x from the initial boundary and D is the diffusion coefficient. Considering the absorption of radioactivity by clay underneath the surface, absorption will follow the exponential law:

$$I = I_0\, e^{-kx}, \qquad \text{(A-1.19)}$$

where I_0 is the measured activity without absorption and I is the activity observed through an absorber of thickness x with absorption coefficient k. Therefore, any radio tracer at a distance x below the surface will contribute an amount of activity at the surface proportional to $c_x e^{-kx} dx$. Therefore, the total activity recorded at the surface of a clay plug will be

$$A_0 = \frac{Q}{\sqrt{\pi Dt}} \int_0^{\infty} e^{-(x^2/4Dt+kx)} dx. \qquad (A-1.20)$$

Similarly, when the surface of a plug has been sliced down to a depth x below the original surface, the radioactivity measured at the new surface will be given by

$$A_x = \frac{Q}{\sqrt{\pi Dt}} \int_0^{\infty} e^{-(x^2/4Dt+kx)} dx. \qquad (A-1.21)$$

Setting

$$y = \frac{x}{2\sqrt{Dt}} + k(\sqrt{Dt}), \qquad (A-1.22)$$

and integrating between $y = y_0 = k\sqrt{Dt}$ and $y = \infty$ the following equation will be obtained:

$$A_0 = Q e^{k^2 Dt}(1 - \operatorname{erf} y_0), \qquad (A-1.23)$$

where $\operatorname{erf}(y)$ is the error function or probability integral.

Equation (A-1.23) can also be written

$$A_x = Q e^{k^2 Dt}(1 - \text{erf } y). \qquad \text{(A-1.24)}$$

Combining Equation (A-1.23) and (A-1.24)

$$\frac{A_x}{A_0} = \frac{1 - \text{erf } y}{1 - \text{erf } y_0}. \qquad \text{(A-1.25)}$$

The condition $A_x/A_0 \leq 1$ is fulfilled when the measurement of activity of the clay plug is made at any appreciable depth below the original boundary surface. Since $\text{erf } y_0 < 1$, Equation (A-1.25) can be reduced approximately to

$$\text{erf } y = 1 - \frac{A_x}{A_0}. \qquad \text{(A-1.26)}$$

G.R. Dutt and P.F. Low (1962)

For one dimensional, steady-state diffusion in a clay system, Fick's law obtains

$$J = -DA \frac{dc}{dx}, \qquad \text{(A-1.27)}$$

where J is the amount of the constituent diffusing per unit time, D is the apparent diffusion coefficient, A is the externally measured cross-sectional area, c is the concentration of the solution,

and x is the externally measured distance along the diffusion path. Separating the variables in Equation (A-1.27) and integrating yields

$$J \int_0^S \frac{dx}{D} = -A(c_2 - c_1), \qquad \text{(A-1.28)}$$

where S is the total external length of the diffusion path and c_2 and c_1 are the concentrations of the diffusing constituents at the ends of the path. For a clay system in which D varies with distance along the diffusion path $\overline{D}$, the integral diffusion coefficient, is given by

$$\overline{D} = -\frac{JS}{A(c_2 - c_1)} \quad . \qquad \text{(A-1.29)}$$

Combining Equation (A-1.28) and (A-1.29) we have

$$\overline{D} = \frac{S}{\int_0^S \frac{dx}{D}} \quad . \qquad \text{(A-1.30)}$$

T.M. Lai and M.M. Mortland (1968)

A grain boundary exists between crystal lattices in polycrystalline forms of some metals. Movement of metallic atoms in such systems is by diffusion (D_b) along the grain boundary and diffusion (D_ℓ) into the adjoining crystal lattices. According to Fisher's (1951)

equation:

$$\log c = \text{constant} - [2^{1/2}/(\pi D_\ell t)^{1/4}(\delta D_b/D_\ell)^{1/2}]y, \qquad \text{(A-1.31)}$$

a plot of $\log c$ vs. y then should give a straight line of slope,

$$-2^{1/2}/(\pi D_\ell t)^{1/4}(\delta D_b/D_\ell)^{1/2}, \qquad \text{(A-1.32)}$$

where t is diffusion time, and δ is the thickness of the grain boundary slab. The ratio of D_b/D_ℓ can then be evaluated.

Fisher's solution is limited to certain simple cases, which Whipple (1954) extended and published with fewer limitations. For the purpose of convenient mathematical manipulation, Whipple (1954) introduced the following dimensionless quantities

$$\eta = \frac{y}{(D_\ell t)^{1/2}} \qquad \zeta = \frac{x - \frac{1}{2}\delta}{(D_\ell t)^{1/2}}, \qquad \text{(A-1.33)}$$

where x and y are ordinary coordinates, a parameter

$$\beta = \frac{D_b \delta}{2D_\ell (D_\ell t)^{1/2}}. \qquad \text{(A-1.34)}$$

Whipple's equation has been rearranged by LeClaire (1963) as follows

$$\frac{c}{c_0} = \operatorname{erfc} \frac{1}{2}\eta + \frac{1.159}{(\eta\beta^{-1/2})^{2/3}} \exp[-0.473(\eta\beta^{-1/2})^{4/3} + 0.396 \frac{(\eta\beta^{-1/2})^{2/3}}{\beta}(1-\beta\zeta)], \quad \text{(A-1.35)}$$

where c_0 is the initial concentration of diffusing substance. From this equation the isoconcentration line of diffusing substance in a system with grain boundary diffusion under different conditions can be calculated.

APPENDIX 2

Computer Analysis Program to Determine the Values of the Diffusion Coefficient of 2,4-D (Carbon-14) for Four Fractions of Glass Beads

```
00001:     PROGRAM XSQFIT
00002:     DIMENSION C(30), X(30), X1(30), P(30), ERF(30)
00003:     N=TTYIN(4HTOTA, 4HL DA, 4HTA P, 4HOINT, 4HS = )
00004:     CO=TTYIN(4HCO = )
00005:     T=TTYIN(4HT = )
00006:     DO 71 I = 1, N
00007:     C(I)=FFIN(10)
00008:71   X(I)=FFIN(10)
00009:     DO 2 I = 1, N
00010:2    C(I)=C(I)/CO
00011:3    XK=TTYIN(4HK = )
00012:     TK=2.*SQRT(XK*T)
00013:     DO 4 I = 1, N
00014:     X1(I)=X(I)/TK
00015:     P(I)=1./(1.+0.32759*X1(I))
00016:     Y=-X1(I)*X1(I)
00017:     ERF(I)=(0.2548296*P(I)-0.2844967*P(I)*P(I)
00018:     1+1.4214137*P(I)**3.-1.453152*P(I)**4.
00019:     2+1.0614054*P(I)**5.)*EXP(Y)
00020:4    CONTINUE
00021:     XS=0.
00022:     DO 5 I = 1, N
00023:     XS=XS+(C(I)-ERF(I))*(C(I)-ERF(I))
00024:5    CONTINUE
00025:     PRINT 6, XS
00026:6    FORMAT(1H, 'XSQUARE=', E16.5)
00027:     XI=TTYIN(4HCHAN, 4HGE K, 4H ?)
00028:     IF(XI.EQ.0.) GO TO 10
00029:     GO TO 3
00030:10   WRITE(5, 7)
00031:7    FORMAT(1H , 5X, 'C/CO', 10X, 'ERFC(X)', 10X, 'X(I)')
00032:     DO 8 I = 1, N
00033:8    WRITE(t, 0)C(I), ERF(I), X1(I)
00034:9    FORMAT(1H , E16.5, 5X, E16.5, 5X, F10.5)
00035:     END
```

APPENDIX 3

Mathematical Models Proposed by Different Authors to Determine Self-Diffusion Coefficients of Various Ions

J.H. Wang and J.W. Kennedy (1950)

The general differential equation for diffusion in one dimension is

$$\frac{\partial c}{\partial t} = \frac{\partial}{\partial x}\left(D \frac{\partial c}{\partial x}\right), \qquad \text{(A-3.1)}$$

where c is the volume concentration of the diffusing species, t the time, x the coordinate along which diffusion takes place, and D is the diffusion coefficient. Since for self-diffusion the diffusion medium at different points along the diffusion path is chemically identical, the value of D, self-diffusion coefficient, is a constant and is independent of the concentration of the diffusing tracer ions or molecules. Consequently, Equation (A-3.1) can be written as

$$\frac{\partial c}{\partial t} = D \frac{\partial^2 c}{\partial x^2}, \qquad \text{(A-3.2)}$$

If the diffusion takes place, as in the present work in a capillary practically infinite in length and if before diffusion the concentration c of tracer ions or molecules is constant in one-half of the capillary but zero in the other half, i.e., at $t = 0$, $c = 0$, for $x < 0$, $c = c_0$

for $x > 0$, then

$$\frac{c}{c_0} = \frac{1}{2}\left[1 + \operatorname{erf}\left(\frac{x}{2\sqrt{Dt}}\right)\right], \qquad \text{(A-3.3)}$$

where $\operatorname{erf}(y)$ is the error function of y defined by

$$\operatorname{erf}(y) = \frac{2}{\sqrt{\pi}} \int_0^y e^{-\xi^2} d\xi .$$

In this work (Wang and Kennedy, 1950) the diffusion time t was so adjusted that the value of Dt was about 0.7. After diffusion the total amount A of tracer in the diffusate between $x = -2.000$ cm and $x = -\infty$ cm was determined. This should be

$$A = \frac{c_0 S}{2} \int_{-\infty}^{-2} \left[1 + \operatorname{erf}\left(\frac{x}{2\sqrt{Dt}}\right)\right] dx, \qquad \text{(A-3.4)}$$

or

$$\frac{2A}{c_0 S} = \int_{-\infty}^{-2} 1 + \operatorname{erf}\left(\frac{x}{2\sqrt{Dt}}\right)] dx, \qquad \text{(A-3.5)}$$

where S is the cross-sectional area of the capillary. Equation (A-3.5) was solved graphically for Dt. Alternatively, Equation (A-3, 4) may be written as

$$A = SD \int_0^t \left(\frac{\partial c}{\partial x}\right)_{x=-2} dt = SD \int_0^t \left(\frac{c_0}{2\sqrt{\pi Dt}}\right) e^{-\frac{1}{Dt}} dt,$$

and

$$A = Sc_0\left[\sqrt{\frac{Dt}{\pi}}\, e^{-\frac{1}{Dt}} + \operatorname{erf}\left(\frac{1}{\sqrt{Dt}}\right) - 1\right)],$$

i.e.,

$$\frac{2A}{c_0 S} = \frac{2\sqrt{Dt}}{\sqrt{\pi}}\, e^{-\frac{1}{Dt}} + 2\operatorname{erf}\left(\frac{1}{\sqrt{Dt}}\right) - 2. \qquad \text{(A-3.6)}$$

J.H. Wang (1951)

In a previous method (Wang, 1950), fine uniform capillaries with lower end sealed were filled with heavy water and held in vertical position in a large circulating bath of pure ordinary water at constant temperature. The deuterium oxide and hydroxide were allowed to diffuse upward, the tracer concentrations at the upper end of the capillaries were kept negligible by convection currents in the large bath. Under these conditions, the solution of the one dimensional linear diffusion equation (A-1.1) becomes

$$\frac{c}{c_0} = \frac{4}{\pi} \sum_{n=0}^{\infty} \frac{(-1)^n}{2n+1} \exp\left[-(2n+1)^2 \pi^2 Dt/4\ell^2\right] \cos\frac{(2n+1)\pi x}{2\ell}, \qquad \text{(A-3.7)}$$

where c_0 is the initial concentration of tracer, and ℓ is the length of capillary. The average concentration of solution in the capillary at time t is given by

$$\frac{c_{av}}{c_0} = \frac{8}{\pi^2} \sum_{n=0}^{\infty} \frac{1}{(2n+1)^2} \exp[-(2n+1)^2 \pi^2 Dt/4\ell^2] . \qquad (A-3.8)$$

Thus determination of average tracer concentration in the capillary after diffusion has taken place for a certain time interval t gives the value Dt/ℓ^2, from which D can be readily calculated.

J.H. Wang (1952)

In a previous experiment (Wang, 1951) average concentration of solution in the capillary at time t was given by Equation (A-3.8). In this equation c_{av} is the average concentration of tracer ion in the capillary at time t, and c_0, ℓ and t were defined above. When the value of Dt/ℓ^2 is greater than 0.2, the series on the right-hand side converges so rapidly that all terms following the first can be neglected with an error smaller than 0.2%. Thus

$$\frac{Dt}{\ell^2} = \frac{4}{\pi^2} \ln\left(\frac{8}{\pi^2} \times \frac{c_0}{c_{av}}\right) . \qquad (A-3.9)$$

From the measured values of c_0 and c_{av}, D can be calculated.

J.H. Wang, C.V. Robinson, and I.S. Edelman (1953)

In this improved method a set of capillaries were used to determine the self-diffusion coefficient of liquid water. Under these

conditions the solution of the one-dimensional tracer diffusion Equation (A-1.1) can be represented with enough accuracy by

$$\frac{Dt_i}{(\ell_i - \Delta\ell)^2} = \frac{4}{\pi} \ln\left[\left(\frac{8}{\pi^2}\right) \frac{c_0}{A_i/(\ell_i - \Delta\ell)a}\right], \qquad \text{(A-3.10)}$$

where c_0 is the initial concentration of tracer, A_i is the total amount of tracer left in capillary i (with length ℓ_i and cross-sectional area a) after diffusion has taken place for the length of time t_i, $\Delta\ell$ is the common difference between lengths of diffusion paths and the geometric lengths of the corresponding capillaries with the same cross-sectional area a and held vertically at equivalent positions in the same circulating bath. The set of Equations (A-3.10) can be solved for both $\Delta\ell$ and D. Obviously for given a, $\Delta\ell$ is a function of stirring rate, shape of vessel and viscosity of solution. In all the present measurements the rate of stirring was so adjusted that $2\Delta\ell/\ell$ is negligible as compared to other experimental uncertainties in the present procedure of diffusion measurement. Thus under the present operating conditions, Equation (A-3.10) can be written as

$$\frac{Dt_i}{\ell_i^2} = \frac{4}{\pi} \ln\left[\left(\frac{8}{\pi^2}\right)\frac{c_0}{(c_{av})_i}\right],$$

where $(c_{av})_i = A_i/\ell_i a$. From this the value of D can be calculated.

R.K. Schofield and I.J. Graham-Bryce (1960)

The value of the coefficient of diffusion (D) from Fick's law can be obtained when at the time two sections of soil are placed in contact, the amount of the ion under investigation is equal in the two halves, but in one a proportion consists of a radioactive isotope. The quantity of material Q which is diffused across the boundary in time t can be calculated from

$$\frac{Q}{Q_\infty} = 1 - \frac{8}{\pi^2}\left[e^{-At} + \frac{e^{-9At}}{9} + \frac{e^{-25At}}{25} + \ldots\right], \qquad \text{(A-3.11)}$$

where $A = \frac{D\pi^2}{4\ell^2}$, ℓ is the distance of one half of soil section, and Q_∞ is the quantity which would cross the boundary in infinite time. When the value of $\frac{Q}{Q_\infty}$ is less than 0.5 Equation (A-3.11) may be replaced by

$$\frac{Q}{Q_\infty} = \frac{2}{\ell}\sqrt{\frac{Dt}{\pi}} \; . \qquad \text{(A-3.12)}$$

Measuring Q and Q_∞, D can be calculated.

R.J. Kunze and D. Kirkham (1961)

Consider the concentration in Equation (A-1.1) to be $c = N_D/(N_D+N_H)$, where N_D = moles of D_2O and N_H = moles of H_2O.

Let c_{L0} be the average concentration of D on the left hand of the soil core at $t = 0$, and let c_{R0} be the corresponding quantity for the right half. c_{R0} is small since it refers to deuterium concentration in normal soil water. The initial and boundary conditions are

$$c = c_{L0} \quad \text{for} \quad t = 0 \quad \text{at} \quad 0 < x < a/2,$$

$$c = c_{R0} \quad \text{for} \quad t = 0 \quad \text{at} \quad a/2 < x < a,$$

$$\partial c/\partial x = 0 \quad \text{for all} \quad t \quad \text{at} \quad x = 0,\ x = a.$$

Solution can be simplified by letting

$$F(x,t) = c(x,t) - c_{R0}/(c_{L0}-c_{R0}). \qquad \text{(A-3.13)}$$

With this transformation the basic differential equation is found to be

$$\partial F/\partial t = D_s(\partial^2 F/\partial x^2). \qquad \text{(A-3.14)}$$

After the transformation, the initial and boundary conditions become

$$F = 1, \quad t = 0, \quad 0 < x < a/2,$$

$$F = 0, \quad t = 0, \quad a/2 < x < a,$$

$$\frac{\partial F}{\partial x} = 0 \quad \text{for all} \quad t \quad \text{at} \quad x = 0,\ x = a.$$

A solution of Equation (A-3.14) which satisfies the boundary and initial condition is found to be

$$F = 1/2 + (2/\pi) \sum_{n=1}^{\infty} (1/n)\sin(n\pi/2)\cos(n\pi x/a)e^{-D_s t(n\pi/a)^2} \quad . \quad (A\text{-}3.15)$$

F_L and F_R, the average values of F in the left and right side of the core can be computed in terms of D_s and t from Equation (A-3.15) by the formulae

$$F_L = (2/a) \int_0^{a/2} F dx, \quad (A\text{-}3.16)$$

$$F_R = (2/a) \int_{a/2}^{a} F dx, \quad (A\text{-}3.17)$$

A procedure for converting measured deuterium concentrations to self-diffusion is given by Obermayer (1880). Obermayer combines Equations (A-3.16) and (A-3.17) which results in

$$(F_L - F_R)/(F_L + F_R) = (8/\pi^2) \sum_{n=1}^{\infty} (1/n^2)e^{-D_s t(n\pi/a)^2}, \quad (A\text{-}3.18)$$

Obermayer (1880) has published a table for obtaining values of $D_s t$ corresponding to $(F_L - F_R)/(F_L + F_R)$. The exact values of $D_s t$ may be obtained by interpolation since the relationship of $D_s t$ and $(F_L - F_R)/(F_L + F_R)$ approaches linearity over small intervals of $D_s t$.

I. J. Graham-Bryce (1963)

The coefficient of self-diffusion (D) may be calculated from the quantity of radioactive ions (Q) diffusing from the initially radioactive section to the initially inactive section in time t by solving Equation (A-1.1) for the appropriate set of boundary conditions. For the system used in this work the following solution applies (Barrer, 1951):

$$Q = Dc_0A[4\ell^2\{I - \exp(-Dt[\pi/2\ell]^2)\}/D\pi^2 + 4\ell^2\{I - \exp(-9Dt[\pi/2\ell]^2)\} + \ldots]/\ell, \qquad (A\text{-}3.19)$$

which may be rearranged to:

$$Q = c_0A\ell/2 - 4c_0A\ell[\exp(-Et)+\exp(-9Et)/9+\exp(-25Et)/25+\ldots]\pi^2, \qquad (A\text{-}3.20)$$

where $E = D\pi^2/4\ell^2$, ℓ is the length of each soil section, c_0 is the initial concentration of radioactive ions in labelled section, A is the cross-sectional area of soil sections.

The quantity of ions which would move across the boundary in infinite time is given by:

$$Q_\infty = c_0A\ell/2,$$

so that

$$Q/Q_\infty = I - 8[\exp(-Et)+\exp(-9Et)/9+\exp(-25Et/25)+\ldots]/\pi^2. \qquad (A\text{-}3.21)$$

In practice a graphical procedure based on this equation was used for the calculation of D.

S.R. Olsen, W.D. Kemper, and J.C. Van Schaik (1965)

The equation relating the mutual diffusion coefficient to the individual ion diffusion coefficient is

$$D_{12} = \frac{D_1 D_2 (c_1 + c_2)}{c_1 D_1 + c_2 D_2} , \qquad (A-3.22)$$

which indicates that the diffusion coefficient of the ion present in low concentration will largely control the mutual diffusion coefficient. In this equation D is the diffusion coefficient, c the ion concentration, and the subscripts 1 and 2 represent, respectively the given ion and co- or counter diffusing ion.

The diffusion of ions in the soil solution was considered with surface diffusion along soil particles assumed to be small or negligible. Some of the P in the solid phase contributed to the total amount of P diffusing by renewing the solution concentration. This fraction of the solid phase P plus the P in solution has been termed labile P or potentially diffusible P (Olsen et al., 1962). This means that the relation must be known between the concentration of P in solution and the labile portion of the solid phase P. The rate of equilibrium between P in these two phases was observed to be fast

compared to the rate of diffusion and rate of uptake by roots (Fried et al., 1957).

Steady-State System

The self-diffusion coefficient for P was calculated as follows from Equation (A-3.23) based on Fick's law,

$$\frac{\Delta Q}{\Delta t} = DA\alpha\gamma(L/L_e)^2\theta \frac{\Delta c}{\Delta x} . \qquad (A-3.23)$$

Equation (A-3.23) may be simplified by the substitution,

$$D_p = D\alpha\gamma(L/L_e)^2\theta, \qquad (A-3.24)$$

so that

$$\frac{\Delta Q}{\Delta t} = D_p A \frac{\Delta c}{\Delta x} , \qquad (A-3.25)$$

where D_p is a porous system self-diffusion coefficient, D is the diffusion coefficient for P in bulk solution ($cm^2 sec^{-1}$), ΔQ is the amount of P^{32} diffusing through the soil plug into the solution (counts/min cc times the volume), Δt is the time (seconds) over which ΔQ is measured, A is the cross-sectional area of the soil (cm^2), Δc is the difference in P^{32} activity between each side (counts/min per cc), Δx is thickness of soil (cm), α is a factor for viscosity, γ is a factor for negative adsorption, $(L/L_e)^2$ is a

tortuosity factor, and θ is the volumetric moisture content.

Equation (A-3.25) for porous systems takes into account three important departures from classical diffusion theory, (i) diffusion occurs through the fraction of the pore space filled with water, (ii) the path length for diffusion is longer (tortuosity), and (iii) the negatively charged clay minerals cause negative adsorption of anions and a portion of the soil water near the clay mineral surface is more viscous. These two factors were combined formerly in the γ term (Olsen et al., 1962; Porter et al., 1960), but recent research has shown a way to separate them into α and γ terms for the viscosity and negative adsorption effects, respectively (Kemper et al., 1964).

The diffusion cell contained two porous steel plates as well as moist soil and the correction for diffusion in the steel plates was introduced into Fick's law as follows $\Delta c = \Delta c_p + \Delta c_s$, where the subscripts p and s represent the soil and porous steel phases, respectively. The concentration difference in the porous steel is then

$$\Delta c_s = \frac{(\Delta Q/\Delta t)\Delta x_s}{D_s A}, \qquad \text{(A-3.26)}$$

and the porous system self-diffusion coefficient in the soil is

$$D_p = \frac{(\Delta Q/\Delta t)\Delta x_p}{A\Delta c_p}. \qquad \text{(A-3.27)}$$

By substituting $\Delta c - \Delta c_s = \Delta c_p$ into Equation (A-3.27) and the value of Δc_s from Equation (A-3.26) into Equation (A-3.27), the result is

$$D_p = \frac{\Delta x_p}{A\frac{\Delta c \Delta t}{\Delta Q} - \frac{\Delta x_s}{D_s}}, \qquad \text{(A-3.28)}$$

where Δx_p is the thickness of the soil, Δx_s is the thickness of two porous steel plates, Δc is the concentration difference across the total cell thickness of cross-sectional area A, and ΔQ is the amount of P diffusing across the cell in time, Δt, when a steady state condition is satisfied. Equation (A-3.28) was used to obtain values for D_p. The correction due to diffusion in the porous steel amounted to less than 15% of the value for D_p.

A capacity factor does not enter into Equation (A-3.25) because there will be no net exchange of ions between the liquid and solid phase when $\Delta c/\Delta t = 0$, i.e., a steady state condition that must be achieved experimentally.

Transient State System

Equation (A-3.29) was developed for the time dependent problem by Olsen et al. (1962), using Fick's first law and the equation of continuity.

$$\partial c/\partial t = \frac{D_p}{b+\theta} \frac{\partial^2 c}{\partial x^2}, \qquad \text{(A-3.29)}$$

where D_p, t, θ, and x have the same meaning as above, b is a capacity factor, and c is the concentration of P in the soil solution (g/cm^3). In this equation b and D_p are assumed to be constant and independent of c, t, and x. A capacity factor enters this equation because there is a large labile portion of solid-phase P that goes readily into solution when the P concentration in solution is reduced by diffusion. Thus, a measure of D_p in Equation (A-3.29), comparable with D_p in Equation (A-3.25), requires an independent estimate of b. When $b > 100$, θ becomes insignificant, and the effect of θ is only about 5% when b is around 10.

Porter et al. (1960) presented an integrated form of an equation similar to Equation (A-3.29) which is applicable for measuring D_p in a transient state experiment,

$$\frac{D_p}{b+\theta} = \frac{\pi}{t}(q/q_0)^2 \ell^2, \qquad \text{(A-3.30)}$$

where q is the total quantity diffused per unit of soil, q_0 is the initial quantity of diffusible ion per unit soil, ℓ is the thickness of the soil into which net diffusion occurs, b is a capacity factor and D_p, θ and t have been described above.

W. J. Farmer and C.R. Jensen (1970)

The following solution for the transient diffusion system used was adapted from Crank (1956)

$$\frac{M_{\ell/2}}{M_{\ell}} = \frac{1}{2} - \frac{4}{\pi^2} \sum_{n=1}^{\infty} \frac{\exp-[(2n-1)^2 \pi^2 Dt/\ell^2]}{(2n-1)^2}, \qquad (A-3.31)$$

where $M_{\ell/2}$ is the dieldrin activity in untreated half of cell after diffusion, M_{ℓ} is the total dieldrin (activity) in cell after diffusion, D is the diffusion coefficient (mm^2/week) of dieldrin, t is the time (weeks), and ℓ is the depth of diffusion cell (mm).

APPENDIX 4

Mathematical Model Used to Generate Theoretical Curves for the Transport of Chemicals into a Water Saturated Sorbing and Non-Sorbing Porous Media

Dispersion Model

Following the approach of Lindstrom et al. (1967), the following dispersion equation is assumed to hold during the course of the afore mentioned experiments.

$$D_\ell \frac{\partial^2 U}{\partial x^2} - v_c \frac{\partial U}{\partial x} = \frac{\partial U}{\partial t}, \qquad \text{(A-4.1)}$$

$$(x,t) \in \{(0 < x < \infty) \times (0 < t < \infty)\}$$

$$\text{I.C.} \qquad U(x,0) = 0 \qquad \text{(A-4.2)}$$

$$\text{B.C.} \quad \text{(i)} \quad U(0,t) = U_0, \; 0 \leq t \leq T_1, \; T_1 = \frac{\ell}{v_c} \qquad \text{(A-4.3)}$$

for ℓ small and v_c large.

$$\text{(ii)} \quad \lim_{x \to \infty} \left(-D_\ell \frac{\partial U}{\partial x} + v_c U\right)\Big|_x = 0, \qquad \text{(A-4.4)}$$

where

$U(x,t)$ = free phase chemical concentration distribution function (gm/cm^3),

U_0 = free phase chemical concentration at source-column

interface (gm/cm^3),

D = reduced dispersion coefficient for each particular porous medium (cm^2/day),

v = reduced average hydrodynamic flow velocity in void spaces (cm/day), and

ℓ = length of injecting pulse (cm).

Actually,

$$D = \frac{D_L}{1+\phi\gamma}$$

and

$$v = \frac{v_c}{1+\phi\gamma},$$

where

ϕ = dimensionless parameter. Ratio of the specific void surface area for sorbtion to the average hydrodynamic flow area, and

γ = energy and temperature dependent partition coefficient of chemical between free and sorbed phases.

Thus,

v_c = average sorbtion free hydrodynamic flow velocity in the voids (cm/day), and

D_ℓ = dispersion coefficient for each particular porous medium (cm^2/day).

It is to be noted here that the reduced coefficients are obtained by coupling the free phase chemical distribution to an instantaneous

pointwise equilibration isotherm such as the Freundlich isotherm with exponent equal to one. Also, it can be shown (Lindstrom et al., 1967), that when average hydrodynamic flow velocities are high, $v_c > 20$ cm/day, and $\ell \leq 1$ cm, that the boundary condition (A-4.3), which we assume, is a good approximation to the real case for rapid plug flow dispersion in a porous medium.

The solution to system (A-4.1)-(A-4.4), obtained by taking the limiting case of large v_c, yielding the free phase chemical distribution function has been given by Lindstrom et al. (1967) as

$$U(x,t) = \frac{U_0}{2}\{H(t)\mathcal{L}(x,t) - H(t-\frac{\ell}{v_c})\mathcal{L}(x,t-\frac{\ell}{v_c})\}, \qquad (A\text{-}4.5)$$

$$t > 0, \quad x \geq 0,$$

and where

$$\mathcal{L}(x,t) = \operatorname{erfc}\frac{x-\frac{v_c t}{1+\phi\gamma}}{2\sqrt{\frac{D_\ell t}{1+\phi\gamma}}} + e^{\frac{xv_c}{D_\ell}}\operatorname{erfc}\frac{x+\frac{v_c t}{1+\phi\gamma}}{2\sqrt{\frac{D_\ell t}{1+\phi\gamma}}} \quad . \qquad (A\text{-}4.6)$$

Appendix 4, (Numerical Evaluation Scheme) lists the high order modified inverse polynomial approximation actually used in a computer scheme to evaluate $\mathcal{L}(x,t)$ for prescribed values of the parameters and independent variables.

Numerical Evaluation Scheme

The equation

$$\mathcal{L}(x,t) = \operatorname{erfc}\left(\frac{x-vt}{2\sqrt{Dt}}\right) + e^{x\frac{v_c}{D_\ell}} \operatorname{erfc}\left(\frac{x+vt}{2\sqrt{Dt}}\right), \qquad \text{(A-4.7)}$$

with

$$D = \frac{D_\ell}{1+\phi\gamma}, \quad \text{and} \quad v = \frac{v_c}{1+\phi\gamma},$$

is to be evaluated.

Following Abramowitz and Stegun (1965), define

$$\text{(i)} \quad \delta_1(x,t) = \frac{x-vt}{2\sqrt{Dt}},$$

$$\text{(ii)} \quad \delta_2(x,t) = \frac{x+vt}{2\sqrt{Dt}},$$

$$\text{(iii)} \quad \theta_1(x,t) = \frac{1}{1+p\delta_1}, \qquad \text{(A-4.8)}$$

$$\text{(iv)} \quad \theta_2(x,t) = \frac{1}{1+p\delta_2},$$

where

$$p = 0.47047.$$

The following constants are also used in the computation

$$A_1 = 0.34802$$

$$A_2 = -0.09587$$

$$A_3 = 0.74785.$$

Two cases arise immediately for each (x, t).

Case I. If $\delta_1 \leq 0$, $\delta_2 > 0$, then

$$(x, t) = 2 - (A_1(\theta_1^{(1)} - \theta_2) + A_2((\theta_1^{(1)})^2 - \theta_2^2) + A_3((\theta_1^{(1)})^3 - \theta_2^3))e^{-\delta_1^2} + \epsilon(x, t),$$

where

$$\theta_1^{(1)} = \frac{1}{1+p|\delta_1|},$$

and $\epsilon(x, t)$ is the error term for the high order inverse modified polynomial approximation. Magnitude wise

$$|\epsilon| < 2 \times 10^{-5} \quad \text{for all} \quad (x, t) > (0, 0).$$

Case II. If $\delta_1 > 0$, $\delta_2 > 0$, then

$$\mathcal{L}(x, t) = (A_1(\theta_1+\theta_2)+A_2(\theta_1^2+\theta_2^2)+A_3(\theta_1^3+\theta_2^3))e^{-\delta_1^2} + \epsilon(x, t).$$

For each ordered pair (x, t), the above scheme is followed via a Fortran 4 computer program.

Dispersion Coefficient Estimation

The dispersion coefficients used in evaluationg Equation (A-4.6), the free phase chemical distribution function, are obtained by using

the distribution data in sorbption free form, i.e., $\phi = 0$ or $\gamma = 0$ or both ϕ and $\gamma = 0$, i.e., the medium does not sorb chemical from the free phase or the partition is very small or both phenomena occur simultaneously. The equation used to achieve initial estimates is

$$x_p \cong v_0 t \sqrt{(1 - \frac{\ell}{v_0 t})(1 - \frac{2D_\ell}{v_c \ell} \ln(\frac{t - \frac{\ell}{v_c}}{t}))} , \qquad (A\text{-}4.9)$$

where, x_p is the peak position at time t, and all other parameters have been defined previously. To arrive at Equation (A-4.9) all one needs to do is to differentiate Equation (A-4.5) with respect to x and set the derivative equal to zero. By keeping the major contribution portion to the derivative the following approximation is obtained

$$\sqrt{\frac{t - \frac{\ell}{v_c}}{t}} \cong e^{-\frac{(x_p + \ell - v_c t)^2}{4D_\ell (t - \frac{\ell}{v_c})} + \frac{(x_p - v_c t)^2}{4D_\ell t}} \qquad (A\text{-}4.10)$$

In Equation (A-4.10) we simply solve for x_p which results in Equation (A-4.9). It must be remembered that $\ell / v_c \ll 1$ for the approximations to be reasonably accurate.